UNIVERSITAT POLITÈCNICA DE CATALUNYA
BARCELONATECH
Departament de Teoria del Senyal
i Comunicacions

Radio Resource Management Strategies for Interference Mitigation in 4G Heterogeneous Wireless Networks

PH.D. THESIS DISSERTATION

By
Koutlia Aikaterini

A thesis submitted to the
Department of Signal Theory and Communications
of the Universitat Politècnica de Catalunya (UPC)
in Partial Fulfillment of the Requirements for the Degree of

DOCTOR OF PHILOSOPHY

Barcelona, March 2016

Thesis Advisors: Dr. Jordi Pérez-Romero and Dr. Ramon Agustí Comes
Mobile Communication Research Group (GRCM)
Department of Signal Theory and Communications (TSC)
Universitat Politècnica de Catalunya (UPC)

To my parents

Στους Γονείς μου

Abstract

The new era of mobile communications is dictated by the user demand for robust and high speed connections, data hungry applications and seamless connectivity. Operators and researchers all over the world are challenged to fulfill these requirements by providing enhanced coverage, increased capacity and efficient usage of the scarce spectrum. The introduction of the fourth generation systems (4G), LTE and LTE-A, have set the initiative for a technology evolution that offers new possibilities and is able to satisfy the user requirements and overcome the imposed challenges.

However, and despite the improvements brought by the LTE and LTE-A systems, there are certain constraints that still need to be surpassed. LTE for example adopts innovating technologies, such as Orthogonal Frequency Division Multiplexing Access (OFDMA) that improves the spectral efficiency and reduces the Intra-Cell Interference. Nevertheless, Inter-Cell Interference (ICI) remains a constraining factor that can degrade the system capacity and limit the overall performance of the network. On that respect, Inter-Cell Interference Coordination (ICIC) techniques are adopted with target the interference mitigation. One of the limitations of these techniques is that follow static configurations lacking of flexibility and adaptation on network changes.

Moreover, LTE-A employs enhanced and new techniques and involves alternative strategies. A promising solution lies on the introduction of Heterogeneous Networks (HetNets), which are networks that include low power small cells under the already existing macro cellular network and exploit several other technologies, such as WiFi. HetNets can further improve the network capacity, enhance the coverage and provide higher speed data transfer. However, due to the heterogeneous nature of the network, traditional methods for the user association, resource allocation and interference mitigation may not always be suitable since their design was based on homogeneous deployments. As such, new and enhanced methods are introduced, such as enhanced ICIC (eICIC), with their accompanied requirements and challenges.

Motivated by the abovementioned aspects, this thesis has been focused on the study of ICIC and eICIC schemes, the identification of the related challenges, the enhancement of existing schemes and the proposal of novel solutions. In particular in the initial stages of the work, ICIC techniques have been studied and analyzed. A distributed algorithm that performs dynamic channel allocation has been developed for homogeneous deployments and extended later on to include heterogeneous networks. The solution has been optimized with the use of the Gibbs Sampler, while the setting of algorithm related

parameters has been addressed through a detailed analysis. Moreover, a possible implementation of the solution has been presented in detail. The efficiency of the proposed schemes has been demonstrated through simulations and comparisons with benchmark schemes.

In the next steps, the work has targeted eICIC techniques with purpose the investigation and analysis of the main constraining issues related to the user association, resource management and interference mitigation. Novel eICIC schemes that aim a better resource management and the overall capacity improvement have been developed and presented in detail, while the performance of the solutions has been shown through simulations and comparisons with reference schemes. Moreover, an optimized eICIC solution has been implemented based on genetic algorithms. Simulation results and comparisons with reference schemes have demonstrated the efficiency of the solution, while the selected configurations are discussed and analyzed.

Acknowledgements

During the implementation of this thesis I have gained valuable experiences and lessons. Starting my story from leaving my country Greece and my parents' home, I learnt to live alone, to be independent, to cook (what a challenge!), to speak Spanish, to eat chorizo, to make new friends and learn about other cultures, I have matured as a person, but most important I have entered the world of investigation. This world has always fascinated me and at this moment of my life I can say that I have achieved to make my dream come true. However, this dream would never have been a reality without some persons that have supported me each one with its own way.

First of all, I would like to thank Dr. Jordi Pérez Romero. You have been my mentor. Without you the implementation of this thesis would never be possible. Thank you for your innovating ideas, for giving me solutions whenever I was desperate, for motivating me, for your time, for your patience and for your unconditional support during all these years. You are a brilliant person and I feel honored to have worked with you.

I would like to express my sincere gratitude to Dr. Ramon Agustí Comes first of all for believing in me and giving me the opportunity to be part of the GRCM group. Moreover, I am grateful for his support, his valuable comments and ideas for the implementation of this thesis and most of all his guidance during all these years.

Although words in this case are not enough, I would like to thank my parents for being always there for me, even though they still think I am finishing my master studies. They have made me the person I am, they have given me unconditional love and they have let me go and chase my dreams even if my absence has been painful for them. What can I say, you are awesome. Moreover, I thank my brother for giving me the most wonderful family comprised by my sister in law and my three nephews. Nothing has been more relaxing than their laughs.

I am thankful for the precious friends this life has given me. Theodora, you know that without you I wouldn't be what I am and where I am. Thank for your support in my most difficult moments and the laughs that made our stomachs ache and our eyes cry. Aris, you have been and are my family here. Thank you for being always there for me and sharing the same craziness with me. I would also like to thank the people in the UPC that have been part of my life for the last four years. Liliana, Alessandro, Tauseef, Juan, Martin and the IT department.

Last but not least, I want to say thank you to the most special person in my life, Sergio. Thank you for your patience and tolerance whenever I was full of stress and anxiety, thank you for giving me strength, thank you for motivating me in my most difficult moments, thank you for listening to me, but most importantly, thank you for making my life beautiful.

I. Table of Contents

II. List of Figures

III. List of Tables

IV. List of Abbreviations

3GPP	3rd Generation Partnership Project
ABS	Almost Blank Subframes
BS	Base Station
CA	Carrier Aggregation
CoMP	Coordinated Multipoint Transmission and Reception
CP	Cyclic Prefix
C-RAN	Cloud-Radio Access Networks
CRE	Cell Range Expansion
CSG	Closed Subscriber Group
DFT	Discrete Fourier Transform
DL	Downlink
DSL	Digital Subscriber Line
DSP	Digital Signal Processors
EDGE	Enhanced Data rates for Global Evolution
eICIC	enhanced Inter-Cell Interference Coordination
eNodeB	evolved Node B
EPC	Evolved Packet Core
EPS	Evolved Packet System
ETSI	European Telecommunications Standard Institute
E-UTRAN	Evolved-Universal Terrestrial Radio Access Network
FFR	Fractional Frequency Reuse
FFT	Fast Fourier Transform
FPGA	Field Programmable Gate Array
GPRS	General Packet Radio Services
GRF	Gibbs Random Field

GS-ICIC	Gibbs Sampler-based dynamic frequency allocation
GSM	Global System for Mobile Communications
HeNB	Home evolved Node B
HetNets	Heterogeneous Networks
HGS-ICIC	Gibbs Sampler-based dynamic frequency allocation for HetNets
HS	Hot Spot
HSPA	High Speed Packet Access
HSS	Home Subscriber Server
ICI	Inter-Cell Interference
ICIC	Inter-Cell Interference Coordination
IFFT	Inverse Fast Fourier Transform
ISI	Inter-Symbol Interference
ITU	International Telecommunications Union
LP-ABS	Low Power –ABS
LPN	Low Power Node
LTE	Long Term Evolution
LTE-A	Long Term Evolution – Advanced
MAC	Medium Access Control
MAI	Multiple Access Interference
MCD	measurement-capable devise
MIMO	Multiple Input Multiple Output
MINLP	Mixed integer non-linear programming
MME	Mobility Management Entity
MRF	Markov Random Field
NFV	Network Function Virtualization
NUSGS-ICIC	Negative User SINR GS-ICIC
OFDM	Orthogonal Frequency Division Multiplexing

OFDMA	Orthogonal Frequency Division Multiplexing Access
OSG	Open Subscriber Group
OTFP-eICIC	Optimized TFP-eICIC
PDCP	Packet Data Convergence Protocol
PDN	Packet Data Network
PDN-GW	PDN – Gateway
PFR	Partial Frequency Reuse
QAM	Quadrature Amplitude Modulation
QoS	Quality of Service
RAN	Radio Access Network
RB	Resource Block
REM	Radio Environment Maps
REM SA	REM data storage and acquisition
RFO	REM-based Frequency Optimization
RLC	Radio Link Control
RN	Relay Nodes
RRM	Radio Resource Management
RSS	Received Signal Strength
SAE	System Architecture Evolution
SC	Single Carrier
SC-FDMA	Single Carrier - Frequency Division Multiple Access
SDN	Software Defines Networking
SFR	Soft Frequency Reuse
S-GW	Serving – Gateway
SINR	Signal to Noise and Interference Ratio
TDMA	Time Division Multiple Access
TFP-eICIC	Time-Frequency-Power eICIC

TTI	Transmission Time Interval
UIGS-ICIC	User Interference GS-ICIC
UL	Uplink
UMTS	Universal Mobile Telecommunication Systems
USGS-ICIC	User SINR GS-ICIC
WCDMA	Wideband Code Division Multiple Access

1. Introduction

1.1 Brief History – Early Generation Systems

Several decades ago, a wireless call was a utopia that lived in the imagination of some writers and ambitious inventors. While various attempts for wireless communications were made earlier, the basis for what evolved later on as todays cellular networks started in the early 80s'. The networks developed at that time made use of analog technologies and are known as the first generation (1G) of cellular systems. However the potentials of these systems were limited in the voice domain and provided basic mobility. As such they could not meet the demands of the users and the performance requirements.

In 1991, the second generation systems (2G) were introduced that were based on digital technologies. Among other standards, the most popular is the Global System for Mobile Communications (GSM) developed by the European Telecommunications Standard Institute (ETSI) and adopted mainly in Europe. The objective was to have a unified technology throughout the different countries with purpose to make roaming easier to be carried out. GSM was using Time Division Multiple Access (TDMA) and circuit-switched technology. Initially, it was intended for voice services, however later on it was modified to support also circuit-switched data services. The main problem was that the supported data rates were very low. For this reason, the initial concept of GSM was enhanced to support packet-switched services with the addition of the General Packet Radio Services (GPRS) and a further enhancement was introduced with the Enhanced Data rates for Global Evolution (EDGE), with target to increase the offered data rates.

Despite the success of GSM, the target of a global standard was not completely achieved. Moreover, the user demand was growing continuously with higher requirements in terms of traffic volume and data services. As such, while GSM was being established, a new standard has been developed under the 3rd Generation Partnership Project (3GPP). This standard is the Universal Mobile Telecommunication Systems (UMTS) and represents the third Generation (3G) of mobile communication systems. The advantage of UMTS is that it supports both circuit-switched and packet-switched modes, it improves spectral efficiency and offers higher transmission rates thanks to the use of Wideband Code Division Multiple Access (WCDMA) as air interface.

Mobile communications have become nowadays an essential part of our lives. As technology evolves and user demand increases, the requirements are growing exponentially. Smartphones, laptops, tablets, i-watches and other bandwidth greedy devices are taking leading roles in the daily life. As such, there is the

need for new technologies that will satisfy the continuously increasing demands. The standards that the future technologies must fulfil are becoming more and more exigent. On that respect, fourth Generation (4G) mobile communications systems have been introduced, including a number of new and evolved technologies. As this work mainly focuses on the 4G systems, a brief introduction is given in the next section.

1.2 Fourth Generation Systems (4G)

Device proliferation dominated by data hungry applications and user demand for higher data rates impose a set of challenges, such as improved capacities and coverage that operators and researchers all over the world need to surpass. The initiative for a new era in the mobile communications has been set with the introduction of the fourth generation systems such as Long Term Evolution (LTE) and LTE-Advanced (LTE-A).

The first steps towards the technology evolution have been made with the development of LTE. The architecture of LTE was based on homogeneous deployments of macrocells that involved novel and enhanced techniques. Examples include the Orthogonal Frequency Division Multiplexing (OFDM) and the use of Multiple Input Multiple Output (MIMO) antennas. Higher data rates and better user experience were provided; however with no margins for further improvements since the Shannon capacity limits were approached in terms of spectral efficiency per link [1]. Moreover, the uneven nature of the user distribution and data traffic was remaining a constraining factor [2]. Despite the possibilities of LTE, it could not meet all the specifications defined by the International Telecommunications Union (ITU) for a truly 4G system. As such, alternative strategies that will allow further improvement in the cells capacity and the spectrum efficiency, yet in low expenditure cost, became a necessity. On that respect, 3GPP developed the framework of LTE-A with target to overcome these challenges and further improve the overall network performance. This framework involves the enhancement of existing technologies, as well as the adoption of new ones, such as Coordinated Multipoint Transmission and Reception (CoMP) and Carrier Aggregation (CA).

One of the most promising solutions in the context of LTE-A consists in the Heterogeneous Networks (HetNets), a transition from traditional homogeneous deployments to more complex patterns. This novelty was able to enhance the coverage in hot spot areas and allow higher data rate transmissions. The concept of HetNets includes the addition of different types of small cells, such as pico and femto cells, as well as the incorporation of different types of technologies (e.g. WiFi). With HetNets it is possible to further improve the system performances in terms of capacity, coverage and data rates in a cost effective way, reasons that drawn the attention of the researchers [3] and Standardization Bodies [4].

Nevertheless, due to the diversity and the different characteristics of the involved cells in a HetNet, new challenges arise that include the areas of user-to-cell association, interference management and utilization of resources [5]. In [6] a survey of challenges is presented, including some suggestions and potentials for the different topics that need modifications and enhancements.

In this thesis, the main target is to address radio resource management issues in 4G systems with special focus on the interference management. Throughout this work, the theory behind existing technologies has been studied and the associated challenges have been identified. The research has been focused on the optimization of existing schemes and the development of new techniques. The implementation process started considering homogeneous deployments based on frequency reuse schemes and later on it extended to include heterogeneous networks. More details are given in the following.

1.3 Motivations, Objectives and Contributions

Radio spectrum is a scarce and therefore an expensive resource that undergoes regulations imposed by the governments or organizations like the ITU. For this reason, efficient utilization of the resources and interference mitigation are crucial issues. The adoption of Orthogonal Frequency Division Multiplexing Access (OFDMA) as air interface in the 4G systems resulted in the improvement of the spectral efficiency and in the reduction of the intra-cell interference due to the orthogonality of the users. However, inter-cell interference (ICI) remains a constraining factor, especially for the users located close to the cell borders. On that respect, LTE adopts Inter-cell Interference Coordination (ICIC) techniques that allow the allocation of the available resources to the edge users with higher reuse factors, resulting in the mitigation of the inter-cell interference [7].

Despite the potentials of ICIC schemes, most approaches consider static configurations, constraining in this way the network flexibility and the overall performance. Moreover, the design of these schemes has been carried out based on homogeneous deployments. As such, the deployment of small cells (e.g. femto cells) in the macrocell environments sets additional challenges with respect to the frequency planning and the interference management. On that respect, in the context of LTE-A ICIC techniques are evolved and enhanced ICIC (eICIC) schemes are introduced. eICIC takes into account the network heterogeneity, however new challenges and constraints arise with respect to the interference management and the resource utilization.

Based on the above, the main objective of this thesis is to study, analyze and propose interference management solutions under the LTE and LTE-A frameworks that allow the mitigation of the interference, the efficient utilization of the available resources and the improvement of the network capacity. Investigation focuses on the identification of the technical challenges and the possible implementation

constraints of both ICIC and eICIC schemes. Initial work considers ICIC solutions for resource allocation in homogeneous deployments and targets the optimization of them. Then, this work is extended to include heterogeneous networks. Taking advantage of the knowledge acquired through the study of ICIC scenarios, eICIC techniques are investigated and the related problems are identified. Novel solutions are proposed for the management of the interference in heterogeneous networks scenarios. Finally, the optimization of a novel solution developed throughout this work is carried out.

As such the contributions of this thesis can be summarized as follows:

1. The ICIC constraints under homogeneous deployments are investigated and identified and a distributed algorithm, known as Gibbs Sampler-based ICIC (GS-ICIC), that performs dynamic frequency allocation is developed. The proposed solution targets the mitigation of the ICI in tri-sectorial frequency reuse scenarios and is based on the Gibbs Sampler as optimization tool. The interference problem is formulated accordingly so that the algorithm minimizes the network interference through the proper allocation of the available frequencies. The solution results in the improvement of the overall network capacity, with special focus on the users located in the cell edges, which are the most vulnerable to interference. Moreover, an analysis is carried out with respect to variations of algorithm related parameters and how these affect the performance of the algorithm in terms of interference reduction, capacity improvement and convergence.
2. The above solution is further investigated through variations of the formulation of the interference problem and the impact they have to the algorithm performance is analyzed. Examples include the consideration of the user interference instead of the total and the inclusion of the Signal to Noise and Interference Ratio to the formula. The former targets the interference minimization by taking into account the number of the network users, while the later aims the capacity maximization along with the interference mitigation.
3. The GS-ICIC scheme is extended to include heterogeneous deployments. The proposed solution is known as GS-ICIC for HetNets (HGS-ICIC). Investigation starts from simple scenarios in order to study the behavior of the algorithm when small cells are included in the network topology and how their locations can impact on the algorithm decisions. Then, more complicated topologies are studied consisting in several macrocells and small cells. The benefits brought by the HGS-ICIC solution in terms of interference mitigation and capacity increment are demonstrated through simulations.
4. An implementation of the proposed HGS-ICIC scheme is studied considering the Radio Environment Maps (REM) concept, which is a database for storing dynamically information about the radio environment. The REM-based Frequency Optimization (RFO) uses the information stored in the database related to the propagation in order to estimate the received and generated

interference and the resource allocation is carried out accordingly. Simulation results show the efficiency of the scheme in terms of capacity improvement.

5. Based on the knowledge gained throughout the previous work, a novel eICIC solution is presented for heterogeneous networks based on the joint exploitation of the time-frequency and time-power dimensions. The solution aims the efficient utilization of the available resources and the mitigation of the interference generated to the small cells from the macrocells with target the improvement of the network capacity. The selection of the mechanism that is applied is based on the location of the small cells with respect to the macro Base Station (BS). It is shown that the management of the resources performed by the algorithm brings significant improvements in the network capacity.
6. The previously presented solution is extended to include only one mechanism that exploits jointly the time, frequency and power dimensions (TFP-eICIC). As such, an alternative and more flexible management of the available resources is proposed that results in the mitigation of the small cell interference, the increment of the macrocell and the overall network capacity and the efficient utilization of the resources.
7. In the last part of this work the TFP-eICIC scheme is optimized and the OTFP-eICIC scheme is proposed. The optimization framework of the OTFP-eICIC solution is based on genetic algorithms and adjusts the configuration of the system parameters depending on the network environment with result the minimization of the interference, the efficient load balancing and resource utilization and the maximization of the network capacity.

1.4 List of Publications

The work carried out throughout this thesis has been published and/or submitted for publication in journals, conferences and funded research projects. A list of the related publications is given in the following.

Journals

[J1] K. Koutlia J. Pérez-Romero, R. Agustí, “On jointly exploiting the frequency, time and power dimensions for optimizing eICIC in Heterogeneous Networks”, *Journal on Wireless Communications and Networking*, *EURASIP*, (submitted for publication)

[J2] J. Pérez-Romero, A. Zalonis, L. Boukhatem, A. Kliks, K. Koutlia, N. Dimitriou, R. Kurda, "On the use of radio environment maps for interference management in heterogeneous networks," in *Communications Magazine, IEEE* , vol.53, no.8, pp.184-191, August 2015

Conference Papers

[C1] K. Koutlia, M. Žiak, J. Pérez-Romero, R. Agustí, "On the Use of Gibbs Sampling for Inter-Cell Interference Mitigation under Partial Frequency Reuse Schemes", *Proc. The Third International Conference on Mobile Services, Resources, and Users* (MOBILITY), Lisbon, Portugal, Nov. 2013

[C2] K. Koutlia, J. Pérez-Romero, R. Agustí, "Novel eICIC scheme for HetNets exploiting jointly the frequency, power and time dimensions", in *Personal, Indoor, and Mobile Radio Communication (PIMRC), 2014 IEEE 25th Annual International Symposium on*, pp.1078-1082, 2-5 Sept. 2014

[C3] K. Koutlia, J. Pérez-Romero, R. Agustí, "On enhancing Almost Blank Subframe Management for efficient eICIC in HetNets", *2014 IEEE 81st Vehicular Technology Conference (VTC Spring)*, May 2015

Contributions to Research Projects

- NEWCOM# : Network of Excellence in Wireless Communications#, funded by the European Commission (Contract Number 318306). Contribution to Deliverables:

  [D1] A. Zalonis (Editor), "D13.1 Fundamental issues on energy- and bandwidth-efficient communications and networking", Deliverable del proyecto NEWCOM#, Febrero, 2014

  [D2] A. Zalonis (Editor), "D13.2 Techniques and performance analysis on energy- and bandwidth-efficient communications and networking", Deliverable del proyecto NEWCOM#, Noviembre, 2014

  [D3] A. Zalonis (Editor), "D13.3 Overall assessment of selected techniques on energy- and bandwidth-efficient communications", Deliverable del proyecto NEWCOM#, Octubre, 2015

- ARCO : "Opportunistic and Cognitive Radio Access," original title in Spanish: "Acceso Radio Cognitivo y Oportunista", funded by CICYT Ref. TEC2010-15198
- RAMSES : Redes móviles eficientes para la AMpliación de SErvicios a nuevos Sectores profesionales, funded by CICYT Ref. TEC2013-41698-R

Finally it has to be referred that the work has been supported by a scholarship from the Spanish Ministry of Education, Culture and Sports (Ref. FPU 12/02088).

1.5 Organization of the Thesis

This PhD Thesis is organized in 5 chapters. The structure of the thesis is graphically summarized in Figure 1 and a brief overview of each chapter is given in the following.

Chapter 2 discusses the fundamental concepts and characteristics of the fourth generation systems. The main features of the network architecture of LTE and LTE-A are presented and the new technologies adopted by the standards are discussed in detail. Special emphasis is given on the concept of Heterogeneous Networks. An overview of the different elements and their main features that comprise the network is presented, while the challenges imposed by the combination of the different cell types and technologies are addressed.

Chapter 3 targets on the management of the Inter-Cell Interference in the frequency dimension. A discussion on the main reasons that make the usage of ICIC techniques indispensable is given. Moreover, the most important ICIC schemes for channel allocation are presented in detail and the related constraints are identified. Based on the limitations studied in this chapter, a distributed algorithm that performs dynamic channel allocation in homogeneous networks is proposed that targets the minimization of the ICI and the network capacity increment. The details of the mathematical framework and the algorithm implementation are presented. The efficiency of the proposed solution in terms of interference reduction and capacity improvement is demonstrated through simulations and comparisons with a traditional frequency allocation scheme. Additional analysis is carried out with respect to the algorithm convergence and the possibility of an online implementation. Furthermore, the algorithm behavior is further studied with respect to variations of different algorithm related parameters and alternative mathematical frameworks. The analysis is focused on the impact they have on the performance of the algorithm in terms of interference mitigation, capacity improvement and algorithm convergence. The proposed solution is extended to heterogeneous networks comprised of macrocells and small cells. Simulation results and comparisons with a reference scheme prove that the proposal introduces significant benefits in the network capacity and mitigates the ICI. Finally, a possible implementation of the proposed scheme based on a concept of a dynamic database known as REM is discussed in the end of the chapter.

Chapter 4 is dedicated on the management of interference under heterogeneous topologies. A brief introduction is given related to the challenges arising in the field of user association and interference management. Possible solutions adopted by the LTE-A framework are presented in detail, while the limitations and constraints are identified and discussed. A novel solution for the management of the available resources is proposed taking into advantage the knowledge acquired during chapter 3. In particular the solution consists of two mechanisms that exploit either the time-frequency domain or the time-power domain depending on the position of the small cells in the network topology with purpose to mitigate the interference seen by the small cells and increase the capacity of the macrocells. Simulations and comparisons with benchmark schemes are presented that show the effectiveness of the proposal in terms of resource utilization, interference reduction and capacity improvement. The proposed solution is

modified and enhanced with target the further improvement of the network performance and the elimination of certain constraints that are identified. The new solution employs only one mechanism that exploits jointly the time, frequency and power dimensions with target to balance more effectively the trade-off between small cell interference mitigation and the capacity degradation on the macrocells. The additional benefits and the overall improvements brought by the scheme are demonstrated through simulations and comparisons with different reference schemes. Finally, the solution is optimized using genetic algorithms that are used to find the most appropriate configuration of parameters related to the partitions on the three dimensions and the user association. Results presented reveal that the optimized scheme presents significant benefits in terms of load balancing, resource utilization and capacity improvement with respect to a fixed configuration and to reference schemes existing in the literature. The results are concluded with an analysis and discussion of the selected configurations.

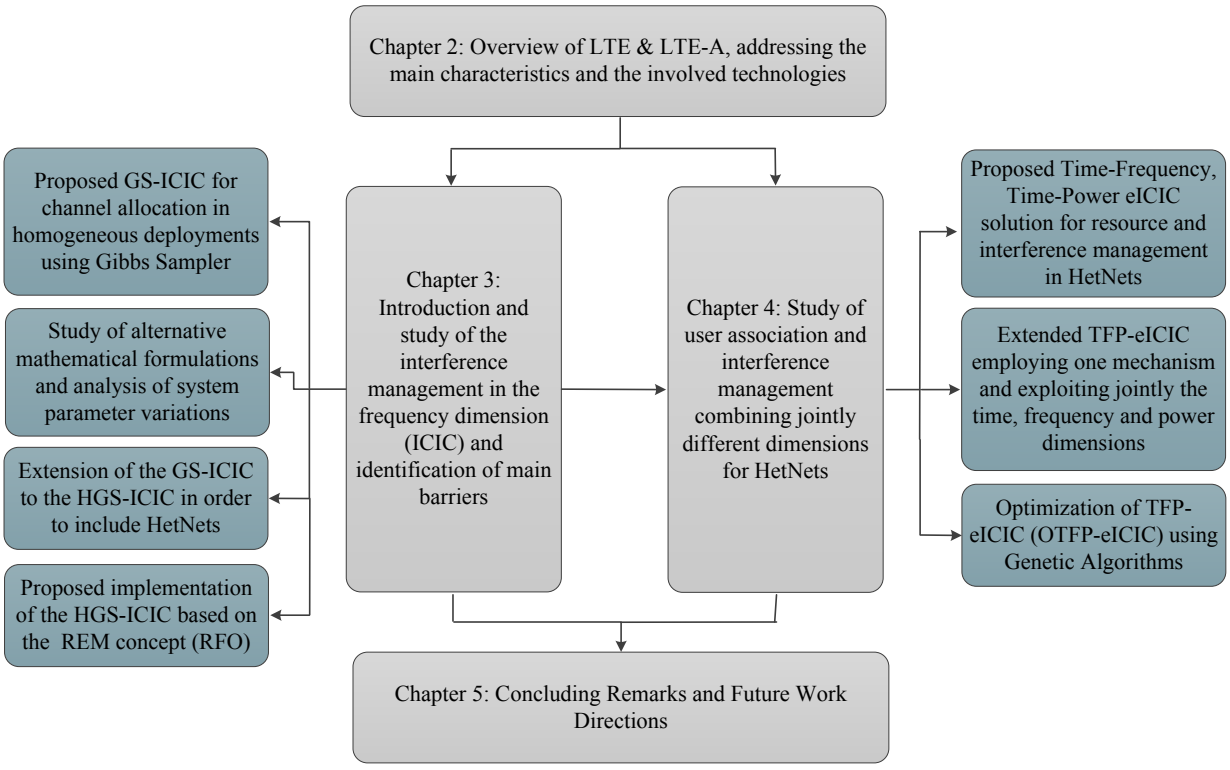

Figure 1: Thesis Structure

Finally, Chapter 5 summarizes the work presented in this PhD thesis and the most important conclusions. In addition, future possible directions are discussed related to the further analysis of the performance of the solutions presented throughout this work, as well as several implementation considerations and the addition of other technologies related to the current 4G and the envisaged 5G networks.

2. Fundamental Concepts

2.1 LTE & LTE-A Overview

Long Term Evolution has been developed by the 3rd Generation Partnership Project (3GPP), which is one of the most prominent Standardization Groups on the field of the mobile communications. Work on the LTE has been going on since 2004 [8] when a number of mobile communication companies presented what they envisioned for the next generation communication systems. The main purpose was to create a new technology that fulfilled a set of requirements, such as higher user data rates, improved spectral efficiency, and seamless mobility. The first complete specification on LTE was released on March 2009 (3GPP-Release 8) [9], while some additional enhancements were added with Release 9 [10].

Despite the potentials of LTE, it did not meet all the requirement specifications envisaged by the ITU IMT-Advanced for the fourth generation cellular systems. As such, 3GPP presented a new release under the name of LTE-Advanced (Release 10) [11], which includes further improvements and enhanced features. Additional features and refinements of the standard were introduced with Release 11 and Release 12, while Release 13 is under development introducing great potentials and opening the way towards the fifth generation (5G) systems. For an overview of the related releases the reader is encouraged to refer to [12]. This chapter addresses the main features of LTE and LTE-A with special focus on the involved technologies adopted by the standards.

2.1.1 Network Architecture Overview

The success of the LTE/LTE-A is based on the evolved technologies that are used, as well as on the design of the network following a fully packet-switched model. In Release 8, two important aspects are specified by 3GPP. These are the Radio Access Network (RAN) known as Evolved-Universal Terrestrial Radio Access Network (E-UTRAN) and the System Architecture Evolution (SAE). The SAE includes the Evolved Packet Core (EPC) network and, together with the E-UTRAN, they comprise the Evolved Packet System (EPS) [10].

In contrast to the previous mobile generations (2G, 3G), EPS is designed to support only packet-based services and is responsible for the seamless connectivity of the users with the external Packet Data Network (PDN). Furthermore, functionalities such as the QoS, security and privacy issues are related to

the elements comprising the network (EPC and E-UTRAN elements). Finally, EPS ensures interoperability among different vendor technologies [13]. Figure 2 gives an overview of the EPS architecture.

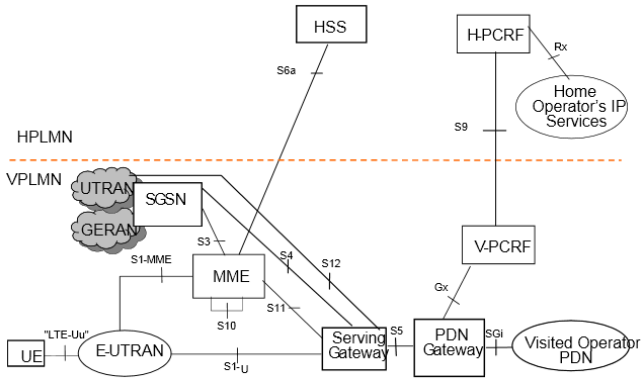

Figure 2: Evolved Packet System (EPS) Overview [9]

The Core Network (EPC) follows a flat IP-based structure that enables reliable and cost-effective transfers of the data-traffic [10][14]. The architecture has been simplified by means of involved nodes and the flexibility of the network has been increased due to the separation of the user plane and the control plane [14]. Moreover, the architecture of the EPC focuses on three main aspects: the mobility, the security and the policy management [15].

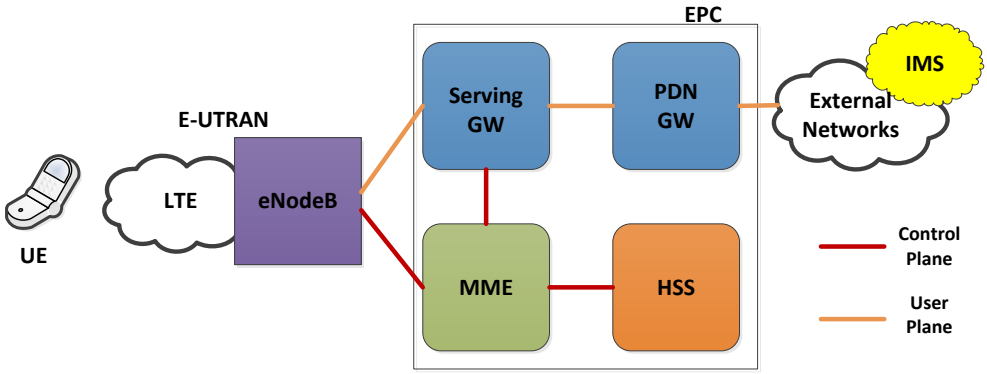

Figure 3: Evolved Packet Core (EPC) architecture

The Core Network, depicted in Figure 3, is comprised by the following elements:

- *The PDN Gateway* (PDN-GW): It serves as the interconnection point between the core network (EPC) and the external network (PDN).
- *The Serving Gateway* (S-GW): It serves as the interface between the core network (EPC) and the radio access network (RAN).

  Both the P-GW and the S-GW manage functionalities related to the user data plane.
- *The Mobility Management Entity* (MME): It is the node that deals with the control plane.

- *The Home Subscriber Server* (HSS): It is a database that holds the user and the subscription information. In addition, it holds information related to security, user authentication and mobility and session management.

The Evolved - Universal Terrestrial Radio Access Network (E-UTRAN) provides the connection of the users with the Core Network [16]. In contrast to the previous technologies, the E-UTRAN does not include a centralized Radio Network Controller (RNC) and is comprised only of a number of Base Stations known as evolved NodeBs (eNodeB). The communication between the eNodeB and the core network takes place through the S1 interface, while the eNodeBs are physically interconnected through the X2 interface (Figure 4) [8]. The X2 interface allows the hand-over between the eNodeBs in a direct manner achieving in this way, faster transitions.

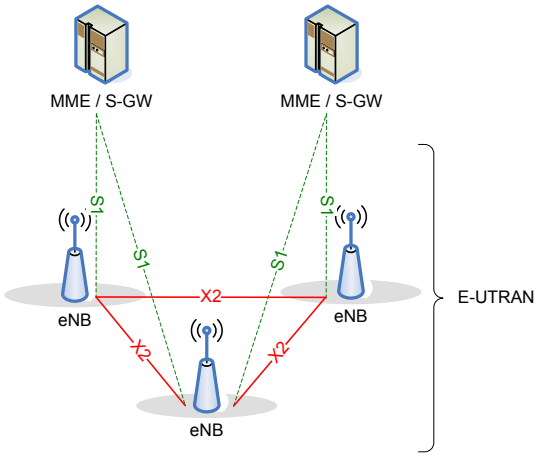

Figure 4: E-UTRAN [17]

The E-UTRAN protocol stack, hosted by the eNodeB, includes the Medium Access Control (MAC), the Radio Link Control (RLC) and the Packet Data Convergence Protocol (PDCP) [10]. The eNodeB is also responsible for a number of radio related functions. Examples include Radio Resource Management (RRM), Connection Mobility control, Dynamic Resource Allocation, routing of the user data traffic towards the S-GW, hand-over management, header compression and encryption of the user data (measurements) [17].

One of the key characteristics of the LTE/LTE-A Access Network is the use of the Orthogonal Frequency Division Multiplex (OFDM) as transmission scheme and the associated multiple access schemes for the downlink and uplink, Orthogonal Frequency Division Multiple Access (OFDMA) and Single Carrier - Frequency Division Multiple Access (SC-FDMA), respectively. The main reason for adopting the OFDM scheme is the improvement of the spectral efficiency. A detailed description of the radio access scheme is given in the section that follows.

2.1.2 OFDM

LTE has adopted Orthogonal Frequency Division Multiplexing (OFDM) as radio access technology, due to the advantages it offers that meet the 4G requirements. OFDM is based on a multicarrier transmission as shown in Figure 5. This means that the available bandwidth is divided into several narrowband sub-channels (sub-carriers), which are overlapping but they are orthogonal to each other (using the Inverse Fast Fourier Transform - IFFT) [10]. The data is transmitted in parallel with lower rates using these sub-carriers. This implies that the channel for each sub-carrier can be considered as flat fading, resulting in this way in a significant reduction of the Inter-Symbol Interference (ISI). On the receiver side this implies that the signals can be easily separated without imposing the need for guard bands [18][19]. As such, OFDM presents high spectral efficiency and allows a low-complexity implementation of the receivers.

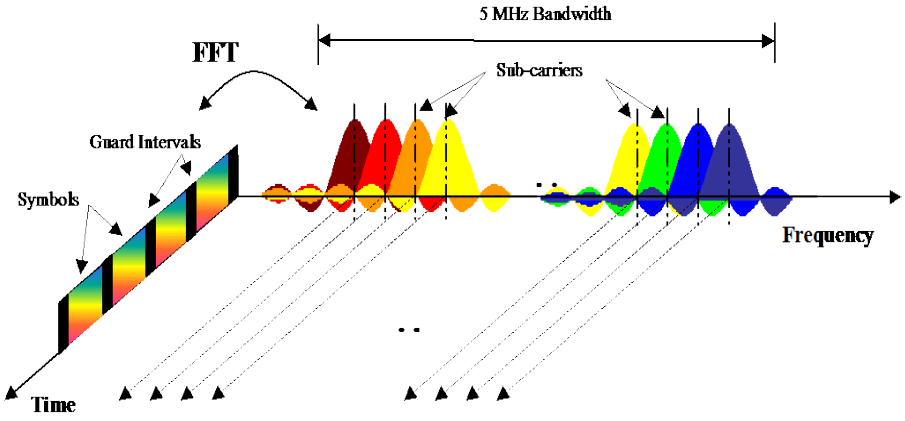

Figure 5: OFDM Sub-carriers [20]

Moreover, OFDM is considered an attractive modulation technology because it is robust to the frequency selective fading thanks to the high symbol duration it offers, which when combined with a Cyclic Prefix (CP), results in the complete elimination of the ISI and of the Inter-Carrier Interference. The CP is simply a duplication of the last part of the signal, which is added in the beginning of the OFDM symbol and as long as it is longer than the channel delay spread, the ISI is negligible [21]. In addition, CP plays significant role in the maintenance of the orthogonality between the sub-carriers. As such, the equalization needed to recover the data is substantially simplified because frequency domain equalizers can be used [19][22].

Finally, the incorporation of channel coding and interleaving techniques provides robustness against the frequency selective fading and allows the data retrieval in cases of erroneous transmissions [10][23].

2.1.3 Multiple Access Schemes

In order to achieve higher capacities, Multiple Access techniques are used to share the available spectrum among a set of users. As such, the users are permitted to transmit their information simultaneously without interfering with each other. OFDM can be combined with a variety of Multiple Access schemes such as FDMA and TDMA. In LTE and LTE-A, two schemes have been adopted, the Orthogonal Frequency Division Multiple Access (OFDMA) and the Single Carrier Frequency Division Multiple Access (SC-FDMA) for the downlink and the uplink, respectively [8].

2.1.3.1 OFDMA

OFDMA is a Multiple Access technique based on OFDM that allows the sub-carriers to be shared among multiple users for simultaneous transmissions [10]. Each sub-carrier is used to carry the data symbol of one user. Since the sub-carriers are orthogonal to each other, the Multiple Access Interference (MAI) is not a subject of concern. As such, the spectral efficiency is significantly improved and therefore OFDMA is a technique that satisfies the LTE requirements. Moreover, OFDMA allows the exploitation of dynamic frequency allocation techniques, which provide flexibility in the management of the available resources and further increase the spectral efficiency of the system [24]. Another characteristic of OFDMA is the support of different modulation schemes (e.g. QAM) and variable user data rates according to the QoS requirements or the channel conditions [19][25]. Furthermore, as in OFDM, with the insertion of the CP OFDMA is robust against the ISI that arises from the multipath propagation and the channel distortion can be easily compensated with simple equalization techniques [24][26]. Finally, OFDMA is a very attractive scheme because it requires low-complexity implementation. More particularly, thanks to the evolution of the Digital Signal Processors (DSPs), the IFFT/FFT processes required in transmission/reception can be implemented easily and in a cost-effective way [25][26].

2.1.3.2 SC-FDMA

The uplink transmissions differ from the downlink with respect to the user equipment requirements. In order to have a successful technology, the performance of the user equipment needs to be improved; that is power-efficient devices are needed, yet with simple design and low-cost implementation. SC-FDMA is a Multiple Access scheme that combines the advantages of a single carrier (SC) transmission with these of OFDMA, constituting in this way the most appropriate technology for the LTE uplink. In particular, SC-FDMA offers high data rates, robustness against multipath propagation, and allows the exploitation of dynamic resource allocation [27].

From implementation perspective, SC-FDMA can be seen as a modified form of OFDMA with main difference the addition of a precoding scheme carried out with the use of the Discrete Fourier Transform (DFT) before the standard OFDM process. Similarly to OFDMA, SC-FDMA divides the available spectrum in multiple sub-carriers which are orthogonal to each other, and the orthogonality is maintained with the addition of the CP [10].

2.1.4 MIMO

Multiple Input Multiple Output (MIMO) is a technology that makes use of multiple antennas and is adopted by LTE in order to achieve higher spectral efficiency and higher data rates. MIMO in combination with OFDM offers several advantages over traditional technologies [21]. The main functionality of MIMO is the division of the data stream into multiple data streams in order to be transmitted by the multiple antennas, taking advantage of the decorrelation existing between multipath transmissions.

The key MIMO features that are exploited in LTE are the *spatial multiplexing* and the *diversity*.

The *spatial multiplexing* results from exploiting the effects of multipath propagation to perform multiple parallel transmissions. The data stream is divided into multiple data streams in order to be simultaneously transmitted by the multiple antennas. On the receiver side, the streams are separated according to their spatial signatures. This allows the system capacity to be significantly enhanced without imposing the need for additional bandwidth usage [28][29]. However, it has to be noted that this technique requires good channel conditions and complex signal processing [10].

The *diversity* is a technique with which the multipath fading and the ISI are minimized in the cases where the user experiences lower SINR (Signal to Noise and Interference Ratio). Reception diversity is achieved when the same signal is received from multiple antennas, thus travelling through independently fading paths. The receiver then combines the independently fading copies of the signal avoiding this way erroneous receptions [30][31]. In this way, the receiver can operate with lower SINR conditions, thus resulting in a diversity gain. A similar effect can be achieved with diversity at the transmission side (i.e. transmitting replicas of the same signal through different antennas, with the appropriate weights and obtaining the combined signal at the receiver).

2.1.5 Radio Resource Management

Mobile communication systems are challenged by the constant change of the network conditions, such as propagation conditions, user mobility, traffic conditions and the interference levels. As such, the management of the network should be characterized by flexibility, and thus to be able to adapt itself

according to the network evolution. Radio Resource Management (RRM) techniques allow the system to adapt to variations of the network environment by controlling the use of the available resources. The main purpose is to satisfy each time the performance targets by dynamically changing the system parameters in order to optimize the network efficiency and provide better services. Frequency allocation, transmission power and coding schemes are some examples of the parameters that can be adapted in order to meet QoS requirements, enhance the cell coverage and improve the overall network capacity [26][32].

In LTE, the main functions of RRM are specified [33], however without specifying the algorithms and strategies to be adopted. As such, LTE provides the manufacturers and the operators with a degree of freedom to use the RRM functions according to the different design issues of the particular networks. Due to the lack of specification, a large amount of RRM algorithms has been presented in the literature; however they all can be classified in different categories according to the general aspects they serve. Some examples are presented below:

- *Radio Admission Control*: It handles the connection requests according to the availability of the resources and the network load. A connection may be established if the QoS requirements are satisfied, provided that the already established connections are not affected; otherwise it is rejected [32].
- *Dynamic Packet Scheduling*: This function is responsible for the allocation of resources to the users in the short term so that they will be able to carry out their transmissions. The operation of the packet scheduling will take into account the QoS requirements, channel conditions, interference levels and the buffer status [34].
- *Power Control*: It adapts the transmit power levels with main purpose to ensure that certain SINR criteria are met, while taking under consideration the overall interference and the battery life constraints of the user equipment [26]. It may take place either on the eNodeB or the user side.
- *Inter-Cell Interference Coordination (ICIC)*: These techniques are used in LTE in order to mitigate the ICI. Adjacent cells can cooperate, in order to avoid for example the same resource usage, by exchanging information related to the resources they occupy and the traffic load conditions [26]. This thesis deals with ICIC techniques and the accompanied issues, therefore a thorough description will be given in chapter 3. Moreover, it has to be referred that in LTE-A eICIC techniques are adopted, which are presented in detailed in chapter 4.

The above presented technologies are part of both LTE and LTE-A systems. However, in LTE-A new and improved features are adopted with target to fulfil all the requirements imposed by the ITU for a truly

4G system. As such, LTE-A is not a new technology, but it can be considered as an overhaul of LTE. Carrier Aggregation (CA), enhanced use of multi-antenna techniques, Coordinated multipoint transmission and reception (CoMP) and support for Relay Nodes (RN) and HetNets are the main concepts added to the standard aiming to provide higher data rates (up to 100 Mbps for high and 1Gbps for low mobility), enhanced coverage, improved spectral efficiency, reduced latencies, and all this with lower deployment cost and cost per megabyte [35][36]. The rest of this section gives a brief description of the main characteristics of these concepts.

2.1.6 Carrier Aggregation

One of the main requirements that the IMT-Advanced has issued is the support of higher data rates. This goal may be achieved by increasing the transmission bandwidth, which as envisioned by the IMT-Advanced may reach the 100 MHz [37]. However, since the contiguous spectrum is scarce and in order to ensure backward compatibility with LTE, LTE-A has incorporated as key technology the logical concatenation of single carriers through Carrier Aggregation (CA) [36]. The concept behind CA is the aggregation of contiguous or non-contiguous single carriers (up to 5 for LTE-A) in order to virtually create wider transmission bandwidths, enabling in this way higher data rates and throughputs [38].

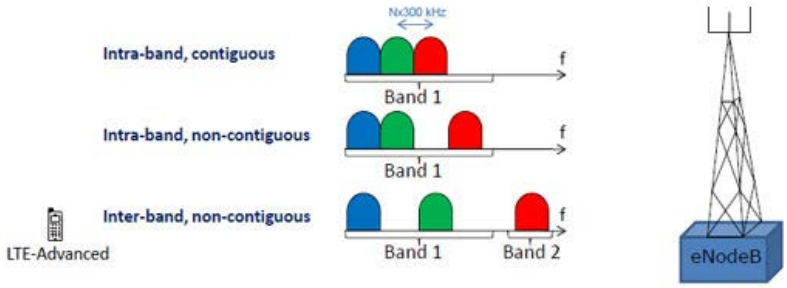

Figure 6: Carrier Aggregation Types [36]

In the 3GPP context, the single carriers are referred to as *component carriers*. Three different types of CA are identified, depending on the type of the carriers used (Figure 6). These would be:

- ✓ Intra-Band Contiguous CA: It is considered to be the simplest form of aggregation since the component carriers belong to the same frequency band and are adjacent to each other. However finding contiguous spectrum is not always possible.
- ✓ Intra-Band Non-Contiguous CA: In this case the component carriers belong to the same frequency band, but they are not adjacent. This introduces a degree of complexity, especially

when considering the user equipment side, for which space, power and cost are of great importance [39].

- ✓ Inter-Band Non-Contiguous CA: It is the most complex form of CA because the component carriers belong to different frequency bands and hence it requires multiple transceivers. Apart from the increased complexity and the higher cost, additional problems can be introduced due to the multiple transceivers, such as the inter-modulation and cross modulation among the transceivers [39].

2.1.7 MIMO and CoMP

One of the main differences of LTE-A and LTE is the number of the antennas that the base stations and the user terminals will be equipped with, in order to further improve the spectral efficiency and allow higher data rates. In LTE-A, higher order MIMO are employed; the downlink (DL) is envisioned to support spatial multiplexing configurations of up to 8x8, while in the uplink (UL), the user terminals will support up to 4 transmitters, thus up to 4x4 transmissions will be possible [40]. Moreover, the number of the employed transmission modes is enhanced in order to support the additional introduced configurations. Several techniques have been added to the standard, such as advanced MU-MIMO beamforming, in order to improve the performance in terms of spectral efficiency and average throughput.

Coordinated multipoint transmission and reception (CoMP) is also introduced in order to allow higher cell throughputs and improve the cell edge performances. CoMP is a set of several techniques that can exploit the MIMO antennas in order to enhance the transmission/reception of signals by the edge users and the eNodeBs. Let us consider for example a user located in the cell edge and that is prepared for handover. At this moment the user will be able to communicate with two or more geographically spaced eNodeBs. Through coordination between these base stations (BSs), it is possible to schedule transmissions/receptions in order to serve the same user. As such, CoMP can be characterized as a distributed MIMO system that improves the signal quality and minimizes the co-channel interference [41]. However CoMP has also raised some controversy: In fact, in [6] it is claimed that in practice, taking into account all the needed realism, no gain at all is perceived.

2.1.8 Relay Nodes

Despite of the significant improvement in terms of throughput and capacity with the use of MIMO, OFDMA and other techniques, the cell edge users may still suffer from low data rates. In order to further

increase the performance when needed, LTE-A exploits the concept of Relay Nodes (RN). RNs are low power small cells that are easy to deploy and can extend the cell coverage in a cost effective way since they don't require a fixed backhaul connection.

The RN is wirelessly connected to a donor eNodeB through the Un interface. Its main responsibility is to relay the data between a user and the base station in a multi-hop manner, similarly to a repeater. However, RNs differ from repeaters because they also support functionalities as demodulation and decoding of the relayed data and error correction in addition to the signal retransmission. As such, the signal quality is not degraded, but instead it is improved [42].

2.2 Heterogeneous Networks ("HetNets")

Current cellular networks, including LTE, follow usually homogeneous deployments of macro cellular architecture, with some micro or pico cells deployed under special situations (e.g. traffic hotspots, etc.). The base stations work under similar characteristics, such as transmit powers, antenna patterns, number of serving users and backhaul connections. Thus, in order to provide good coverage, while minimizing interference, a sophisticated network planning is necessary [43]. However, with the exponentially growth of the data demand, cell splitting, additional bandwidth and new macrocell deployments are necessary to fulfill the needs in terms of coverage, capacity and high data rates. Moreover, it is very common that the data traffic is presented in hotspots; that is for example in stadiums hosting big events or campuses. The traditional acquisition of macrocell sites, not only is costly, but in addition it cannot adapt to the uneven user allocation and traffic demand [2]. In addition, cell splitting is complex and the usage of more frequencies is widely known that is infeasible due to the scarce nature of the radio spectrum [43].

Standardization Bodies have turned in alternative cost-effective solutions that will allow the further improvement of the network performance by deploying more advanced network topologies, known as Heterogeneous Networks (Figure 7). The HetNets include the addition of smaller low power cell sites, such as pico and/or femto cells throughout the macrocell sites, and they also involve the combination of different radio access technologies, such as WiFi and HSPA. HetNets are envisioned to be the future in wireless communications since they allow flexible cost-effective deployments in order to provide additional coverage in areas that cannot be covered by the macrocells and enhance the capacity in hotspots [2].

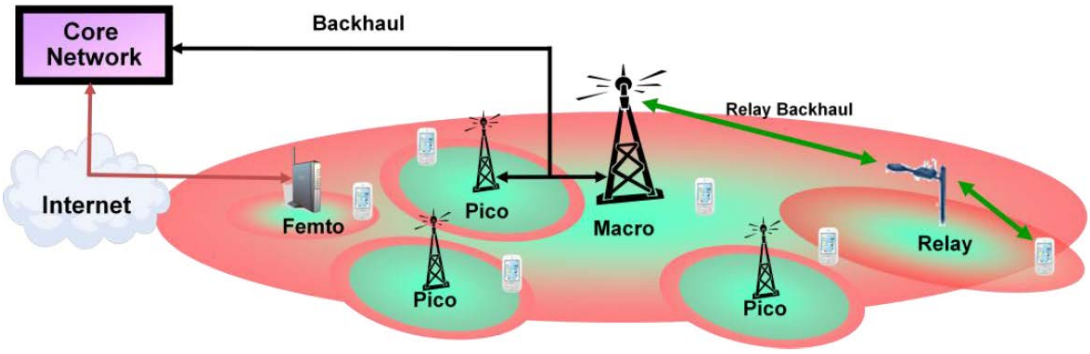

Figure 7: HetNet Topology Example [43]

According to [2], the addition of low power small cells in a traditional cellular network enhances significantly the performance of the network, while offering improved coverage. Figure 8 presents the gain in the spectral density depending on the network topology. As it can be observed, the gain is tremendously increased as cells of smaller radius are used to serve the data traffic.

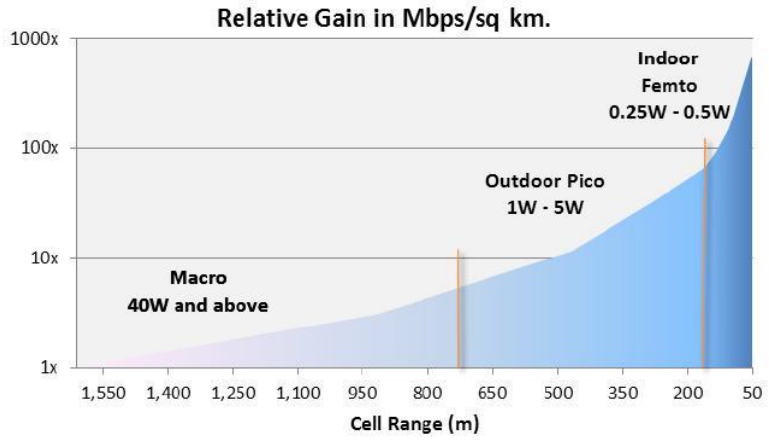

Figure 8: Spectral Density Gain with respect to the network topology [2]

Moreover, simulation results conducted by 3GPP [44] have shown that with the deployment of HetNets a macrocell can provide higher capacities since the number of the users it serves is decreased (less users share the same capacity), thus allowing higher data rate transmissions. In addition, the users that are served by the small cells (pico/femto) experience high quality transmissions with higher data rates and due to the low power transmissions the battery life of the terminals is significantly extended.

2.2.1 Network Overview

For the formation of a HetNet a variety of low power small cells is used, in order to off-load the macrocell when necessary and to provide better user experience. These low power cells are classified

according to their different characteristics, such as the size and the transmit power, and they are the pico cells, the femto cells and the relay nodes. In 2.1.8, an overview of the relay nodes has been given, therefore more details about the characteristics of the pico and femto cells are presented in this section.

Pico cells follow the same concept as the eNodeBs; however they utilize lower transmission powers and they cover smaller areas. Moreover, they cannot be equipped with sectorized antennas (only omni-directional). Their deployment is carried out in an operator planned manner in order to serve indoor or outdoor applications. Depending on the deployment, the transmit power may vary between 250mW and 2W for outdoor and up to 100 mW for indoor scenarios [45]. The connection to the core network is carried similarly as with the eNodeBs, therefore pico cells can make use of the X2 interface and benefit from the ICIC techniques.

Femto cells on the other hand, are intended to serve only indoor scenarios. They employ only omni-directional antennas and their transmit power does not exceed the 100 mW. Due to the low transmit power the interference is kept in low levels. In addition, since femto cells offer small coverage, the distance between the user and the femto cell is quite low providing in this way better signal quality [46]. The installation usually is carried out by the consumers in an unplanned manner, thus operators may not be aware of the changes that may occur to the network structure and this becomes one of the greatest challenges for the interference management. Moreover, femto cells are not connected to the backhaul of the cellular network; instead they utilize the DSL connection or the cable modem of the subscriber. With that approach however, the X2 interface is not accessible, thus ICIC techniques are more difficult to be implemented. In order to mitigate the femto related interference alternative techniques are studied (e.g. [47]). Finally, femto cells can operate in two manners, open and closed. In the closed mode (CSG), only a specific group of users is allowed to access the network, which is defined by the subscriber who installed the femto cell. In the open mode (OSG), the femto cell can be accessed by all the users [43].

2.2.2 HetNets Challenges

In addition to the small cells, a HetNet may include the combination of different radio access technologies, such as HSPA, UMTS, EDGE, WiMax and WiFi in order to offload the highly congested network and boost performances whenever this is feasible. As such, despite the attractive features of the HetNets, several challenges are imposed due to the co-existence of such diversity of technologies. These issues include the necessity for new metrics in order to accurately evaluate the performance of the HetNet network. The outage probability distribution and the area spectral efficiency are considered to be two prevalent metrics. Moreover, the way the network topology used to be modeled has to be changed since

the deployment of the small nodes usually takes place in areas under the coverage footprint of a macrocell and does not follow a regular rule. In addition to this, due to the disparity among the transmit powers the coverage area of each node differs substantially. However, the same does not apply for the uplink (users transmit with the same power), thus dissimilarities in the SINR of the DL and UL may occur. As such, the option that a user may be connected with different cells during the DL and the UL transmissions should also be taken into account. This will imply that the interference for a given user will require different models in the DL and in the UL. Furthermore, the way the users are associated to each cell needs to follow other criteria than these used in traditional macro cellular networks. Similarly, for the user mobility alternative solutions should be considered. The handoff decisions should be based on different parameters, such as the speed of the user (if a user travels too fast it would be suboptimal to perform several handoffs between small cells and macrocells) and the overall interference. Finally, intelligent resource and interference management techniques are necessary to cope with the above issues and to increase network performance. This work deals with the user association and the interference management in HetNets, thus a thorough description will be given in chapter 4. However, for more details on the challenges imposed by HetNets the reader is encouraged to refer to [6].

3. Interference Management in the Frequency Dimension

3.1 Inter-Cell Interference Management

Two types of interference are mainly distinguished, the intra-cell interference that occurs among users of the same cell and the inter-cell interference (ICI) that occurs when adjacent cells utilize the same frequencies. LTE and LTE-A are "immune" to the intra-cell interference thanks to the use of OFDM, which guarantees orthogonality among the users of the same cell. The ICI however, remains a challenge that limits the system performance in terms of capacity especially for the edge users, since these users are more susceptible to ICI. Among others, one method that substantially reduces ICI is to apply frequency reuse, meaning that adjacent cells utilize different frequencies; however on the cost of spectrum underutilization. For this reason, 4G systems employ ICI coordination (ICIC) techniques that are based on the frequency reuse, although only for a portion of the users. In particular, the edge users are assigned the resources with higher reuse factors compared to the users located at the cell-center, so that an effective reuse factor which is slighter greater than 1 is obtained, thus contributing to the mitigation of the ICI while utilizing the resources more efficiently [48]. This concept is generally called Fractional Frequency Reuse (FFR) [7][49] and is presented more detailed in the following section.

3.1.1 Fractional Frequency Reuse (FFR)

The concept of FFR has been initially presented for the GSM network [49], and later on it has been adopted by the 4G systems [7] since the flexibility of the frequency allocation provided by the OFDM makes its implementation quite easy. FFR is a low complexity technique that is based on the division of the cell area in two regions, the inner and the outer. Users in the inner part are located closer to the base station than users in the outer part and consequently, they are more protected against inter-cell interference. The classification of the users between inner/outer can be carried out based on their location, path loss or SINR metrics. Furthermore, the available bandwidth is partitioned in two groups, the inner and the outer. The outer group consists of the set of sub-bands that can be assigned to the outer users with reuse factors greater than 1, while the inner includes the frequencies that can be assigned to the inner users with reuse

factor equal to 1 (Full Reuse). Several FFR variants have been presented in the literature, with the most prominent being the Soft Frequency Reuse (SFR) [50] and the Partial Frequency Reuse (PFR) [51][52]. A brief description of the main idea behind these techniques is given in the following.

- *Soft Frequency Reuse (SFR)*

SFR is a variation of FFR that targets the efficient bandwidth utilization. The main characteristic of the SFR scheme is that the whole bandwidth is available to all the cells; however each cell can transmit in different frequencies with different powers [53], as shown in Figure 9.

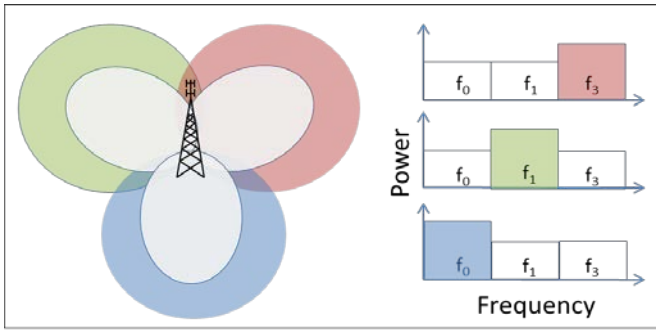

Figure 9: Soft Frequency Reuse

As it can be seen from the figure, the outer users are allowed to utilize only part of the spectrum with a reuse factor greater than 1 (equal to 3 in the example), while the inner users may also have access to the frequencies reserved for the outer users of the adjacent cells. This forces the restriction of the transmit powers of the inner parts to lower levels than the outer parts in order to reduce the interference of the network.

Compared to other FFR schemes, with this technique it is possible to achieve higher data rates for the inner users, while the outer users do not suffer from high interference. With this approach, the spectrum efficiency can be significantly improved, although outer users still experience some interference from the inner part of other cells. Finally, it has to be referred that the transmit powers can be adjusted according to the desired reuse factor [50].

- *Partial Frequency Reuse (PFR)*

Another variant of FFR is the Partial Frequency Reuse (PFR), which is a reuse scheme that focuses on the reduction of the ICI by splitting the cell in two parts, the inner and the outer. Moreover, the available bandwidth is divided into the inner band which is assigned with a reuse-1 factor and which is common to all the cells, and the outer band which is assigned with a higher reuse factor (Partial Reuse). As such, the

users located in the inner part utilize a common frequency, while the outer users benefit from the allocation of non-overlapping frequency sub-bands. The advantage of this strategy is the mitigation of the interference experienced by the outer users of the cell since neighboring cells utilize different frequency sub-bands (which are orthogonal to each other due to OFDMA), while keeping the interference experienced by the inner users in low levels [53].

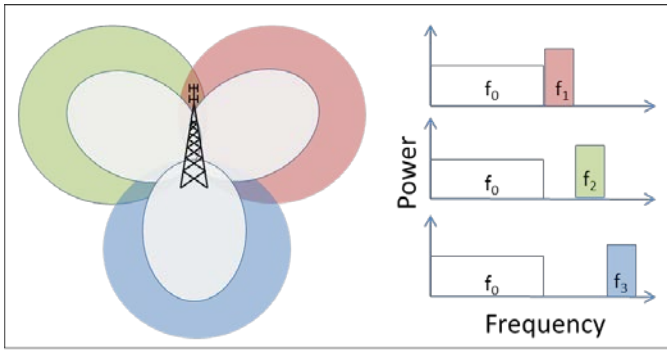

Figure 10: Partial Frequency Reuse

In Figure 10, an example of the PFR technique is presented, which allocates the inner band with reuse factor 1 and the outer with reuse factor 3. If we consider that the total bandwidth *BW* is divided in the inner part BW_1 and the outer BW_2, then the effective frequency reuse factor will be $BW/(BW_1 + BW_2/3)$ [48]. Moreover, similar to SFR, the transmit power between the outer and the inner part may differ.

3.1.2 Problem Identification and Literature Review

Despite the fact that the above presented ICIC schemes introduce improvements in terms of spectral efficiency and interference reduction, if the allocation of the resources remains static they wouldn't be able to adapt to the network changes, such as in spatial traffic loads that vary over time. Moreover, in heterogeneous deployments such static patterns may result sub-optimal. The dynamic allocation allows higher performances to be achieved. As such, research has been focused on dynamic ICIC techniques. A Dynamic Fractional Frequency Reuse (D-FFR) scheme has been presented in [54], where the resources are re-allocated depending on cell load variations. The proposed scheme has been carried out using a graph-based framework. It has been shown through simulations that the proposed solution presents throughput and data rate improvement in scenarios with un-equal cell loads. In [55], the authors presented a dynamic Soft Frequency Reuse (ND-SFR) scheme that mainly deals with uneven traffic loads. Two algorithms are used, one for resource allocation and another one for power control, which significantly improved the network capacity and the energy efficiency. In [56], an Adaptive Partial Frequency Reuse (APFR) scheme

has been developed based on an off-line genetic algorithm. Through simulations, it has been demonstrated that the proposed solution outperforms the classical PFR scheme in terms of edge user throughput.

Based on the above, a novel ICIC scheme that allocates the available frequencies (channels) in a dynamic manner is presented in this chapter. Initial work targets the mitigation of the ICI and the capacity improvement in homogeneous networks, while later on the work is extended to heterogeneous deployments that consist in macrocells and small cells. On the contrary to other solutions (e.g. [56]) the proposed scheme is based on a distributed algorithm, which as it will be demonstrated in the following offers the possibility of an online implementation.

3.2 Gibbs Sampler-based ICIC (GS-ICIC)

Under the previously presented framework, a dynamic ICIC scheme for frequency allocation has been developed throughout this work and presented in [57]. The solution targets the minimization of the downlink ICI in PFR deployments and is based on the Gibbs Sampler [58][59] algorithm as optimization tool. In particular, the algorithms' target is to find the most appropriate allocation of the available resources in a distributed manner so that the network interference is minimized. Before proceeding to more details about the implementation of the scheme, the basic theory behind the Gibbs distributions and the Gibbs Sampler will be presented first.

3.2.1 Markov Random Fields and Gibbs Distributions

Probabilistic approaches are considered as useful tools for the estimation of parameters or random variables based on probability distributions that involve the variability of the random variables and their interaction with other random variables of the structure (known as *neighbors*). A key concept lies on the fact that when specifying joint distributions based on local interactions, a global model can be considered. As such, for solving a problem one can target two things; sampling the variables from the joint distribution or some form of conditional distribution and maximizing some form of distribution [60].

Based on the above, let us consider a finite set S of cardinality H that consists of elements that are called *sites*. The sites in this context can be thought as the network cells. Moreover let us consider that $s=1,2,\ldots H$ and $S=\{1,2,\ldots,H\}$. Then, at each site there will be a random variable X_s that takes values from the *phase space* for the sites $s \in S$ denoted as Λ. The collection (or vector) $X=\{X_s\}_{s \in S}$ of random variables

is a *random field* on S, while a realization of the field $x=\{x_s, s\in S\}$ is called a *configuration* and the *configuration space* is denoted as Λ_s. The objective of the problem is to find the adequate configuration of each site.

Two sites can be related to each other and therefore be neighbors. $N_s \subset S$ corresponds to the *neighborhood* of s, while a *neighborhood system* on S is a collection $N=\{N_s\}_{s\in S}$ of subsets of S such that satisfies two conditions: 1. a site is not a neighbor of itself and 2. two sites are mutually considered neighbors to each other. These conditions are expressed as follows:

$$\forall s \in S \begin{cases} s \notin N_s \\ t \in N_s \Rightarrow s \in N_t \end{cases} \tag{1}$$

Then, the above can be interpreted in graphs topology, where S corresponds to the vertices of the graph and N to the edges. Therefore, it can be said that the *sites* s and t can be considered as neighbors only when they are connected with an edge. Then, a set $\mathcal{C} \subset S$ is said to be a *clique* if all of its sites are neighbors with each other.

The random field X is said to be a Markov Random Field (MRF) with respect to the neighborhood system N if $\forall s \in S$:

$$P(X_s = x_s \mid X_{S\setminus s} = x_{S\setminus s} = P(X_s = x_s \mid X_{Ns} = x_{Ns}) \tag{2}$$

implying that the distribution of X_s depends directly on the distributions of its neighbors.

With the proper definition of the neighborhood system, any random field can be handled as a MRF. However, as with MRFs the construction of the global distribution is not always straightforward, Gibbs distributions are needed.

For the Gibbs distributions the concept of cliques and potentials is of a great importance. Previously, the notion of cliques has been presented; therefore let us focus on the potentials:

A Gibbs potential on Λ_s is a collection of functions $\{V_O\}_{o\in \mathcal{C}}$ such that:

1. $V_O(x) \equiv 0$ if O is not a clique
2. $\forall x, x' \in \Lambda_s$ and $o \in \mathcal{C}$,

$$x(O) = x'(O) \Rightarrow V_O(x) = V_O(x') \tag{3}$$

As it can be observed, $V_O(x)$ depends only on the configurations of the elements of the clique $\mathcal{C}$.

Moreover, let us define as ε the *energy function* that derives from the potential $\{V_O\}_{o\in\mathcal{C}}$:

$$\varepsilon(x)=\sum_{O\in\mathcal{C}}V_O(x) \tag{4}$$

With all the above, a Gibbs distribution is defined as:

$$\pi(x)=\frac{1}{z_T}e^{-\frac{1}{T}\varepsilon(x)} \tag{5}$$

and the random field X is said to be a Gibbs Random Field (GRF) if and only if it follows the Gibbs distribution.

In (5) T is the *temperature* parameter, $\varepsilon(x)$ is the *energy* of the configuration x and Z_T is the normalization constant also known as the *partition function*. More details about the MRF and the Gibbs distributions can be found in [58][59] and [61].

In the following subsections all the above general concepts are particularized for the ICIC problem considered here.

3.2.2 Gibbs Sampler-based Optimization Model

Gibbs Sampler based solutions have been presented in the literature in a variety of subjects including the optimization of problems related to channel allocation, as well as power management and user association. In [62], the authors proposed a set of distributed algorithms for unmanaged WiFi networks that are based on Gibbs Sampler. The algorithms perform channel allocation and user association with target the minimization of the interference and the fair sharing of the bandwidth, respectively. In [63], the Gibbs Sampler concept is exploited by the authors with target the joint and separate optimization of the transmit power and user association in homogeneous cellular networks. A joint optimization of the channel allocation, power control and user association for heterogeneous networks that is based on the Gibbs Sampler is presented in [64].

More details about the optimization algorithm for channel allocation in PFR deployments are given in the following sections, although before proceeding to this the system model used for the development of the scheme will be presented.

3.2.2.1 System Model and Notation

For the development of the Gibbs Sampler based ICIC scheme we consider an undirected graph where each vertex (site) corresponds to a base station (BS). If two sites are within communication range of each other, they are considered as neighbors. Each BS is spatially divided with the use of directional antennas in three sectors (cells), resulting in a set of X cells. A set of users is randomly distributed in the scenario and denoted as U, while the subset of users that are associated to BS $x \in X$ is denoted as $u_x \in U_x \subseteq U$. The association process is carried out according to the minimum experienced path loss, as described by the following equation:

$$L_{u,x}(dB) = l_A + l_B \log d(km) - B(\phi,\theta) + S \tag{6}$$

where d is the distance between user u and cell x, l_A and l_B are parameters of the propagation model that depend on the considered environment, S is a Gaussian random variable representing the Log-Normal Shadowing and $B(\phi,\theta) = B_H(\phi) + B_V(\theta)$ is the antenna pattern calculated using the following formulas in dB [65]:

$$B_H(\phi_{u,x}) = -min\left(B_o, 12 \cdot \left(\frac{\phi_{u,x} - \Phi}{\Delta_\phi} \right)^2 \right) \tag{7}$$

$$B_V(\theta_{u,x}) = -min\left(B_o, 12 \cdot \left(\frac{\theta_{u,x} - \Theta}{\Delta_\theta} \right)^2 \right) \tag{8}$$

where $\phi_{u,x}$ and $\theta_{u,x}$ are the azimuth and elevation angles, respectively between user u and cell x. Moreover, Φ and Θ are the azimuth and downtilt orientations of the antennas, respectively, Δ_ϕ is the horizontal antenna beam width, Δ_θ is the vertical antenna beam width and B_o is the backward attenuation.

Furthermore, as it has presented in the theory behind the PFR, the users of a cell are classified into inner and outer. The criterion used for the classification in this case is based on a path loss threshold, defined as:

$$L_{th}(dB) = l_A + l_B \log R_{in}(km) \tag{9}$$

where R_{in} is the radius of the inner part of the cell. As such, if the path loss $L_{u,x}$ of user u_x is below the threshold L_{th}, the user is considered as inner, otherwise as outer. With this classification two more subsets are defined; the subset of the inner users $U_{x,in} \subseteq U$ and the subset of the outer users $U_{x,out} \subseteq U$. It has to be noted that since the shadowing is included in the path loss calculations, the classification of the users is

carried out not only based on the distance of the user from the BS, but also by taking into account the randomness in the propagation that reflects real wireless scenarios.

Additionally, the total band is split into segments denoted as *channels*. Following the Gibbs terminology, the set of channels C corresponds to the set of states. As such, each cell is characterized by its state (c). The bandwidth of each channel c is B_c. In the current implementation we assume for simplicity reasons that each cell can be assigned only one channel for the inner and one for the outer part, although it can be easily modified in order to include a set of channels for each cell. Therefore, at any instance each cell x can be characterized by the state $c_x=(c_{x,in},c_{x,out})$ that is represented by the configuration of the inner $c_{x,in}\in C$ and outer $c_{x,out}\in C$ channels. Moreover, the transmit power for the inner and the outer part of each cell x in channel c is described as:

$$P_{x,c}=\begin{cases} P_{x,out} & \text{if } c=c_{x,out} \\ P_{x,in} & \text{if } c=c_{x,in} \text{ and } c_{x,in}\neq c_{x,out} \\ 0 & otherwise \end{cases} \tag{10}$$

where $P_{x,in}$ and $P_{x,out}$ are the transmit power in (W) of cell x for the inner and the outer parts, respectively. Note that the last expression (10) assumes the more general case in which it may be allowed that the channels $c_{x,in}$ and $c_{x,out}$ may be the same. In this respect, different possibilities about making or not this consideration will be analyzed later on.

With all the above, the Signal to Interference and Noise Ratio (SINR) can be formulated. Considering an inner user $u_{x,in}$, the downlink SINR is given by the following formula:

$$SINR_{u_{x,in}}=\frac{P_{x,c_{x,in}} \Big/ L_{u_{x,in},x}}{P_N+\sum_{k\neq x}\left(P_{k,c_{x,in}} \Big/ L_{u_{x,in},k}\right)} \tag{11}$$

Where P_N is the noise power and $k\in X$ denotes the interfering cells. $L_{u_x,x}$ and $L_{u_x,k}$ stand for the path loss of user u_x with its serving cell x and with the interfering cell k, respectively.

Moreover, for the calculation of the capacity it is assumed that the bandwidth of a channel assigned to the inner or the outer part of the cell is equally shared among the users of the corresponding part. As such, the scheduling can be considered as a round robin, although it can be extended to other scheduling schemes through the consideration for example of the user diversity model, and therefore in this case the total capacity achieved by user $u_{x,in}$ can be formulated as:

$$C_{u_{x,in}} = \frac{B_{c_{x,in}}}{K_{x,in}} \log_2\left(1 + SINR_{u_{x,in}}\right) \tag{12}$$

where $K_{x,in} = \begin{cases} \left|U_{x,in}\right| & \text{if } c_{x,in} \neq c_{x,out} \\ \left|U_{x,in}\right| + \left|U_{x,out}\right| & \text{if } c_{x,in} = c_{x,out} \end{cases}$

and |.| denotes cardinality. It has to be referred that for the outer users, the same formulas as in (11) and (12) can be applied by simply replacing the index *in* by *out*.

Then, the average capacity per user in the scenario is:

$$C_{user,avg} = \frac{\sum_x \sum_{u_{x,in}} C_{u_{x,in}} + \sum_x \sum_{u_{x,out}} C_{u_{x,out}}}{\sum_x \left(\left|U_{x,in}\right| + \left|U_{x,out}\right|\right)} \tag{13}$$

3.2.2.2 Algorithm

Based on the mathematical background for the Gibbs Sampler and the system model presented in the previous sections, the optimization framework is formulated in accordance to the current problem.

Let us recall that when a system can be described by an *energy function ε(c)* which takes real values depending on the configuration *c* and derives from a potential function $\{V_O\}_{O \in X}$, then the Gibbs Sampler can be applied [62]. As such, in the following the formulation of the *energy function* related to the current PFR frequency allocation concept is presented.

The proposed solution aims at finding the states c_x, i.e. the channel allocation for the network cells that minimizes the global inter-cell interference. On that respect, it is defined a function that describes the total interference of the network, the *global interference*. This will be the aggregation of the interference seen by all the cells and the total noise:

The *energy function* or the *global energy* in our problem is the global interference, while the *local energy* is the interference at each BS. Then, the *global energy* is defined as follows:

$$\varepsilon = \sum_x \left[P_N + \frac{1}{\left|U_{x,in}\right|} \sum_{u_{x,in}} \sum_{k \neq x} \frac{P_{k,c_{x,in}}}{L_{u_{x,in}\,,\,k}} + \frac{1}{\left|U_{x,out}\right|} \sum_{u_{x,out}} \sum_{k \neq x} \frac{P_{k,c_{x,out}}}{L_{u_{x,out}\,,\,k}} \right] \tag{14}$$

where $k \in X$ denotes all the neighboring base stations of x, $v \in U_k$ denotes the users associated with the neighboring base stations k, and P_N denotes the noise power. It has to be noted that in (14) it is considered the average interference seen by the users of each cell.

Then, the *energy function* can be reformulated as:

$$\varepsilon = \sum_{x} P_N + \sum_{(x,k)} \left(f\left(k,x\right) + f\left(x,k\right) \right) \tag{15}$$

where $f(k,x)$ is the interference generated by cell k to cell x:

$$f\left(k,x\right) = \frac{1}{\left|U_{x,in}\right|} \sum_{u_{x,in}} \frac{P_{k,c_{x,in}}}{L_{u_{x,in},k}} + \frac{1}{\left|U_{x,out}\right|} \sum_{u_{x,out}} \frac{P_{k,c_{x,out}}}{L_{u_{x,out},k}} \tag{16}$$

As such, it can be stated that the *energy function* derives from a *potential function* V_O:

$$\varepsilon = \sum \left\{ V_O \middle| O \subseteq X \right\} \tag{17}$$

where O represents any possible subset of cells that can be included in X, and V_O is given by

$$V_O = \begin{cases} P_N & \text{if } \; O = \{x\} \\ f\left(k,x\right) + f\left(x,k\right) & \text{if } \; O = \{x,k\} \\ 0 & \text{if } \; \left|O\right| \geq 3 \end{cases} \tag{18}$$

Gibbs Sampler is based on the local interactions in order to minimize the global energy. In other words, it aims as at finding the states that minimize the energy function, which results from minimizing the *local energy* at each site [64][66]. As such in the current problem the purpose is to find the channel allocation c_x at each cell that will minimize the global inter-cell interference through the minimization of the interference at each cell, i.e. the local energy:

$$\varepsilon_x = \sum \left\{ V_O \middle| x \in O, O \subseteq X \right\} = P_N + \sum_{k \neq x} \left(f\left(k,x\right) + f\left(x,k\right) \right) \tag{19}$$

The Gibbs sampler will compute the *local energy* for each possible state $c_x=(c_{x,in},c_{x,out})$, given by the allocated channels, that is:

$$\varepsilon_x\left(c_{x,in},c_{x,out}\right)=P_N+\sum_{k\neq x}\left(\frac{1}{\left|U_{x,in}\right|}\sum_{u_{x,in}}\frac{P_{k,c_{x,in}}}{L_{u_{x,in},k}}+\frac{1}{\left|U_{x,out}\right|}\sum_{u_{x,out}}\frac{P_{k,c_{x,out}}}{L_{u_{x,out},k}}\right)+$$

$$+\sum_{k\neq x}\left(\frac{1}{\left|U_{k,in}\right|}\sum_{u_{k,in}}\frac{P_{x,c_{k,in}}}{L_{u_{k,in},x}}+\frac{1}{\left|U_{k,out}\right|}\sum_{u_{k,out}}\frac{P_{x,c_{k,out}}}{L_{u_{k,out},x}}\right) \tag{20}$$

It has to be noted that the *local energy* function actually results from the measurement of the mutual interference, i.e. the interference that users of cell x will receive from the other cells (second term of the equation), as well as the interference that cell x will cause to the neighboring cells (third term of the equation).

The procedure for the minimization of the *energy function* presented above is described by *Algorithm 1* which is executed at each cell. Assuming that the system time starts at t=0, each cell is assigned with an exponentially distributed timer with mean t_a. The algorithm is executed whenever a cells' timer expires. Then the channel allocation c_x (state) is selected by sampling a random variable λ according to the following probability distribution that represents the probability of selecting state c_x among the set of all possible states denoted as C_P.

$$\pi\left(c_x\right)=\frac{e^{\left(-\varepsilon_x\left(c_{x,in},c_{x,out}\right)/T\right)}}{\sum_{c'\in C_P}e^{\left(-\varepsilon_x\left(c'_{x,in},c'_{x,out}\right)/T\right)}} \tag{21}$$

where T is the *temperature* parameter and is calculated according to the following equation:

$$T=\frac{T_0}{\log\left(2+t\right)} \tag{22}$$

In (22) T_0 is a constant and t is the age variable (t shows the time passed since the simulation started). When the state selection is carried out for a cell, a new timer is assigned to this cell to schedule the subsequent execution of the algorithm. It has to be noted that the probability distribution described (21) favors the lower energy states and with $T\rightarrow 0$ it will converge to a configuration (state) that minimizes the global interference [62][64].

Algorithm 1: Gibbs Sampler Procedure

1: ***if*** *cell x timer (T_x) expires at time t*
2: *calculate the temperature parameter T* (22)
3: ***for*** *each state $c_x \in C_p$*
4: *calculate the Local Energy* $\varepsilon_x\left(c_{x,in}, c_{x,out}\right)$ (20)
5: *calculate the Selection Probability* $\pi\left(c_x\right)$ (21)
6: ***end for***
7: *sample a random variable λ with law $\pi(c_x)$*
8: *assign channels $(c_{x,in}, c_{x,out})$ according to the outcome of λ*
9: *sample an exponential random variable μ with mean t_a*
10: *assign a new timer ($T_x=t+\mu$)*
11: ***end if***

3.2.3 Simulation Results

The proposed solution has been evaluated through simulations and comparisons with conventional schemes. The evaluation is carried out according to two different criteria. First, the benefits brought from the optimization process on respect to the interference mitigation (energy minimization) are studied. Moreover, the impact of the algorithm to the network and the edge user capacity is analyzed. For the evaluation, the classical PFR scheme (as depicted in Figure 11) is used as benchmark, where the channel allocation follows a static configuration. Moreover, a study related to the algorithm convergence and real time implementation possibilities is presented. Finally, variations of the different algorithm related parameters are studied in order to study the impact they have on the algorithm performance and evaluate the proper setting of them.

The simulation scenario consists of 4 tri-sectorial BSs forming a total of 12 cells, as shown in Figure 11. The possible states are formulated by the set of frequencies $C=\{f_0,f_1,f_2,f_3\}$ that can be assigned to the set of cells with the restriction that the inner and the outer part cannot be assigned simultaneously the same channels ($c_{x,in} \neq c_{x,out}$). Therefore the total number of states that the algorithm can choose from is 12. It has to be noted that the selection of the restriction has been carried out after testing different approaches and finding out that when this restriction is applied, better performances are achieved. More details about the other approaches and the simulation results are given in 3.2.4.

Each cell serves 10 users that are distributed uniformly in a circular area with range $R = 1km$. The duration of each simulation is set to $1200 \cdot t_a$ and the simulation step to t_a /24. T_o is set to 0.7 and the energy values in (20) are given in dBW. Simulations are performed for variations of the inner cell range R_{in}, while in each experiment the initial allocation that is considered is the one depicted in Figure 11.

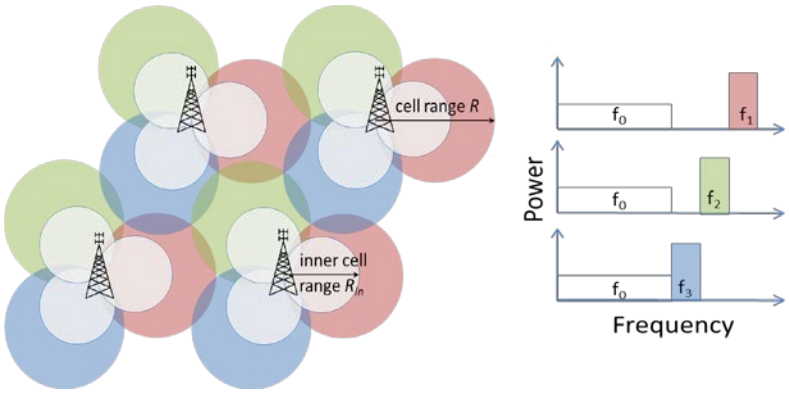

Figure 11: System topology and frequency allocation for the benchmark scheme

The transmit power for the outer part of the cell ($P_{x,out}$) is fixed at 43dBm for all the experiments, while the power for the inner part ($P_{x,in}$) depends to the inner cell range (or equivalently L_{th}) in each experiment and is calculated according to the following expression:

$$P_{x,in}\left(dBm\right) = P_{x,out}\left(dBm\right) - l_A - l_B \log R\left(km\right) + L_{th} \tag{23}$$

This formulation achieves the assignment of the same average received power level for an outer user located at a distance equal to the cell range R and for an inner user located at a distance equal to the inner cell range R_{in}.

The results for each value of the inner cell range R_{in} are the average of 500 experiments. In each experiment the simulation randomly distributes uniformly the users in the scenario. The users' positions are kept static during the experiment. The different users experience independent shadowing conditions. Table I presents the rest of the simulation parameters.

TABLE I: SIMULATION PARAMETERS

Antenna Pattern	Δ_ϕ=70º, Δ_θ=10º, B_o=20 dB, Φ=120º, Θ=0º
Shadowing Std. Deviation	10 dB
Path Loss Parameters	l_A= 128.1 dB , l_B= 37.6
Bandwidth per channel B_c	5 MHz
Noise Power P_N	-100 dBm

1. *Global Energy Reduction*: As it has been referred, the first part of the analysis focuses on the energy reduction or in other words the interference mitigation. Figure 12, shows the comparison between the Gibbs Sampler based dynamic frequency allocation scheme (GS-ICIC) and the classic PFR where the Gibbsian optimization model is not applied. From the figure it can be observed that the algorithm achieves a significant reduction of the global energy, especially in the cases of inner cell range above 400m. The maximum gain is achieved for inner cell range 900m and is equal to

13.43 dB, while the average gain for all the inner cell ranges is 8.47 dB. The proposed solution accomplishes such an energy reduction not only due to the proper channel assignment in the outer parts of the cells that are the most affected from interference, but also due to the fact that the inner parts are also assigned different frequencies on contrast to the reference scheme where all the inner parts utilize the same frequency (f_0). Having such an allocation increases the interference for the users of the inner parts, especially for high inner cell ranges. This justifies the increasing behavior of the global energy when increasing the inner cell range.

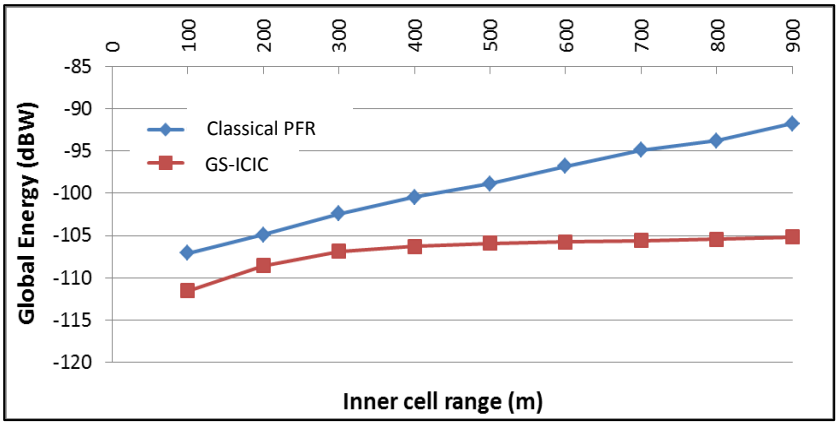

Figure 12: Global Energy

2. *Capacity Improvement*: As a second part of the analysis of the algorithm performance, the impact of the algorithm in the user capacity is studied. Subject of interest are both the average user and the edge user capacity. In the former case, all the users in the cell are taken into account, while in the latter case only the "edge users", assumed to be those located at a distance higher than $0.9R$, are taken into account. Note that in this way, edge users may be either outer or inner users depending each time on the considered inner cell range of the experiment, as well as on the shadowing conditions. Figure 13 presents the comparison of the average edge user capacity between the proposed solution and the reference scheme. It can be clearly observed that the benefits brought from the Gibbs optimization are remarkable, having an average gain of 11.64%, while the highest gain is observed for inner cell range 900m and reaches the 17%.

   Similarly, Figure 14 depicts the comparison of the average user capacity between the proposed solution and the classic PFR scheme. It can be seen that also in this case the capacity improvement that is offered by the Gibbs optimization is significant, especially for the inner cell ranges above 400m.

   By studying Figure 13 and Figure 14 together, it can be noticed that the maximum capacity in each case occurs for different inner cell ranges. In the case where the capacity of all the cell users is considered, the maximum capacity is observed when the inner cell range is 400m, while for the

edge users, the highest values occur for higher ranges. In addition to the interference reduction, this behavior is also related to the fact that, as the inner range is set larger, the outer area is reduced and therefore the available capacity is shared by fewer users. Then, the optimal setting of the inner cell range would result from the trade-off between average and cell-edge capacity, in accordance with network operator policies.

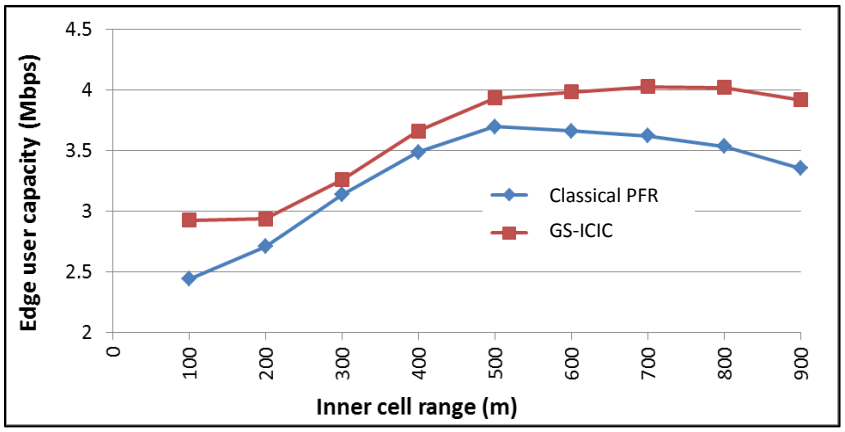

Figure 13: Average Edge User Capacity

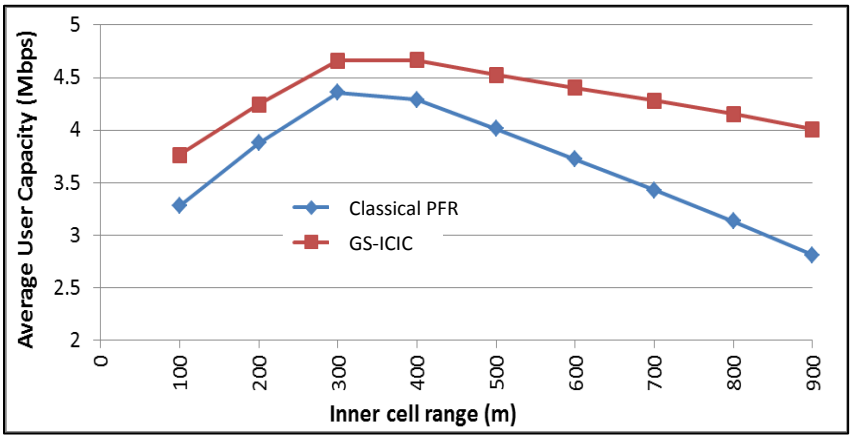

Figure 14: Average User Capacity

3. *Convergence of the algorithm*: As it has been stated, additional information will be presented related to the convergence of the algorithm to an optimal solution, as well as for the feasibility of implementing it in real time scenarios. In the current problem it has been considered that the algorithm is executed either until a convergence criterion is met or the total simulation time ($12000 \cdot t_a$) is reached. The criterion used in this work in order to evaluate the convergence of the algorithm is based on the selection probabilities (21). In particular, when all the selection probabilities of all the network cells are above the value of 0.99 for one of the possible states, then the algorithm is considered to have converged to an optimal solution.

In Figure 15, it is depicted the average number of experiments that have reached convergence according to the criterion presented above as a result from the execution of 500 experiments for each inner cell range. As it can be observed, above the 400m the majority of the executed experiments converge. However, below this range it can be noticed that a significant number of experiments do not meet the convergence criterion. This behavior was expected due to the fact that in these ranges only a few or zero users belong to the inner part, therefore the experienced interference is negligible. This results in multiple optimal solutions since the inner channel does not affect the received inter-cell interference. In cases like this, it has been noticed that the algorithm instead of converging to a given state, it was presenting similar probabilities for all the optimal states. Therefore, the algorithm behavior is adequate although the convergence criterion is not met.

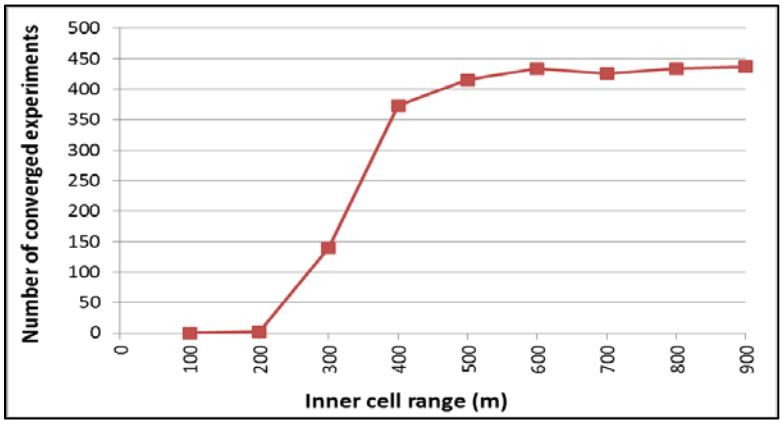

Figure 15: Number of experiments that have reached convergence according to the criterion used in this work

Finally, the required number of algorithm executions in order to reach the convergence criterion has been studied. Figure 16 depicts the evolution of the global energy of a random experiment with respect to the times that the algorithm has been executed until it reaches convergence. As it can be noticed, after 19 executions the convergence criterion is met. This means that the algorithm finds an optimal configuration quite quickly. Furthermore, as it can be seen in the figure, the energy follows a continuously decreasing form. This implies that an online algorithm implementation would be feasible due to the fact that throughout the algorithm execution the impact on the network interference is positive. In particular, it can be observed that even though in the first steps of the simulation the algorithm does not reach convergence, the channel allocation that it is performed results in the reduction of the interference. Therefore, the benefits brought in the network performance are significant form the very beginning of the algorithm execution, making an online implementation possible.

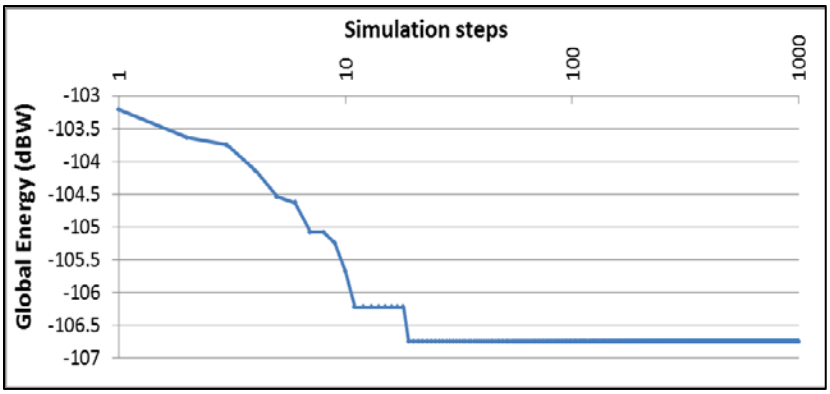

Figure 16: Global Energy Evolution

3.2.4 Parameter Analysis

Further analysis has been carried out with respect to different algorithm related parameters in order to study the impact they have on the algorithm performance. These parameters include the restrictions on the channels used by the inner and outer parts and how they impact on the network capacity, the temperature parameter and how it affects the network interference, capacity and algorithm convergence and the number of the users and the impact it has on the network interference.

- Impact of the restrictions applied to the channels used by the inner and outer parts

The restriction of ($c_{x,in} \neq c_{x,out}$) used in the proposed GS-ICIC scheme has been selected after a careful evaluation of other possible options. In particular, the same experiments have been evaluated under the following options:

a) GS-ICIC – 1 inner channel: The inner part of the macrocell is allowed to be assigned only one channel (i.e. $c_{x,in} = f_0$), therefore the algorithm is actually applied only to the outer part.

b) GS-ICIC – Restricted: Refers to the case where the inner and the outer parts of the macrocell are restricted from utilizing the same channel (i.e. $c_{x,in} \neq c_{x,out}$).

c) GS-ICIC – No restrictions: Corresponds to the case where the channels (f_0, f_1, f_2, f_3) are available for both parts without any restrictions, so the same channel could be assigned to the inner and outer part.

The analysis is carried out in terms of capacity improvement. In particular, the different approaches are compared in terms of average user and the average edge user capacity, which are depicted in Figure 17 and Figure 18, respectively.

As it can be observed from the figures, the solution where the restriction is applied (GS-ICIC – Restricted) outperforms the rest of the cases in terms of average user capacity gain, while in the case of average edge user capacity gain it presents a similar behavior as the GS-ICIC – 1 inner channel, where only one channel is considered for the inner part. As such, overall it can be said that the best behavior is achieved when applying the restriction of ($c_{x,in} \neq c_{x,out}$).

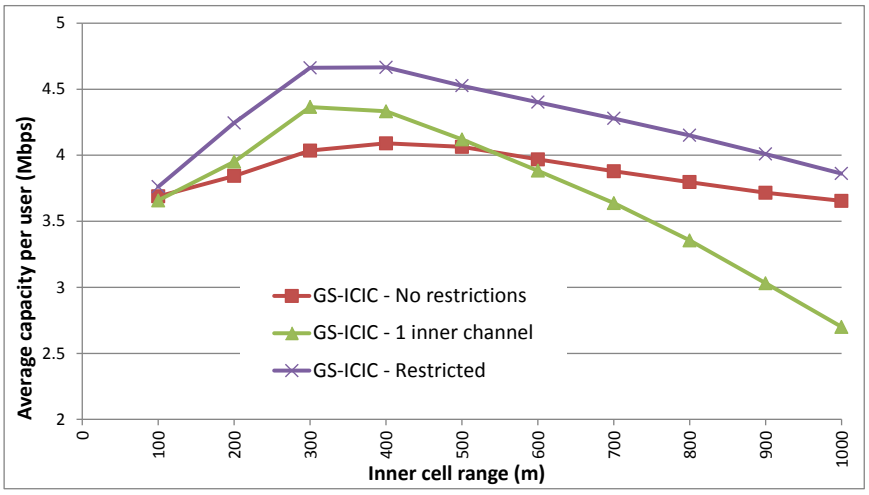

Figure 17: Average user capacity comparison

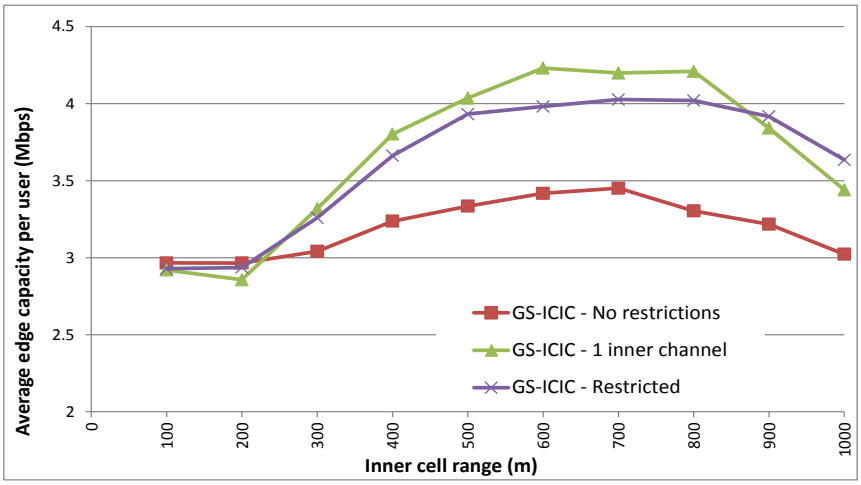

Figure 18: Average edge user capacity comparison

- Temperature Parameter Variations

The impact that the temperature parameter (T_o) has on the algorithm performance has been studied thoroughly through simulations. The considered network is as presented in Figure 11, while the approach under test is the GS-ICIC – 1 inner channel. It is reminded that in this approach only one channel is allocated to the inner part of the macrocell (i.e. $c_{x,in} = f_0$) and therefore the algorithm is applied only to the outer part. However it has to be noticed that the effect of the T_o variations is similar for all the approaches.

Simulations have been carried out for different values of inner cell range (R_{in}) and of T_o, while the results are the average of 100 experiments. The analysis has been focused on the global energy reduction and the energy reduction that the proposed solution achieves with respect to the classical PFR scheme considering the inner and outer parts separately. Moreover, the average user and the average edge user capacity improvement are studied, while a discussion about the time required by the algorithm to reach convergence is also given.

Figure 19a depicts the inner energy reduction (in dB), while Figure 19b the outer energy reduction achieved by the algorithm with respect to the reference scheme for 4 different values of the temperature parameter (T_o). Starting from the inner energy, it can be seen that for inner cell ranges above 300m, the gain for all the values of T_o is zero. This occurs due to the fact that the inner users do not benefit from the algorithm execution since it is applied only in the outer part of the macrocell. Moreover, it can be observed that for the ranges below 300m, the inner users see more interference. The reason for this lies on the fact that since the restriction ($c_{x,in} \neq c_{x,out}$) is not applied in this case, in some experiments the algorithm assigns f_0 in the outer part which results in higher interference for the inner users. However, looking at Figure 19b it can be seen that the benefit for the outer users is significant, and by considering that for these cell ranges the number of the inner users is quite small, the impact it has in the global energy is insignificant as it will be shown later on.

Focusing on the outer energy reduction for inner cell ranges above 300m, the gain follows a positive slope, although it has to be noted that as the range increases the number of the outer users decreases. For ranges up to 800m all the values of T_o present similar results, however above this range the difference is noticeable. Since the number of the outer users is very small, the algorithm for high values of T_o does not reach convergence in most of the experiments due to the fact that as T_o increases, more time is necessary to reach convergence. On the other hand, small values of T_o perform better.

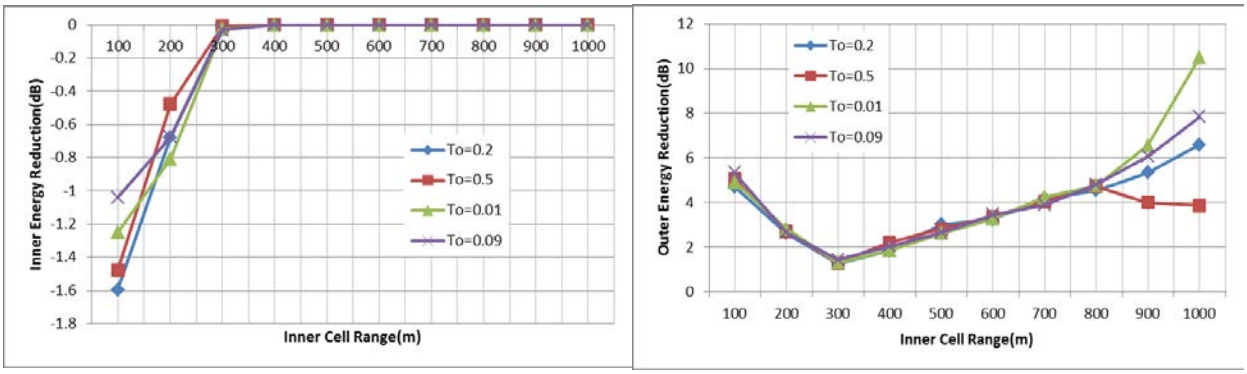

Figure 19: a) Inner Energy Reduction, b) Outer Energy Reduction with respect to the reference scheme

Figure 20 presents the global energy reduction (in dB) for the 4 different values of the temperature parameter (T_o). As it can be observed from the figure, the results for the four values are quite similar since

for small inner cell ranges the contribution of the outer users is more significant, while as the range increases, the inner users contribute more. As such, despite the fact that by looking the inner and the outer energies separately differences in the T_o values can be observed, this is not the case in the global energy.

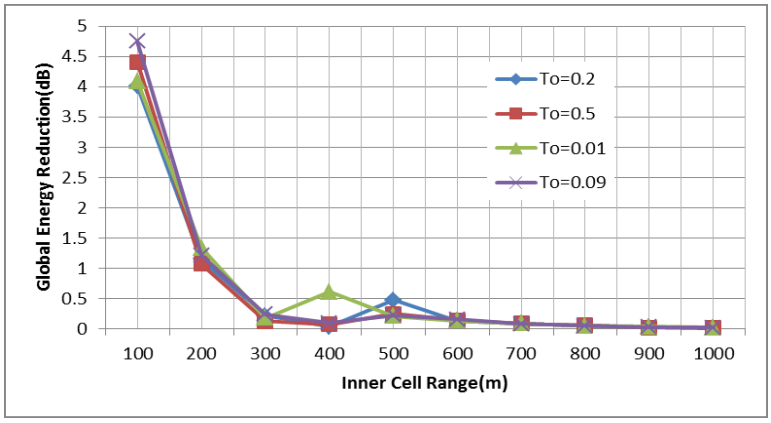

Figure 20: Global Energy Reduction with respect to the reference scheme

As far as for the algorithm convergence, as it was expected results have showed that as the value of T_o is increased the number of experiments that do not reach convergence and the required algorithm executions increase, although the global energy reduction for all the tested values resulted to be very similar.

Finally, Figure 21a and b depict the average user and the average edge user capacity, respectively compared to the classic PFR. From the figures it can be seen that the proposed solution improves the capacity in both cases with higher benefit for the edge users.

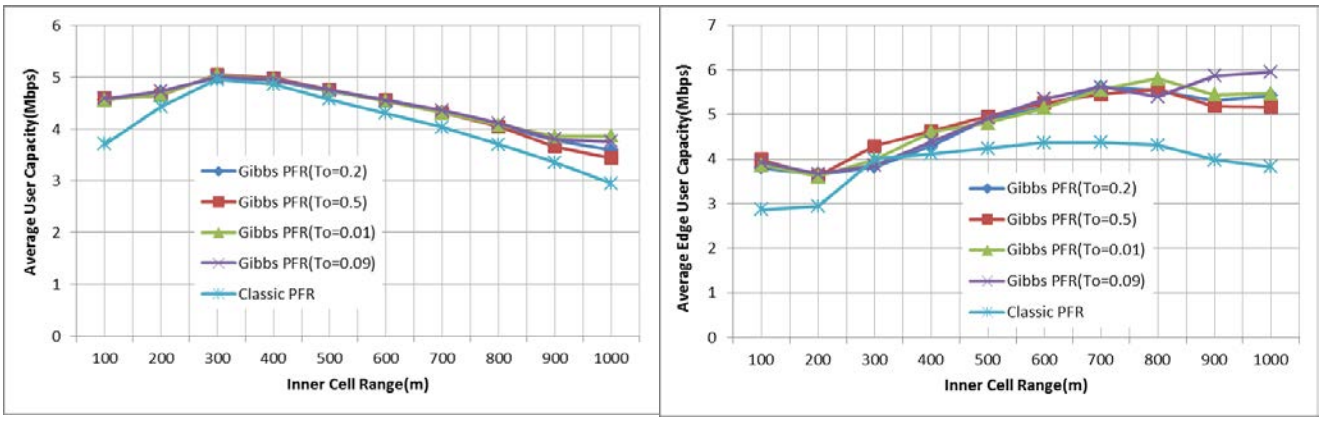

Figure 21: Average User a) and Average Edge User b) Capacity

Further evaluations have been performed in order to estimate the most appropriate value of the temperature parameter (T_o), Examples include variations of T_o for a specific inner cell range R_{in} and analysis of the suggested configurations. It has been observed that very small values of T_o may lead the algorithm to converge in configurations that are not optimal. As such, by considering also the results

presented above, it can be concluded that the temperature parameter must be chosen carefully depending on the network complexity and the requirements of each problem so as to compensate the trade-off between the time of convergence and the accuracy of the solutions given by the algorithm.

- Number of Users Variations

Finally, an analysis has been carried out in order to evaluate the impact of the user variations on the algorithm performance for the GS-ICIC – 1 inner channel scenario. Simulations have been performed for 5, 10, 15 and 20 users in each cell and with T_o = 0.2, which as it has been shown in the previous analysis offers a good trade-off in terms of selected allocation and algorithm convergence.

Figure 22 depicts the outer energy reduction for different number of users. As it can be seen, as the number of users increases, interference is increased as well, although the performance of the algorithm is quite similar in all the cases. Moreover, similar behavior is observed in the average user and the average edge user capacity with gains reaching up to 25% and 36%, respectively.

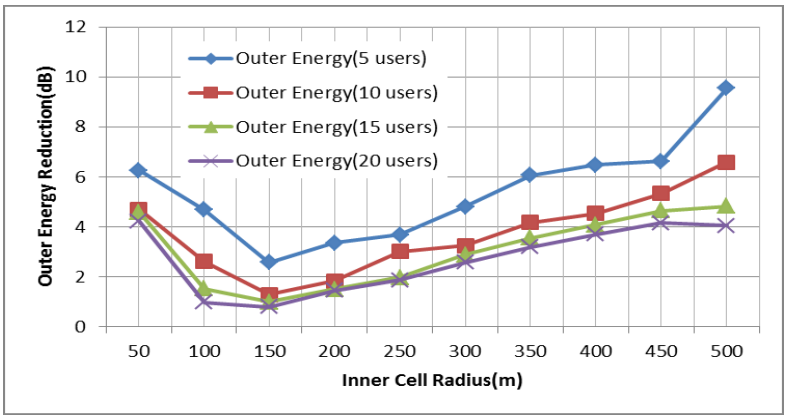

Figure 22: Outer Energy Reduction

3.3 Gibbs-Sampler Formulation Variations

Additional analysis of the Gibbs Sampler-based dynamic frequency allocation scheme (GS-ICIC) has been made with respect to different formulations of the energy function and the impact they have on the algorithm performance, while having as main target the mitigation of the inter-cell interference and the maximization of the capacity. For this purpose, this chapter presents the mathematical framework used for the implementation of the different formulations, as well as the related simulation results.

3.3.1 User interference based energy function (UIGS-ICIC)

The formulation of the energy function presented above is based on the interference experienced by all the cells of the network. As such, the objective was to minimize the total interference. However, the capacity of a user does not only depend on the experienced interference, but also on the number of the users that are served by the same cell and therefore they share the same bandwidth.

Before proceeding to the energy formulation let us recall the expression of the capacity of an inner user as presented in (12):

$$C_{u_{x,in}} = \frac{B_{c_{x,in}}}{K_{x,in}} \log_2\left(1 + SINR_{u_{x,in}}\right)$$

where $K_{x,in} = \begin{cases} \left|U_{x,in}\right| & \text{if } c_{x,in} \neq c_{x,out} \\ \left|U_{x,in}\right| + \left|U_{x,out}\right| & \text{if } c_{x,in} = c_{x,out} \end{cases}$

Moreover, let us recall that the same expression is valid for an outer user by replacing the index *in* by the index *out*.

One way to consider the impact of the bandwidth sharing is to redefine the energy function to include both the interference and the number of users. Empirically it has been observed that a way to achieve this is by defining the energy to be the product between interference and number of users i.e. $K_{x,in} \cdot I_{ux,in}$ for the inner users and $K_{x,out} \cdot I_{ux,out}$ for the outer users. Based on this, the energy function of (14) is modified empirically and takes the following form:

$$\varepsilon = \sum_x \left[P_N + \frac{K_{x,in}}{\left|U_{x,in}\right|} \sum_{u_{x,in}} \sum_{k \neq x} \frac{P_{k,c_{x,in}}}{L_{u_{x,in},k}} + \frac{K_{x,out}}{\left|U_{x,out}\right|} \sum_{u_{x,out}} \sum_{k \neq x} \frac{P_{k,c_{x,out}}}{L_{u_{x,out},k}} \right] \tag{24}$$

Consequently, the local energy will be:

$$\varepsilon_x\left(c_{x,in}, c_{x,out}\right) = P_N + \sum_{k \neq x} \left[\frac{K_{x,in}}{\left|U_{x,in}\right|} \sum_{u_{x,in}} \frac{P_{k,c_{x,in}}}{L_{u_{x,in},k}} + \frac{K_{x,out}}{\left|U_{x,out}\right|} \sum_{u_{x,out}} \frac{P_{k,c_{x,out}}}{L_{u_{x,out},k}} \right] +$$

$$+ \sum_{k \neq x} \left[\frac{K_{k,in}}{\left|U_{k,in}\right|} \sum_{u_{k,in}} \frac{P_{x,c_{k,in}}}{L_{u_{k,in},x}} + \frac{K_{k,out}}{\left|U_{k,out}\right|} \sum_{u_{k,out}} \frac{P_{x,c_{k,out}}}{L_{u_{k,out},x}} \right] \tag{25}$$

3.3.2 User SINR based energy function (USGS-ICIC)

Another approach that has been studied is to consider the Signal to Interference and Noise Ratio (SINR) with purpose the joint minimization of the interference and the maximization of the capacity. Since the Gibbs Sampler targets the minimization of the energy function, then in order to achieve the maximization of the SINR and consequently the users' capacity, the inverse of the SINR can be included in the formulation of the energy function.

Let us start by considering that the user capacity presented in (12) can be rewritten as:

$$C_{u_{x,in}} = \frac{B_{c_{x,in}}}{K_{x,in}} \log_2\left(1 + SINR_{u_{x,in}}\right) = \log_2\left(1 + SINR_{u_{x,in}}\right)^{\frac{B_{c_{x,in}}}{K_{x,in}}} \quad (26)$$

Since the logarithm is a monotonically increasing function, the following equivalence exists between maximization problems:

$$\underset{channel\ allocation}{\arg\max}\ \log_2\left(1 + SINR_{u_{x,in}}\right)^{\frac{B_{c_{x,in}}}{K_{x,in}}} = \underset{channel\ allocation}{\arg\max}\ \left(1 + SINR_{u_{x,in}}\right)^{\frac{B_{c_{x,in}}}{K_{x,in}}} \approx$$

$$\approx \underset{channel\ allocation}{\arg\max}\ SINR_{u_{x,in}}^{\frac{B_{c_{x,in}}}{K_{x,in}}} \quad (27)$$

Based on the above, in order to take into account the impact of the bandwidth sharing, the $Bc_{x,in}/K_{x,in}$ exponent is included in the energy function. However it has to referred that in order to avoid having computational problems in the exponent due to the high value of the bandwidth (i.e. 5 MHz), it has been normalized to $Bc_{x,in} = 1$, assuming it is the same for all the users. On that respect, the energy function is modified as follows:

$$\varepsilon = \sum_{x}\left[\frac{1}{\left|U_{x,in}\right|}\sum_{u_{x,in}}\left[\frac{P_N}{\frac{P_{x,c_{x,in}}}{L_{u_{x,in},x}}}\right]^{\frac{1}{K_{x,in}}} + \frac{1}{\left|U_{x,out}\right|}\sum_{u_{x,out}}\left[\frac{P_N}{\frac{P_{x,c_{x,out}}}{L_{u_{x,out},x}}}\right]^{\frac{1}{K_{x,out}}}\right]$$

$$+\sum_{x}\left[\frac{1}{\left|U_{x,in}\right|}\sum_{u_{x,in}}\sum_{k\neq x}\left[\frac{\frac{P_{k,c_{x,in}}}{L_{u_{x,in},k}}}{\frac{P_{x,c_{x,in}}}{L_{u_{x,in},x}}}\right]^{\frac{1}{K_{x,in}}} + \frac{1}{\left|U_{x,out}\right|}\sum_{u_{x,out}}\sum_{k\neq x}\left[\frac{\frac{P_{k,c_{x,out}}}{L_{u_{x,out},k}}}{\frac{P_{x,c_{x,out}}}{L_{u_{x,out},x}}}\right]^{\frac{1}{K_{x,out}}}\right] \tag{28}$$

Note that in this function two terms are considered. The first term is the inverse of the signal to noise ratio and the second term is the inverse of the signal to interference ratio.

With all the above, the local energy is formulated as follows:

$$\varepsilon_x\left(c_{x,in},c_{x,out}\right) = \frac{1}{\left|U_{x,in}\right|}\sum_{u_{x,in}}\left[\frac{P_N}{\frac{P_{x,c_{x,in}}}{L_{u_{x,in},x}}}\right]^{\frac{1}{K_{x,in}}} + \frac{1}{\left|U_{x,out}\right|}\sum_{u_{x,out}}\left[\frac{P_N}{\frac{P_{x,c_{x,out}}}{L_{u_{x,out},x}}}\right]^{\frac{1}{K_{x,out}}} +$$

$$+\frac{1}{\left|U_{x,in}\right|}\sum_{u_{x,in}}\sum_{k\neq x}\left[\frac{\frac{P_{k,c_{x,in}}}{L_{u_{x,in},k}}}{\frac{P_{x,c_{x,in}}}{L_{u_{x,in},x}}}\right]^{\frac{1}{K_{x,in}}} + \frac{1}{\left|U_{x,out}\right|}\sum_{u_{x,out}}\sum_{k\neq x}\left[\frac{\frac{P_{k,c_{x,out}}}{L_{u_{x,out},k}}}{\frac{P_{x,c_{x,out}}}{L_{u_{x,out},x}}}\right]^{\frac{1}{K_{x,out}}} + \tag{29}$$

$$+\frac{1}{\left|U_{k,in}\right|}\sum_{u_{k,in}}\sum_{k\neq x}\left[\frac{\frac{P_{x,c_{k,in}}}{L_{u_{k,in},x}}}{\frac{P_{k,c_{k,in}}}{L_{u_{k,in},k}}}\right]^{\frac{1}{K_{x,in}}} + \frac{1}{\left|U_{k,out}\right|}\sum_{u_{k,out}}\sum_{k\neq x}\left[\frac{\frac{P_{x,c_{k,out}}}{L_{u_{k,out},x}}}{\frac{P_{k,c_{k,out}}}{L_{u_{k,out},k}}}\right]^{\frac{1}{K_{x,out}}}$$

3.3.3 *"Negative" user SINR based energy function (NUSGS-ICIC)*

The last variation of the energy function that has been studied is based on empirical observations. Throughout the simulations it has been noticed that when multiplying the exponent by a constant (i.e. α), the users' capacity is improved. As such, although the same formulation as previously is carried out, the difference is that the exponent takes the form of ($Bc_{x,in}/\ \alpha{\cdot}K_{x,in}$). Note that also in this case the bandwidth is normalized to 1. On that respect, the energy function is defined as:

$$\varepsilon = -\sum_{x}\left[\frac{1}{\left|U_{x,in}\right|}\sum_{u_{x,in}}\sum_{k\neq x}\left[\frac{\frac{P_{x,c_{x,in}}}{L_{u_{x,in},x}}}{P_N+\frac{P_{k,c_{x,in}}}{L_{u_{x,in},k}}}\right]^{\frac{1}{\alpha.K_{x,in}}}+\frac{1}{\left|U_{x,out}\right|}\sum_{u_{x,out}}\sum_{k\neq x}\left[\frac{\frac{P_{x,c_{x,out}}}{L_{u_{x,out},x}}}{P_N+\frac{P_{k,c_{x,out}}}{L_{u_{x,out},k}}}\right]^{\frac{1}{\alpha.K_{x,out}}}\right] \quad (30)$$

Let us define E as the summation of the average SINR enhanced by ($1/\ \alpha{\cdot}K_{x,in}$) of all the users for all the cells x. Then for E it can be written $E=-\varepsilon$. The objective is to maximize the user capacity, therefore this can be achieved by maximizing the users' SINR. As it has already been stated, Gibbs Sampler targets the minimization of the energy function and since in this case it is defined as $E=-\varepsilon$, then E is maximized. With all the above, the local energy will be:

$$\begin{aligned}\varepsilon\left(c_{x,in},c_{x,out}\right) = &-\frac{1}{\left|U_{x,in}\right|}\sum_{u_{x,in}}\sum_{k\neq x}\left[\frac{\frac{P_{x,c_{x,in}}}{L_{u_{x,in},x}}}{P_N+\frac{P_{k,c_{x,in}}}{L_{u_{x,in},k}}}\right]^{\frac{1}{\alpha.K_{x,in}}}-\frac{1}{\left|U_{x,out}\right|}\sum_{u_{x,out}}\sum_{k\neq x}\left[\frac{\frac{P_{x,c_{x,out}}}{L_{u_{x,out},x}}}{P_N+\frac{P_{k,c_{x,out}}}{L_{u_{x,out},k}}}\right]^{\frac{1}{\alpha.K_{x,out}}}-\\ &-\frac{1}{\left|U_{k,in}\right|}\sum_{u_{k,in}}\sum_{k\neq x}\left[\frac{\frac{P_{k,c_{k,in}}}{L_{u_{k,in},k}}}{P_N+\frac{P_{x,c_{k,in}}}{L_{u_{k,in},x}}}\right]^{\frac{1}{\alpha.K_{k,in}}}-\frac{1}{\left|U_{k,out}\right|}\sum_{u_{k,out}}\sum_{k\neq x}\left[\frac{\frac{P_{k,c_{k,out}}}{L_{u_{k,out},k}}}{P_N+\frac{P_{x,c_{k,out}}}{L_{u_{k,out},x}}}\right]^{\frac{1}{\alpha.K_{k,out}}}\end{aligned} \quad (31)$$

3.3.4 Simulation Results

The evaluation of the different formulations of the energy function has been carried out by means of simulations. The simulation model is the same as presented in 3.2.3, except some differences given in the following.

First, the restriction of ($c_{x,in} \neq c_{x,out}$) is not applied to the different formulations of the energy, thus the number of the possible states increases to 16. This selection has been carried out with the purpose to achieve similar or better results as the GS-ICIC without the usage of any restrictions. Another difference in the simulation setting has occurred due to the fact that the modifications of the energy functions affected the convergence of the algorithm, therefore the value of T_o was adjusted to 0.2 and 0.7. Finally, it has to be mentioned that the results presented for the negative user SINR based energy function are for α equal to 15. This value has been proven to be the most appropriate through simulations and comparisons with several other values; however results are omitted for the sake of brevity.

Figure 23 presents the comparison of the average user capacity achieved by the different energy formulations, while Figure 24 presents the comparison of the average edge user capacity. It has to be noted that the different formulations in the results presentation are given as follows:

GS-ICIC refers to the initial formulation of the algorithm as presented in 3.2. The User Interference formulation presented in 3.3.1 is referred to in the results as UIGS-ICIC, the User SINR based formulation presented in 3.3.2 is referred to as USGS-ICIC and the Negative User SINR formulation presented in 3.3.3 is referred to as NUSGS-ICIC. Finally, the classical PFR scheme is also included in the graph in order to have a reference for the comparisons.

From Figure 23 it can be observed that the interference based formulation (GS-ICIC) and the negative user SINR (NUSGS-ICIC) are proven to be equally beneficial in terms of average user capacity, presenting similar improvements. In Figure 24, it can be seen that the best solution with respect to the edge users' capacity changes with the inner cell range and consequently with the number of the outer users. In the case that the inner cell range is small and therefore the outer users are more, the GS-ICIC formulation achieves higher improvements. On the other hand, as the inner cell range increases the NUSGS-ICIC based solution outperforms the rest. As such, it can be stated that depending on the needs of the current problem, the proper formulation can be chosen accordingly, although the GS-ICIC and the NUSGS-ICIC formulations are the ones that achieve the best performances.

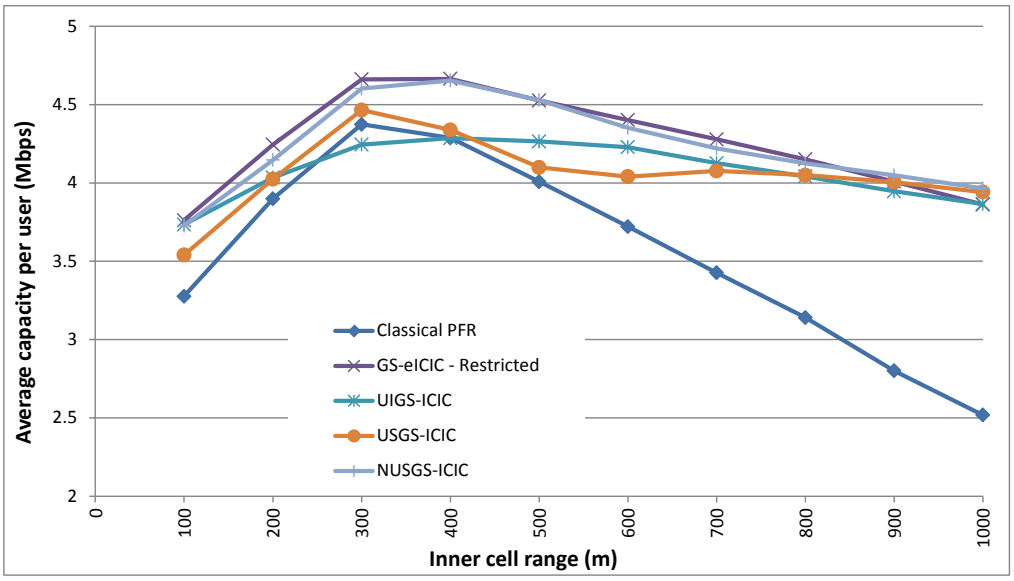

Figure 23: Average User Capacity comparison for different energy function formulations

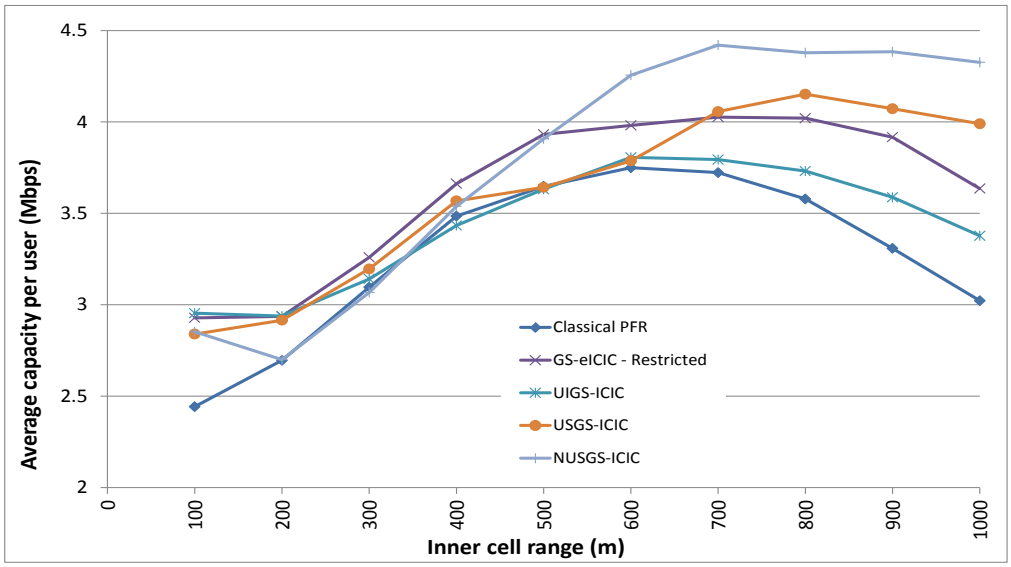

Figure 24: Average Edge User Capacity comparison for different energy function formulations

3.4 Gibbs Sampler-based ICIC for HetNets (HGS-ICIC)

The Gibbs Sampler based frequency allocation model (GS-ICIC) has been extended to the HGS-ICIC scheme in order to include Heterogeneous Networks. On that respect, the proposed solution presented in 3.2 has been formulated accordingly in order to include small cells in the problem of the frequency allocation. The system model used for the implementation of the proposal, the optimization model and the simulation results are presented in the following.

3.4.1 System Model

The system model of 3.2.2.1 is extended to include small cells in the network deployment. As such, apart from the set of X macro base stations, the set S of small cells is introduced. The macrocells may use either omni-directional or tri-sectorial antennas depending on the scenario under test, while the small cells make use of only omni-directional antennas.

The set of the users U is randomly distributed in the scenario, where the association of each user with a cell is carried out according to the maximum received power:

$$P_{R_{(u,(x/s))}}\left(dBm\right) = P_{T_{(u,(x/s))}}\left(dBm\right) - L_{(u,(x/s))}\left(dB\right) \tag{32}$$

where the notation x/s refers to the macrocell x or the small cell s, $P_{R(u,x/s))}$ is the power that a user u receives from the macrocell x or the small cell s, $P_{T(u,x/s))}$ is the transmit power of the macrocell x or the small cell s, and $L_{(u,x/s))}$ is the pathloss as described in (9). Note that when omni-directional antennas are considered the antenna pattern is set to 0 dB.

On a similar way as in 3.2.2.1, the users that are associated with the macrocells are further classified into the subsets $U_{x,in}$ and $U_{x,out}$ depending on whether they belong to the inner or the outer part of the cell. Moreover, the set of channels C can be shared among the macrocell and the small cells, thus let us define as C_{in}, and C_{out}, the subsets of channels for the inner and the outer part of the macrocell, respectively, and as C_{sc} the subset of channels for small cells. Note that $C_{in} \subseteq C$, $C_{out} \subseteq C$ and $C_{sc} \subseteq C$. Also in this implementation we assume for simplicity reasons that each macrocell can be assigned only one channel for the inner and another one for the outer part. Each x macrocell will be then characterized by the state $c_x=(c_{x,in},c_{x,out})$, where $c_{x,in} \in C_{in}$, $c_{x,out} \in C_{out}$ and each small cell s by $c_s \in C_{sc}$. It has to be referred that C_{in}, C_{out}, C_{sc} are not necessarily disjoint sets, meaning that the same channel may be assigned to the inner or outer part of the macrocell and the small cells.

The transmit power of macrocell x in channel c is defined as:

$$P_{x,c} = \begin{cases} P_{x,out} & \text{if } \; c = c_{x,out} \\ P_{x,in} & \text{if } \; c = c_{x,in} \text{ and } c \neq c_{x,out} \\ 0 & \textit{otherwise} \end{cases} \tag{33}$$

while for a small cell s the transmit power in channel c is given by:

$$P_{s,c} = \begin{cases} P_s & \text{if } c_s = c \\ 0 & \text{otherwise} \end{cases} \tag{34}$$

With all the above, the SINR for an inner user $u_{x,in}$ (or outer if replacing the index *in* by *out*) will be formulated in this case as:

$$SINR_{u_{x,in}} = \frac{P_{x,c_{x,in}} / L_{u_{x,in},x}}{P_N + \sum_{\substack{k \neq x \\ k \in X}} \left(P_{k,c_{x,in}} / L_{u_{x,in},k} \right) + \sum_{s \in S} \left(P_{s,c_{x,in}} / L_{u_{x,in},s} \right)} \tag{35}$$

While the SINR for user u_s belonging to the small cell s will be:

$$SINR_{u_s} = \frac{P_{s,c_s} / L_{u_s s}}{P_N + \sum_{\substack{j \neq s \\ j \in S}} \left(P_{j,c_s} / L_{u_s,j} \right) + \sum_{x \in X} \left(P_{x,c_s} / L_{u_s,x} \right)} \tag{36}$$

3.4.2 Gibbs Sampler-based Optimization Model for HetNets

As it has already been stated, in order to minimize the network inter-cell interference the Gibbs Sampler should be defined according to the current problem. In this case the total interference is comprised by the interference in both the macrocells and the small cells. On that respect, it is defined the macrocell global energy and the small cell global energy to be minimized, as the total received interference in the macrocells and the small cells, respectively. As such, the macrocell global energy will be:

$$\begin{aligned} \varepsilon_M = & \sum_x \left[P_N + \sum_{\substack{k \neq x \\ k \in X}} \left(\frac{1}{\left| U_{x,in} \right|} \sum_{u_{x,in}} \frac{P_{k,c_{x,in}}}{L_{u_{x,in},k}} + \frac{1}{\left| U_{x,out} \right|} \sum_{u_{x,out}} \frac{P_{k,c_{x,out}}}{L_{u_{x,out},k}} \right) \right] \\ & + \sum_x \left[\sum_{s \in S} \left(\frac{1}{\left| U_{x,in} \right|} \sum_{u_{x,in}} \frac{P_{s,c_{x,in}}}{L_{u_{x,in},s}} + \frac{1}{\left| U_{x,out} \right|} \sum_{u_{x,out}} \frac{P_{s,c_{x,out}}}{L_{u_{x,out},s}} \right) \right] \end{aligned} \tag{37}$$

where the second term of the summation corresponds to the interference that the inner/outer users of macrocell x receive by the neighboring macrocells k, while the third term represents the interference that the inner/outer users of macrocell x receive by the small cells s.

Similarly, the global energy for a small cell s, will be:

$$\varepsilon_S = \sum_s \left[P_N + \sum_{\substack{j \neq s \\ j \in S}} \left(\frac{1}{|U_s|} \sum_{u_s} \frac{P_{j,c_s}}{L_{u_s,j}} \right) + \sum_{x \in X} \left(\frac{1}{|U_s|} \sum_{u_s} \frac{P_{x,c_s}}{L_{u_s,x}} \right) \right] \tag{38}$$

that includes the interference that the users u_s of small cell s receive by the neighboring small cells j (second term of the summation), as well as the interference that the users u_s of small cell s receive by the macrocells x (third term of the summation).

With all the above, the network global energy will be defined as the sum of the two energy functions:

$$\varepsilon = \varepsilon_M + \varepsilon_S \tag{39}$$

Based on the above global energy function, and following a similar procedure like in 3.2.2, the local energies for each possible state $c_x=(c_{x,in},c_{x,out})$ for the macrocells and $c_s \in C_{sc}$ for the small cells are formulated as:

$$\begin{aligned} \varepsilon_{M_x(c_{x,in},c_{x,out})} = P_N &+ \sum_{k \neq x} \left(\frac{1}{|U_{x,in}|} \sum_{u_{x,in}} \frac{P_{k,c_{x,in}}}{L_{u_{x,in},k}} + \frac{1}{|U_{x,out}|} \sum_{u_{x,out}} \frac{P_{k,c_{x,out}}}{L_{u_{x,out},k}} \right) \\ &+ \sum_{k \neq x} \left(\frac{1}{|U_{k,in}|} \sum_{u_{k,in}} \frac{P_{x,c_{k,in}}}{L_{u_{k,in},x}} + \frac{1}{|U_{k,out}|} \sum_{u_{k,out}} \frac{P_{x,c_{k,out}}}{L_{u_{k,out},x}} \right) \\ &+ \sum_{s \in S} \left(\frac{1}{|U_{x,in}|} \sum_{u_{x,in}} \frac{P_{s,c_{x,in}}}{L_{u_{x,in},s}} + \frac{1}{|U_{x,out}|} \sum_{u_{x,out}} \frac{P_{s,c_{x,out}}}{L_{u_{x,out},s}} \right) + \sum_{s \in S} \left(\frac{1}{|U_s|} \sum_{u_s} \frac{P_{x,c_s}}{L_{u_s,x}} \right) \end{aligned} \tag{40}$$

where the first summation corresponds to the received interference from the neighboring cells k, the second summation represents the generated interference from macrocell x to the neighboring cells k, and the third and fourth summations correspond to the received and generated interference from and to the small cells s, respectively.

And for the small cells:

$$\varepsilon_{S_s} = P_N + \sum_{j \neq s} \left(\frac{1}{|U_s|} \sum_{u_s} \frac{P_{j,c_s}}{L_{u_s,j}} \right) + \sum_{j \neq s} \left(\frac{1}{|U_j|} \sum_{u_j} \frac{P_{s,c_j}}{L_{u_j,s}} \right)$$
$$+ \sum_{x \in X} \left(\frac{1}{|U_s|} \sum_{u_s} \frac{P_{x,c_s}}{L_{u_s,x}} \right) + \sum_{x \in X} \left(\frac{1}{|U_{x,in}|} \sum_{u_{x,in}} \frac{P_{s,c_{x,in}}}{L_{u_{x,in},s}} + \frac{1}{|U_{x,out}|} \sum_{u_{x,out}} \frac{P_{s,c_{x,out}}}{L_{u_{x,out},s}} \right) \quad (41)$$

where the first summation corresponds to the received interference from the other small cells *j*, the second summation represents the generated interference from small cell *s* to the other small cells *j*, and the third and fourth summations correspond to the received and generated interference from and to the macrocells *x*, respectively.

The algorithm is executed when the timer of a macrocell or a small cell expires. The difference with the previous implementation is that a new random variable is added that corresponds to the selection probability of the states of the small cells. As such, the algorithm samples a random variable λ_m (instead of λ) for the macrocell according to equation (21), where instead of ε_x we now have ε_{Mx} and a random variable λ_s for the small cells according to the following probability distribution:

$$\pi(c_s) = \frac{e^{\left(-\varepsilon_{Ss}(c_s)/T\right)}}{\sum_{c_s' \in C_{SP}} e^{\left(-\varepsilon_{Ss}(c_s')/T\right)}} \quad (42)$$

Let us recall that in (21) C_P represents the set of all the possible states for the macrocell, whereas in this case C_{SP} corresponds to all the possible states for the small cells.

Finally, the pseudocode of the execution process of the proposed solution for both the macrocells and the small cells is presented in *Algorithm 2*, below.

Algorithm 2: Gibbs Sampler Procedure for HetNets

1: ***if*** *macrocells x timer (T_x) expires at time t*
2: *calculate the temperature parameter T*
3: ***for*** *each state $c_x \in C_p$*
4: *calculate the Local Energy $\varepsilon_{Mx}(c_{x,in}, c_{x,out})$*
5: *calculate the Selection Probability $\pi(c_x)$*
6: ***end for***
7: *sample a random variable λ_m with law $\pi(c_x)$*
8: *assign channels $(c_{x,in}, c_{x,out})$ according to the outcome of λ_m*
9: *sample an exponential random variable μ with mean t_a*
10: *assign a new timer ($T_x = t+\mu$)*
11: ***end if***
12: ***else if*** *small cells s timer (T_s) expires at time t*
13: *calculate the temperature parameter T*
14: ***for*** *each state $c_s \in C_{sp}$*
15: *calculate the Local Energy $\varepsilon_{Sx}(c_s)$*
16: *calculate the Selection Probability $\pi(c_s)$*
17: ***end for***
18: *sample a random variable λ_s with law $\pi(c_s)$*
19: *assign channels c_s according to the outcome of λ_s*
20: *sample an exponential random variable μ with mean t_a*
21: *assign a new timer ($T_x = t+\mu$)*
22: ***end else if***

3.4.3 Simulation Results

The evaluation of the proposed solutions has been carried out considering initially simple scenarios and extended later on to include more complicated topologies. Although the simulation setup is similar as presented in 3.2.3, due to the addition of the small cells in the network topology some differences occur. These are given in detailed in the following.

The set of channels $C=\{f_0,f_1,f_2,f_3\}$ is common for both the macrocells and the small cells. Moreover, for simplicity reasons, the inner part of the macrocells can be assigned only one frequency (i.e. f_0), therefore we have the following subsets: $C_{in}=\{f_0\}$, $C_{out}=\{f_0,f_1,f_2,f_3\}$, $C_{sc}=\{f_0,f_1,f_2,f_3\}$. The radius of the small cells is set to 100m, where 4 users are distributed uniformly in each of their coverage area. Furthermore, the transmit power of the small cells ($P_{s,c}$) is fixed and set to 20dBm. Due to the addition of the small cells, the temperature parameter needs to be adjusted accordingly. Therefore, several values have been tested and the impact on the algorithm convergence has been studied. Based on this study, the temperature parameter in the majority of the scenarios has been set to the value of 0.2. Finally, the convergence criterion in this case is related with both selection probabilities of the macrocells and the small cells, thus it is considered that the algorithm has reached convergence when both the selection probabilities are above a specific threshold (i.e. 0.99).

The simulation results are mainly divided into two parts. In the first part a simple scenario is considered where the network topology consists in one macrocell and two small cells, while in the second part the network complexity is increased and therefore 12 macrocells and 10 small cells are considered. In both cases the analysis is carried out with special focus on the energy reduction and the capacity improvement.

3.4.3.1 Heterogeneous Study Case with one Macrocell

In the first part, the study has been focused on the frequency allocations performed by the algorithm and how these affect the network interference and capacity in the case where small cells are deployed in the network topology. In order to facilitate the analysis, the simulation scenario has been simplified to one omni-directional macrocell and two small cells in its vicinity. The results have been carried out for two different scenarios. In the first scenario, the PFR technique is not applied in the macrocell, therefore the cell is considered as a whole part and the allocated channel applies for all the users. In the second scenario PFR technique is applied, meaning that the macrocell is divided into the inner and the outer part and that two channels are assigned; one for the inner and one for the outer part. Moreover, in each scenario the position of the small cells is varied in order to evaluate the impact it has to the algorithm performance and the network interference. Finally, for both scenarios simulation results are the average of 100 experiments.

The topologies of the two cases that are considered in the first scenario (where no PFR is applied for the macrocell) are shown in Figure 25. As it can be seen, the locations of the two small cells are changed from being quite far away from each other (Figure 25a) to being really close (Figure 25b) with purpose to include the case where the small cells interfere severely with each other.

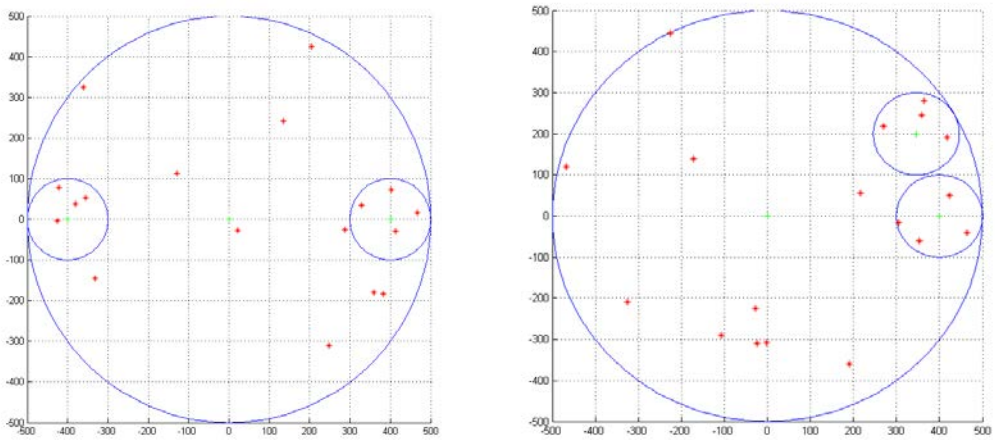

Figure 25: Network topologies for scenario 1 a) case 1 b) case 2

The simulation parameters are the same as presented previously with only difference in the number of the available frequencies that are reduced to three (i.e. f_0, f_1, f_2) since in this case only three cells are involved, and in the transmit power of the small cells that is decreased to -20dBm. It has to be noted that all the experiments were initialized to the same frequency for all the cells (i.e. f_1,f_1,f_1) and that a static user allocation has been considered.

For both scenarios, simulations have been performed in order to calculate the global energy (interference) for all the possible frequency assignments. Some indicative results for the two cases of the first scenario are presented in Table II, where G.E. corresponds to the global energy, MC to the macrocell, SC to the small cell and SYS represents the system, while N/A refers to the cases where interference was equal to 0 W. These calculations have also been compared to the final assignments that the Gibbs Sampler performs. As depicted in Table II with blue color, the best configurations are these where a different channel is assigned among the involved cells (e.g. f_0, f_1, f_2). Moreover, especially for case 2 (Figure 25b) due to the high distance of the small cells, there are configurations that involve the same channel for the small cells and different for the macrocell (indicated by green color in the table) that present results in terms of energy reduction very close to the ones where different channels are assigned. Finally, in both cases and all of the experiments, it was found that the proposed solution was assigning one of the best configurations (i.e. f_1, f_0, f_2) with result the mitigation of the interference and the increment of the capacity as shown in Table III and Table IV. As such, it can be stated that the algorithm correctly finds a proper channel allocation that results in the reduction of the interference and consequently in the capacity improvement.

CASE 1

MC	SC1	SC2	G.E. MC (dB)	G.E. SC (dB)	G.E. SYS (dB)
0	0	0	-132.83926	-99.97577	-99.97353
0	0	1	-132.93739	-100.45545	-100.45300
0	0	2	-132.93739	-100.45545	-100.45300
0	1	0	-146.65153	-109.78095	-109.78006
0	1	1	N/A	-146.93075	-145.18940
0	1	2	N/A	-146.98970	-145.22879

CASE 2

MC	SC1	SC2	G.E. MC (dB)	G.E. SC (dB)	G.E. SYS (dB)
0	0	0	-142.83958	-101.78946	-101.78912
0	0	1	-149.75030	-102.54881	-102.54873
0	0	2	-149.75030	-102.54881	-102.54873
0	1	0	-142.88928	-10973712	-109.73502
0	1	1	N/A	-143.67524	-142.76529
0	1	2	N/A	-146.98970	-145.22879

Table II: Results of the global energy calculations for scenario 1 a) case 1 b) case 2

Av. Energy Gain MC (dB)	Av. Energy Gain SC (dB)	Av. Capacity Gain MC (Mbps)	Av. Capacity Gain SC (Mbps)
39.8521	52.8599	5.35	19.03

Table III: Global Energy and Capacity gain case 1

Av. Energy Gain MC (dB)	Av. Energy Gain SC (dB)	Av. Capacity Gain MC (Mbps)	Av. Capacity Gain SC (Mbps)
37.9917	54.2534	4.91	20.07

Table IV: Global Energy and Capacity gain case 2

In a similar way, it has been analyzed the scenario where the PFR technique is applied to the macrocell, splitting it into the inner and the outer parts. The inner cell radius is fixed and set to 250 meters. Two different cases regarding to the small cells positions were considered, as depicted in Figure 26, with the purpose to study the cases where one of the small cells is located in the inner and the outer part of the macrocell, respectively.

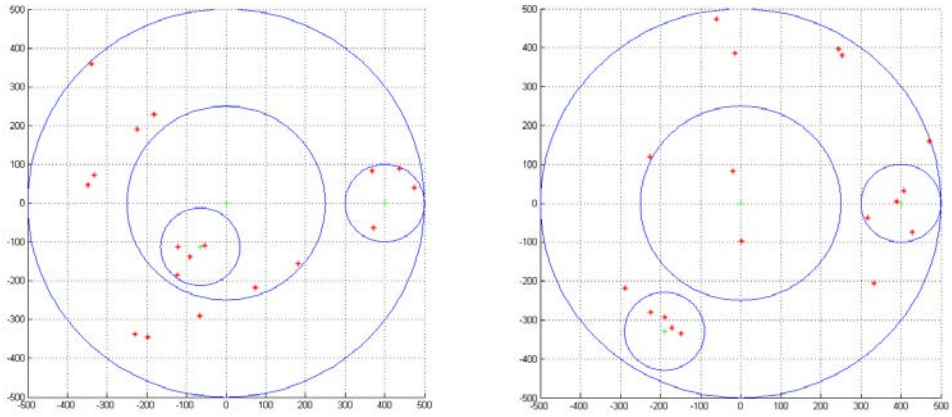

Figure 26: Network topologies for scenario 2 a) case 1 b) case 2

In the first case (Figure 26a) one of the small cells is located in the inner part of the macrocell, while in Figure 26b both of the small cells are positioned in the outer part. In both scenarios the frequency assigned to the inner part of the macrocell is fixed to $\{f_0\}$, while the set $\{f_0, f_1, f_2\}$ to be assigned is common for the outer part of the macrocell and the two small cells.

Indicative results for the global energy calculations for both scenarios are given in Table V. As it can be seen, the two best configurations are these where the inner and the outer part of the macrocell share the same frequency, (i.e. f_0), while the small cells are assigned different channels from the set $\{f_1, f_2\}$ (depicted with blue color). For case 1, the algorithm has converged in these two best configurations in 91/100 experiments, while in case 2 one experiment did not converge and the fraction of best channel assignment was 90/99. It has to noted that in both scenarios the rest of the selected configurations although they were not the optimal ones, they were also presenting a notable energy reduction.

CASE 1

MCin	MCout	SC1	SC2	GE MC (dB)	GE SC (dB)	GE SYS (dB)
0	0	0	0	-107.985	-86.6727	-86.6408
0	0	0	1	-111.719	-87.8641	-87.8462
0	0	1	2	N/A	-146.989	-145.228
0	0	2	0	-110.374	-92.922	-92.8454
0	0	2	1	N/A	-146.989	-145.228
0	1	2	0	-126.101	-115.557	-115.19

CASE 2

MCin	MCout	SC1	SC2	GE MC (dB)	GE SC (dB)	GE SYS (dB)
0	0	0	0	-104.514	-94.720	-94.287
0	0	0	1	-105.125	-95.906	-95.415
0	0	1	2	N/A	-146.989	-145.228
0	0	2	0	-113.330	-100.949	-100.705
0	0	2	1	N/A	-146.989	-145.228
0	1	2	0	-114.498	-123.567	-113.991

Table V: Results of the global energy calculations for scenario 2 a) case 1 b) case 2

In Table VI and Table VII it is depicted the energy reduction and the capacity increment for case 1 and case 2, respectively. As it can be seen, the energy reduction for both the macrocell and the small cells is significant. Moreover, the small cells experience a very high capacity improvement. On the other hand and despite the energy reduction, the macrocells present a small loss in their capacity. This is based on the fact that in the initial allocation the inner and the outer part were assigned different channels, whereas in the end of the simulations they are assigned, in most of the cases, the same channel. Therefore, more users have now to share the same frequency with result a small reduction in the capacity.

Av. Energy Gain MC (dB)	Av. Energy Gain SC (dB)	Av. Capacity Gain MC (Mbps)	Av. Capacity Gain SC (Mbps)
34.8014	60.0428	-0.43	21.19

Table VI: Global Energy and Capacity gain case 1

Av. Energy Gain MC (dB)	Av. Energy Gain SC (dB)	Av. Capacity Gain MC (Mbps)	Av. Capacity Gain SC (Mbps)
34.2783	50.9506	-0.88	18.77

Table VII: Global Energy and Capacity gain case 2

3.4.3.2 Heterogeneous Study Case with 12 Macrocells

The second part of the results can be considered as an extension of the previous analysis with a more complicated topology. This scenario consists of 12 omni-directional macrocells and 10 small cells specifically distributed within each macrocells' area. For the evaluation of the proposed ICIC solution, the analysis is carried out according to the following strategy. Initially the algorithm for the channel allocation is executed in a scenario where no PFR technique is applied for the macrocells and no small cells are deployed and the PFR. This case is referred to as Case 1. Then, in Case 2, small cells are added to the network in order to study the impact of this addition in the network interference and capacity and the performance of the dynamic channel allocation performed by the Gibbs Sampler. Finally, the HGS-ICIC is evaluated, where the PFR technique is applied in the macrocells and the allocation of the channels is carried out in a dynamic manner using Gibbs Sampler as presented in 3.4.2. The evaluation is in this case is carried out for different inner cell ranges.

The simulation setting is given in Figure 27 with the sets of channels being $C_{in}=\{f_0\}$, $C_{out}=\{f_0,f_1,f_2,f_3\}$, $C_s=\{f_0,f_1,f_2,f_3\}$. Moreover, the transmit power of the inner part $P_{x,in}$ depends on the inner cell radius R_{in} and can get the maximum value of $P_{x,out}$=43 dBm when $R_{in}=R$. Finally the simulation results are the average of 500 experiments.

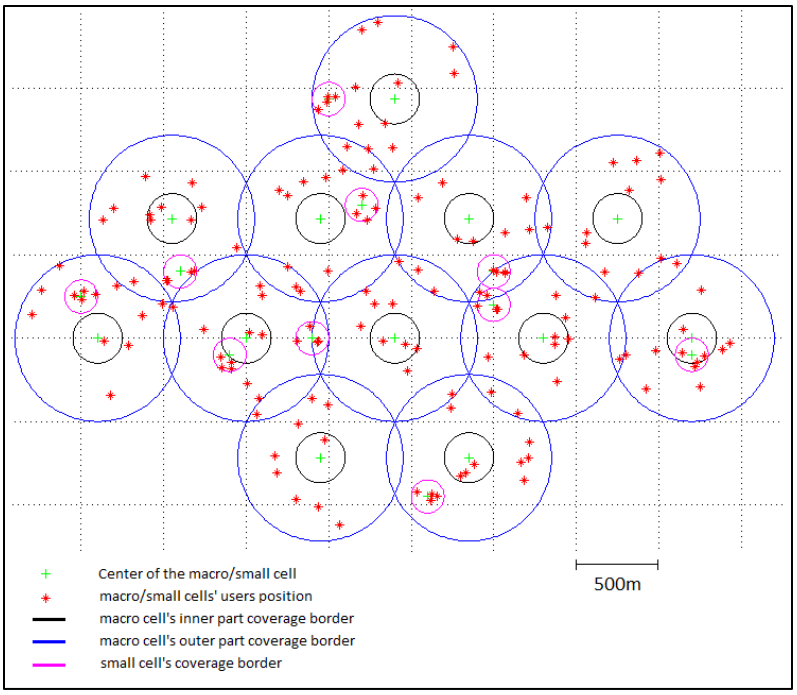

Figure 27: Network Topology with random user distribution

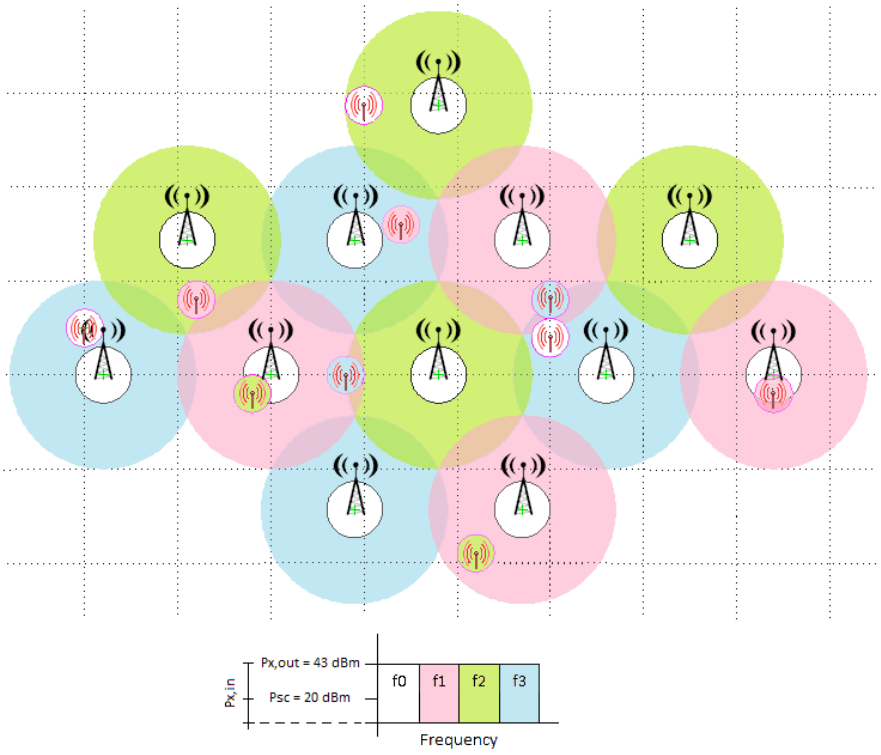

Figure 28: Network Topology and Initial Allocation

In order to understand the benefits offered by the addition of small cells and the PFR technique to the macrocell, a comparison between the three case studies is carried out. The initial allocation and the

topology of HGS-ICIC is depicted in Figure 28. It has to be noted that the topology of Case 1 is the same without the small cells and the cell splitting (PFR technique), while Case 2 consists of the same macrocells and small cells, but it does not include the cell splitting.

The results of all the three case studies in terms of energy and capacity are summarized in Figure 29a and Figure 29b in order to facilitate the comparison. Starting from Case 1, it can be observed in Figure 29a that the algorithm execution in such a simple scenario brings a global energy reduction of 4dB and a capacity gain of 20% (0.58 Mbps) with respect to the initial fixed allocation. The addition of small cells by itself in Case 2 improves the system capacity, although it introduces some level of interference as expected. Then, by applying the Gibbs Sampler a gain in the global energy of approximately 19dB is provided and the capacity is improved by 13% and 5% for the macrocells and the small cells, respectively. Finally, by applying the PFR technique in the macrocells (HGS-ICIC) and testing different inner cell ranges it has been noticed that in all cases the macrocell capacity was increased, while this was not the case for the small cells. With the algorithm execution however, it has been observed that for inner cell ranges 100 and 150m both the macrocells and the small cells capacity presented the maximum values, although there was a small loss in the macrocells capacity compared to the initial allocation. This occurred due to the fact that in the initial allocation the inner and the outer part of the macrocells were assigned different frequency channels, while this was not always the case after the algorithm execution since the same channel could be assigned to the two parts with result more users to share the same bandwidth. Finally, the global energy reduction is observed to present quite high values in these inner cell ranges. Overall, it can be clearly stated that the proposed HGS-ICIC solution offers significant benefits in the network performance, although the system parameters should be carefully selected according to the necessities of each problem.

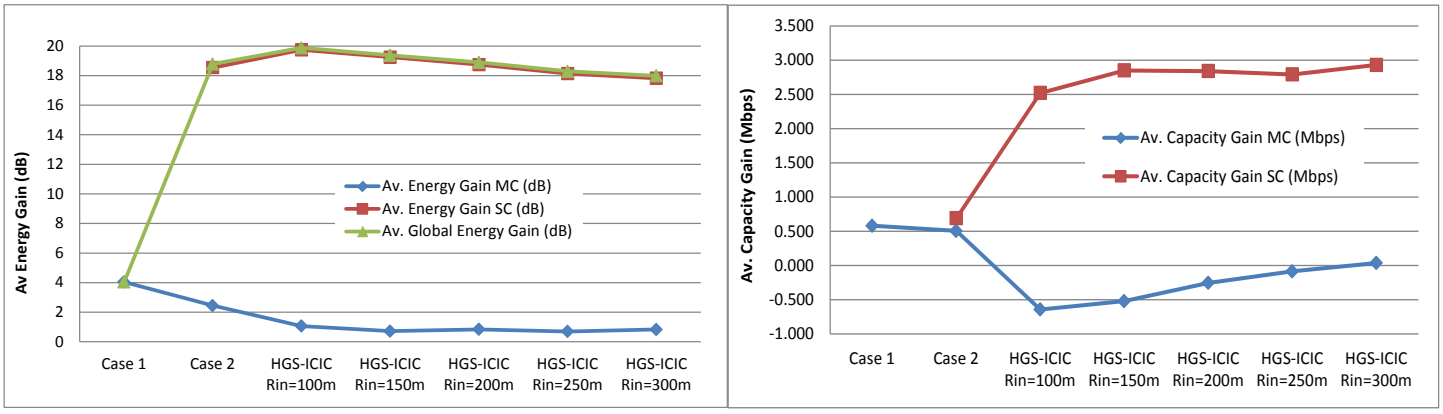

Figure 29: Result Comparison of different implementations a) Av. Energy Gain b) Av. Capacity Gain

3.5 REM based implementation of the HGS-ICIC

Due to the randomness introduced by the user mobility, the data traffic and the propagation characteristics, the radio environment changes continuously. As such, prior knowledge of information related to the radio environment would be beneficial for the implementation of the inter-cell interference coordination (ICIC) techniques. Radio Environment Map (REM) is a database that is used to store information related to the radio environment, such as active users' locations and propagation characteristics, in a dynamic manner [67]. In [68] it is presented an implementation of the HGS-ICIC based on the REM concept, referred to as the REM-based Frequency Optimization (RFO) scheme. A brief introduction on the REM architecture and more details of the RFO implementation are given in the following sections.

3.5.1 REM Architecture Overview

An architectural approach for the REM concept is given in [69], where four main blocks are considered:

- The measurement-capable devices (MCDs), which are the network elements that are responsible for performing spectrum and geo-location related measurements.
- The REM data storage and acquisition (REM SA), which constitutes the storage element for the data resulting from the MCDs, as well as for other processed data.
- The REM manager, which is responsible for requesting measurements, and extracting and processing the data from the REM SA.
- The REM user that corresponds to the network entity that benefits from the REM data.

Let us note that depending on the considered network, the functionalities of the different entities may be adjusted accordingly. As such, when considering for example a heterogeneous network consisting of macrocells and small cells, a layered REM architecture can be considered, meaning that the same REM blocks can be located at different network elements (e.g. macrocells). In this way, the information collection is facilitated because each block is responsible for information related to its local environment.

3.5.2 Implementation Considerations

Depending on the considered network and/or type of ICIC, there are different ways for the implementation of a REM-based ICIC. In general, two types of information are considered, the local and the global. The local REM database can be included in the macrocells (eNodeB)/small cells (HeNB) and

involves information related to their local environment. In particular, the more dynamic parameters are preferably stored in the local REM databases, such as propagation loses, cell and user positions and signal strengths. The global REM can be included in the mobility management entity (MME)/HeNB Gateway, and deals with the less dynamic parameters and/or the parameters that can impact a higher number of network nodes. Examples include QoS metrics, cell positions and information related to other technologies employed in a heterogeneous network. Depending on the problem needs, the type of REM and the type of information may vary.

Table VIII depicts the different parameters that can be exploited for the implementation of an ICIC scheme. Two examples are given, including the proposed RFO approach [68] and a power control ICIC scheme presented in [70]. The REM-based Autonomous HeNB Power Control (RAHPC) ICIC adjusts the transmit power of the small cells in a heterogeneous network according to information obtained by the REM database, in order to achieve a target SINR. As it can be observed from the table, both types of information are exploited, local and global. The RFO scheme on the other hand, can be considered as a fully distributed architecture that makes use only of local information. REM blocks in this case can exchange information using the X2 interface, however with the required signaling to be directly related to the amount of the necessary information, the update rate, etc.

Type of Information		**REM-based Autonomous HeNB Power Control (RAHPC) [70]**	**REM-based Frequency Optimization (RFO) [68]**
Local REM	Location of nodes	Small cell (HeNB), UE locations	
	Radio related information	Propagation loses between network elements	Propagation loses between users and cells
	Transmit Power		Transmit power in each channel
	List of neighboring cells		Set of interfering cells for each cell
Global REM	QoS metrics	SINR target	
	Locations of nodes	Macrocell (eNB) locations	
	Wi-Fi related information		

Table VIII: Parameter usage of the RFO approach [68]

3.5.3 RFO Simulation Results

As it has presented in 3.4, in the proposed solution, the macrocells are split into the inner and the outer part using the PFR technique. In each part of the macrocell different channels are assigned, while the small cells make use of only one channel. The Gibbs Sampler is then applied to perform the channel allocation,

as presented in 3.4 with the difference that the required information for the estimation of the received and generated interference is acquired from the REM database as shown in Table VIII.

The benefits brought by the RFO scheme in terms of capacity improvement and energy reduction have been analyzed by means of simulations and comparisons with a reference scheme where the traditional PFR is applied to the macrocell (static allocation) and the small cells are assigned a random channel selected among the ones that are not used by the closest macrocell. The system model consists of 12 omni-directional macrocells and 8 small cells with cell radius 500 and 100m, respectively. Simulations have been performed for different values of inner cell radius. The transmit power for the outer part and the small cells is fixed to 43 and 20 dBm, respectively, while for the inner part varies according to the R_{in}. Finally different values of the REM information error are considered. The error in the REM is modelled as a uniform random variable distributed between [-ε, ε], applied for each propagation loss value stored in the REM.

Figure 30 presents the average user capacity gain (in %) for the macrocells and the small cells with respect to the reference scheme, for different values of the REM information error ε and for R_{in} equal to 200 and 350 meters. As it can be observed from the figure the gain is significant, reaching values of 30% and 55% for the small cell users when the information error is 0dB corresponding to the ideal case where the information hold by the REM match the real propagation loses. As the error increases, the gain is slightly decreased, however even in the worst case of ε=5dB, the gain reaches the values of 22% and 39%, respectively. On the other hand, the macrocell users present very small losses for the case of R_{in} = 200m, while for the case of 350m the impact is mostly positive although negligible. As such it can be clearly stated that the overall network capacity is increased even in the cases that the information error presents relatively high values.

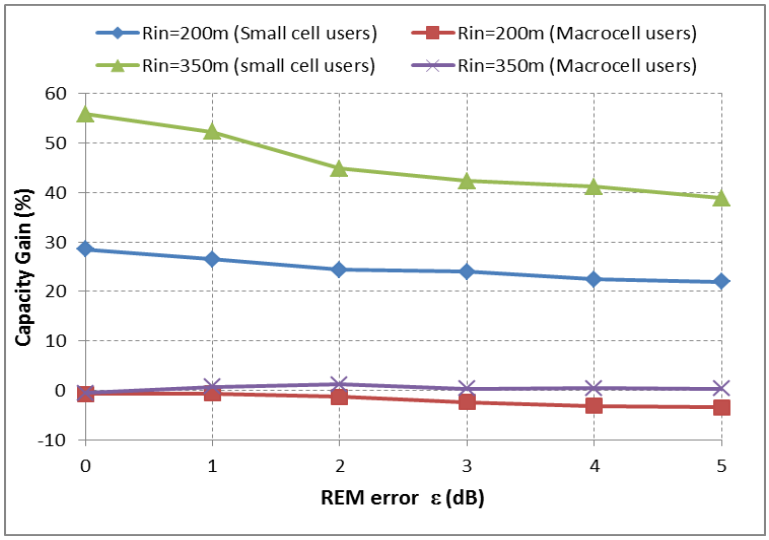

Figure 30: Average user capacity gain for different values of the REM information error

As far as for the network interference, Figure 31 presents the energy reduction (in %) achieved by the proposed solution for different values of the information error ε. As it can be seen from the figure, the small cells are the ones who mostly benefit from the algorithm, having the interference reduced up to 17% and with a minimum value of 13% for the worst case of ε. The macrocell users experience a slight improvement, except for the case of R_{in} = 200m and for ε above 2dB, however it can be stated that in general the impact is positive, although very small.

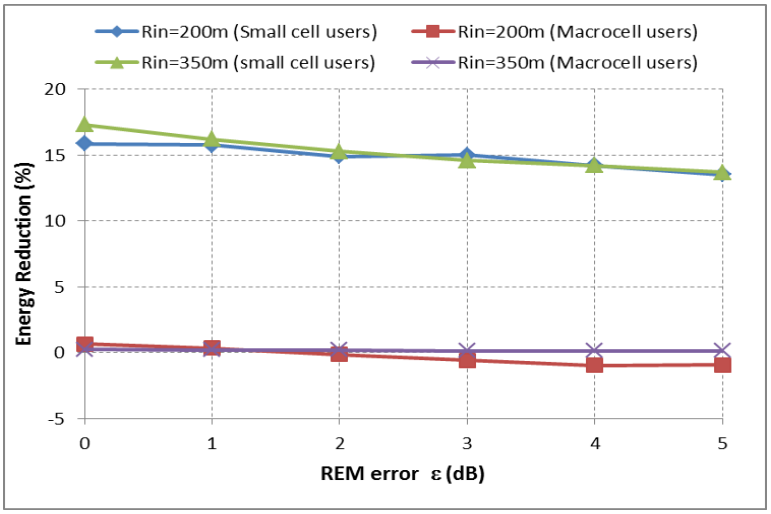

Figure 31: Average energy reduction for different values of the REM information error

4. Interference Management combining Multiple Dimensions

4.1 Inter-Cell Interference Management in Heterogeneous Networks

With the introduction of HetNets in the framework of LTE-A, great potentials have arisen allowing to cope with the requirements imposed by the users and technology evolution. The revolutionary concept of combining different cells sizes and various technologies has opened ways towards new possibilities able to provide cost effective coverage in areas where the macrocells are not sufficient (i.e. hot spot areas), to increase the network capacity and improve the overall system performance. However, due to the heterogeneous nature of the network topology and the diversity of the involved technologies, new challenges emerge. User-to-cell association requires alternative solutions due to the different characteristics of the involved nodes. Moreover, interference becomes more difficult to be controlled since femto cells are deployed by the users in an operator unplanned manner. As such, operators are not always aware of the number of existing nodes and their location in the network topology, making the network planning quite challenging. Another issue arises from the way the small cells can operate. The CGS mode for femto cells presented in chapter 2.2.1 introduces additional interference problems. Users connected to a CSG femto may generate and/or receive interference from unauthorized users which are forced to be connected with a macrocell with which they may not experience high quality transmissions. This makes the usage of the already existing interference management techniques insufficient, and poses the need for more advanced schemes [1]. Based on the above, in this chapter the main constraints and requirements imposed by HetNets are identified and possible solutions are addressed with special focus on the user-to-cell association and the interference management.

4.1.1 User Association: *Cell Range Expansion (CRE)*

In traditional networks that follow homogeneous cell deployments the user-to-cell association is carried out according to the maximum received signal strength (RSS) or Signal to Noise and Interference Ratio (SINR). This means that a user will be connected with the cell with which experiences the highest RSS or SINR. The optimality of this method however is not always guaranteed in the case of HetNets due

to the different characteristics of the involved cells [71]. The small cells have considerably smaller size and consequently smaller coverage footprint compared to the macrocells. Moreover, small cells transmit much lower power levels. As it has presented in chapter 2.2.1, typical values for the small cells are between 250mW and 2W, while for the macrocells these values can be in the order of 40W. Furthermore, the small cells are equipped with antennas of lower gains and in lower heights, which may result in higher path losses. The combination of the above mentioned issues leads the small cells to provide smaller coverage areas, which reduces the number of users that can be offloaded from the macrocell. Moreover, since the available bandwidth is equally shared among the macro and the small cells, this can result in uneven distribution of the capacity [72].

In order to overcome these issues and compensate the traffic distribution with main objective the improvement of the capacity distribution (fairness), the Cell Range Expansion (CRE) concept is introduced [73] depicted graphically in Figure 32. CRE is a user association technique that involves a positive offset, denoted as CRE bias. When the user-to-cell association decision takes place, the CRE bias is added to the user measurements of the RSS or SINR of the small cells (SC), as shown in Figure 32. In this way the coverage footprint of the small cells is extended, reason that explains the name Cell Range Expansion. Having the coverage area of the small cells expanded allows more users to be offloaded from the macrocells and consequently the capacity can be shared more equally between macrocells and small cells.

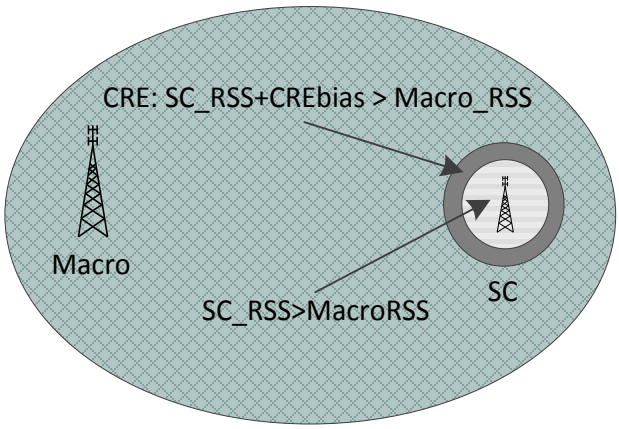

Figure 32: Cell Range Expansion

A crucial factor of the scheme consists the proper setting of the CRE bias, since a too small value may not offload adequately the macrocell, while a too high value may lead to over congested small cells [74][75]. On that respect, research has focused on the setting of the CRE bias. Third Generation Partnership Project (3GPP) reports presented some typical values in [73] and in [76]. Moreover, investigation has also targeted adaptive solutions that configure the value of the CRE bias according to the network conditions. In particular, a solution that adapts the CRE bias based on logarithmic functions and

by taking into account the number of users in the involved cells is proposed in [74]. Another strategy has been presented in [77], where the authors adopted different metrics than the ones of [74] with the purpose to reduce the required signaling and increase the efficiency of the solution. Finally, in [78] an algorithm that updates the values of the CRE bias based on an estimation of the overall system capacity was proposed.

Despite the fact that a proper setting of the CRE bias offers significant benefits, the users that are located in the cell borders (i.e. in the expanded area) and therefore are associated with the small cell thanks to the CRE bias addition, are considerably vulnerable to interference. The reason is that these users experience low SINR values since they actually receive higher RSS from the macrocell than from the associated small cell [79]. As such, enhanced interference coordination techniques are indispensable to protect these users and further improve the performance of CRE [71][80]. An overview of the solutions adopted under the framework of LTE-A is given in the following section.

4.1.2 Enhanced Inter-cell Interference Coordination (eICIC)

In order to cope with the interference related challenges existing in HetNets presented in this chapter, interference management techniques are necessary. However, traditional ICIC techniques may not always be suitable in the case of HetNets since their design implicitly assumes homogeneous deployments [1]. On that respect, in the framework of LTE-A enhanced ICIC (eICIC) techniques are adopted that take into account the heterogeneity of the network. A good introduction to eICIC can be found in [1], while in [81] a survey is presented. In general, three types of eICIC are considered [82]: Frequency-Domain, Time-Domain and Power Control techniques.

Frequency-Domain methods target on carrying out orthogonal user transmissions of the involved cells by scheduling the control channels and the reference signals in reduced bandwidths. The implementation of the orthogonality can be achieved both in a static and in a dynamic manner [1].

Power Control employs techniques that adjust the power of the small cells and that differ from the ones used in the macrocells [83]. The control of the power is carried out by taking into account parameters, such as the power received by a small cell from the strongest interfering macrocell, the path loss and the SINR of the macrocell and the small cell users. For a detailed description on the Power Control one may refer to [84].

In the Time-Domain methods, the control and/or data channels of the users that suffer from interference are scheduled in time domain resources where the interference is suppressed [1],[85]. Two types of Time-Domain eICIC are considered, the OFDM symbol shift and the subframe alignment.

OFDM Symbol Shift is a technique where the subframe boundary of the small cell is shifted by one or more OFDM symbols so that a difference is introduced with respect to the macrocell node. This way, the control channels of the small cell and the macrocell do not overlap, thus interference is avoided. Nevertheless, the macrocell users still experience interference in their control channels from the data channels of the small cell users [1],[85].To cope with this problem, two approaches are used known as PDSCH symbol muting and consecutive subframe blanking. For an overview of these techniques the readers may refer to [85].

Subframe alignment, depicted in Figure 33, is a Time-Domain technique introduced in Release 10 that partitions the total subframes into Normal and Almost Blank Subframes (ABS) [85]. This division allows to periodically mute the transmissions of the aggressor cell (the cell that generates interference), and give the opportunity to the victim cell to transmit under reduced interference conditions [2]. This is achieved by restricting the macrocell transmissions to the Normal subframes, while no data apart from some reference signals are allowed to be transmitted during the ABS subframes. As such, the small cells can schedule their transmissions during the ABS subframes under reduced interference conditions, which results particularly beneficial for the small cell users located in the expanded region.

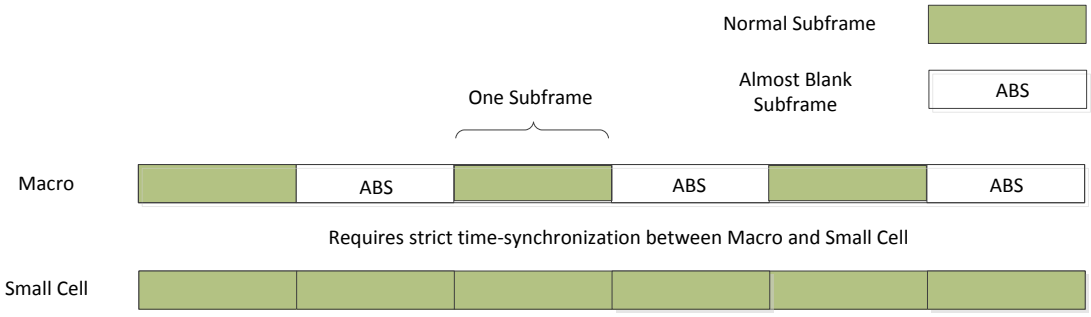

Figure 33: Almost Blank Subframes (ABS)

The proper setting of the number of the ABS subframes plays a significant role in the performance of the scheme. A value too high may result in degradations of the macrocell capacity since the macrocell remains silent during the ABS subframes, while a value too small would imply that a high portion of the resources disposed for small cell transmissions would be characterized of high interference, leading in degradations of the small cells capacity. On that respect, research has been carried out on determining the number of necessary ABS subframes depending on the network conditions. In [86], the authors present a solution for deriving the required number of ABS in macro/pico and macro/femto deployments. The formulation results from stochastic geometry and takes into account the number of the victim users. Another solution that adjusts the number of ABSs dynamically depending on the network load changes is presented in [87].

4.1.3 Problem Identification and Literature Review

The combination of CRE and ABS is used widely since it results in significant improvements in the network performance [80][88]. However, the setting of the two parameters should be directly related due to the fact that the number of ABS subframes depends on the number of the users in the expanded region that in turn are determined by the CRE bias. As such, research has focused on solutions that consider the joint configuration of the two values. In [88] the problem of the joint optimization of the load balancing and resource partitioning (ABS) is addressed. The authors present a general framework and analyze the impact on the data rate and the coverage probability. Another approach has been presented by Deb *et al*. in [89]. The authors provide a mathematical framework and an algorithm for the optimization of the user association and the number of ABS subframes based on propagation and interference data, the users location and the network topology. Exploiting the game theory, the authors of [90] presented a generic framework for the joint optimization of the two schemes. The proposed solution maximizes a network utility function based on statistics such as the RSS measurements.

Moreover and despite the fact that the optimization of the parameters leads to significant benefits in terms of interference mitigation, especially for the users located in the expanded region of the small cells, the ABS faces an important drawback. Due to the silent periods of the macrocell, the available bandwidth is not fully utilized leading in capacity degradations for the macrocell users [90]. Therefore, carefully devised solutions are indispensable in order to balance the trade-off between the interference mitigation in the small cells and the capacity degradation in the macrocells. Recent research has focused on the enhancement or modification of the ABS scheme itself. To the best of our knowledge the majority of existing solutions target the power domain. For example, in some 3GPP contributions [91][92] it is suggested to use lower power in order to allow macrocell transmissions during the ABS subframes. This concept is denoted as Low Power ABS (LP-ABS). An introduction to the LP-ABS is given in [93]. The authors perform an evaluation of the scheme through simulations and address some technical and standardization challenges. A similar approach has been presented by Lopez *et al*. in [79], where the power of the macrocell in the resource blocks used by the edge pico users is adjusted. A resource allocation algorithm is proposed in [94] that handles both the time and power domains. In the time domain the ABS subframes are configured dynamically based on the network load variations. Then, the macrocell transmit power is adjusted according to a utility function that results from game theory. Additionally, a time domain scheduling scheme is proposed in order to protect the picocells edge users.

Based on the above, in this work a novel eICIC scheme for the management of the ABS subframes has been studied, implemented and evaluated. For the formulation of the proposed solution, the knowledge acquired during the study of ICIC schemes has been exploited. As such, it has been considered that the frequency domain can also be combined with the time-domain eICIC. In particular, initial work considers

a solution that depending on the small cells position in the network topology it exploits accordingly the time-frequency or the time-power domains. Later on, the work has been extended to one mechanism that jointly exploits the time, frequency and power domains. Finally, the work has been focused on the optimization of the scheme. The choice of the optimization tool has been carried out based on the type of the optimization problem, therefore heuristic algorithms have been considered. In particular, genetic algorithms have been used as optimization tool, resulting in significant improvements. More details about the proposed solutions, the implementation of them and the benefits acquired as evaluated through simulations are given in the following chapters.

4.2 Time-Frequency/Time-Power eICIC

In order to utilize the available resources in a more efficient way and increase the macrocell users' capacity, while at the same moment allowing the mitigation of the interference seen by the small cells, in this work a novel solution has been proposed, presented in [95], for an alternative management of the ABS subframes. The proposal consists of two mechanisms that exploit the time-frequency or the time-power domains depending on the deployment of the small cells in the network. Thanks to these mechanisms it is possible to allow macrocell transmissions during the ABS subframes under special constraints. Such conditions are expressed in terms of the allowed RBs in the frequency domain or the maximum allowed transmit power. More details about the system model, the implementation of the scheme and the numerical results are given in the following.

4.2.1 System Model

The considered heterogeneous network of this work consists of a set M of macrocells denoted as $i = 1,2...,V$ and a set S of small cells denoted as $k = 1,2,...,P$. The set of users, denoted as U is randomly distributed in the scenario in a non-homogeneous way, forming some hot spot areas with higher user density than other parts. The user-to-cell association is carried out according to the measured RSS with CRE being applied. As such, a user $u \in U$ will be associated to cell x^* according to:

$$x^* = \arg\max_{x \in M \cup S} \left(RSS_{x,u} + \Delta_x \right) \tag{43}$$

where $RSS_{x,u}$ is the received signal strength of cell x measured by user u and Δ_x (dB) is the CRE bias for the small cell $x \in S$, while for macrocells $x \in M$ it takes the value Δ_x=0 dB. Depending on the cell association the set of users is further divided into different subsets. The subset of the users that are

connected to the i-th macrocell is denoted as $U_{M,i}$ and the subset of users connected to the k-th small cell is denoted as $U_{S,k}$. Moreover, the small cell users $U_{S,k}$ are further divided into two subsets depending on whether they receive the highest RSS from the small cell or they have been connected to it thanks to the CRE bias addition (i.e. the users in the extended region). In this way, they are classified as the subset of CRE users ($U_{CRE,k}$), which are the users that belong to the extended region of the k-th small cell so they receive higher RSS from the macrocell than from the small cell and the subset of normal small cell users ($U_{N,k}$), which receive higher RSS from the small cell than from the macrocell. It has to be noted that $U_{CRE,k} \cup U_{N,k} = U_{S,k}$.

We assume communication in the downlink direction, although the same concept can be applied in the uplink. Moreover, it is assumed that all the macrocells and small cells operate in the same LTE carrier. For resource allocation purposes, and following the LTE specifications, the frequency dimension is organized in a total of N Resource Blocks (RBs) of bandwidth B_{RB}=180 kHz and the time dimension in subframes of 1 ms organized in frames of 10ms. Each subframe is a TTI (Transmission Time Interval), meaning that it is the minimum time that a RB is allocated to a user. As result, the available RBs in a frame are numbered as $RB(f,t)$ where f=1,...,N, and t=1,...,10. We assume that the allocation takes place in each frame, where each cell decides the resources to be assigned for the transmissions to its users. The ABS technique is applied, with μ_i denoting the number of ABS subframes per frame for the i-th macrocell and λ_i=10-μ_i denoting the number of Normal subframes. It is assumed that the resource allocation in the k-th small is carried out by taking into account the ABS subframes setting of the macrocell that it receives with highest power, i.e. the macrocell in whose coverage area the small cell is located.

The total propagation losses in the $RB(f,t)$ for a user $u \in U$ with respect to the i-th macro and the k-th small cell are denoted as $L_{M,u,i,RB(f,t)}$ and $L_{S,u,k,RB(f,t)}$, respectively. They include the shadowing and the fast fading due to multipath.

4.2.2 Proposed eICIC Solution

The proposed solution has been designed under the consideration of the drawback that the ABS presents related to the underutilization of the available resources from the part of the macrocell and consequently the capacity degradation that its users experience. In order to overcome this constraint, a modification and enhancement of the scheme has been carried out so as to preserve the main characteristics of the ABS scheme, while allowing a better management of the resources through the employment of smart mechanisms. In particular, the key idea of the proposed eICIC solution is to exploit the knowledge acquired during the study of the ICIC in order to allow the macrocells to utilize the ABS subframes under certain restrictions. On that respect, two mechanisms are applied depending on the

position of the small cells that exploit jointly either the time and the frequency domain or the time and the power domain. The first case employs a set of RBs that can be exploited by the macrocells, while the latter considers the spatial division of the macrocell and the employment of two macrocell transmit power levels. More details about the implementation considerations of the proposed solution are given in what follows.

Let us consider the *i*-th macrocell and the small cells that fall inside its coverage area. Depending on the deployment of the small cells in the network topology two cases are considered, as depicted in Figure 34.

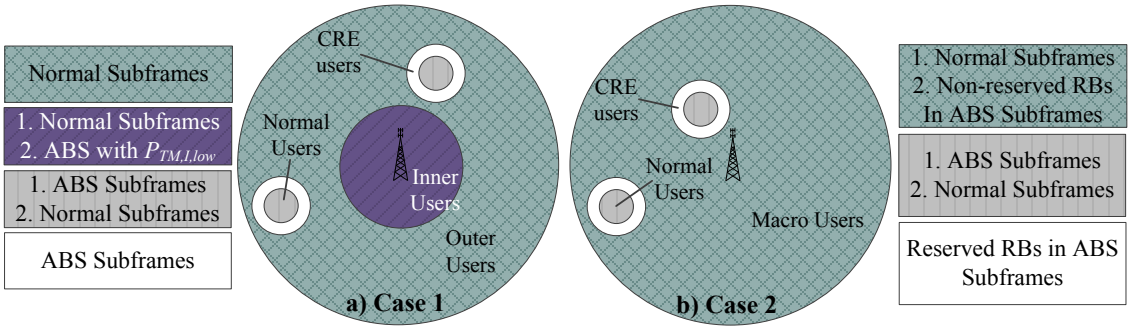

Figure 34: Allocation Criteria for a) case 1 and b) case 2

Case 1: The first strategy is applied in the case where the small cells that fall under the coverage area of the *i*-th macrocell are located at a high distance from the macro BS, specifically if the distance of the closest small cell d_s is above a certain threshold that is denoted as *Ths*. In this case, the time-power technique is applied taking advantage of the fact that the interference experienced by the small cell users is lower due to the high distance. The idea results from the FFR schemes studied in 3.1.1, where the macrocell was spatially divided into two areas; the inner and the outer. As such, by applying a similar concept, the ABS subframes can be utilized by the macrocell for transmissions to their inner users with the restriction of a lower transmit power in order to keep the generated interference in low levels. The macrocell user classification into inner and outer is carried out based on the average propagation loss (i.e. without including fast fading). Users with average propagation loss above a defined threshold (i.e. L_{th}) are classified as outer, while as inner are classified the users with average propagation loss below this threshold. Then, the subset of the outer users is denoted as $U_{O,i}$ and the subset of the inner users as $U_{I,i}$. It has to be noted that $U_{O,i} \cup U_{I,i}=U$. Moreover, the value of the L_{th} is set such that, according to the propagation model, the distance associated to L_{th} is lower than the distance d_s to the closest small cell.

The purpose of the above user classification is to allow transmissions to the inner users to be carried out in the RBs of the μ_i ABS subframes with reduced power level, while transmissions to the outer users are restricted only in the Normal subframes. Then, the transmit power per RB for the *i*-th macrocell will

be $P_{TM,i,low}$ for the ABS subframes allocated for transmissions to the inner users and $P_{TM,i,high}$ for the Normal subframes allocated for transmissions to either outer or inner users.

As for the resource allocation in the small cells, transmissions to the CRE users are allocated only in the ABS subframes, while transmissions to the normal users are allocated preferably in the ABS subframes, but they can also use the Normal subframes when there are not sufficient RBs in the ABS subframes. The transmit power per RB of the *k*-th small cell will be $P_{TS,k}$ in all the subframes allocated for transmissions to the small cell users. The abovementioned allocation criteria for both macro and small cell users in Case 1 are graphically summarized in Figure 34a.

Case 2: The second strategy is followed when at least one of the small cells is located in a closer distance from the macro BS (i.e. when the distance d_s between the macrocell and the closest small cell is below the threshold *Ths*). In this case, the small cells users and especially the CRE users are more susceptible to macrocell interference due to the small distance. As such, simultaneous transmissions during the ABS subframes are not practical even if the macrocell would transmit with reduced power. On that respect, a different approach is adopted where the split takes place in the frequency domain. In particular, a number $\varepsilon_i \leq N$ of RBs is especially reserved in each ABS subframe. These reserved RBs are primarily devoted for transmissions to the CRE users of the small cells, therefore macrocell data transmissions are prohibited in these RBs. In turn, macrocell transmissions can be performed either in the Normal subframes or in the (N- ε_i) non-reserved RBs of the ABS subframes with $P_{TM,i,high}$. In this way, the macrocell can utilize more resources whenever it is necessary, resulting in increasing the capacity. The key factor of this approach is that the number ε_i of reserved RBs may be reconfigured depending on the amount of the CRE users. In particular, in this work we assume the following:

$$\varepsilon = \min([\alpha \cdot numCRE], N) \tag{44}$$

where α is a parameter of the algorithm, *numCRE* is the total number of CRE users in the small cells within the coverage area of the *i*-th macrocell and [·] represents the rounding operation to the nearest integer value.

The purpose of this consideration is that when there are few CRE users, the number of ε_i is reduced in order to dispose additional resources for macrocell transmissions, while as the number of CRE users increases we approach the conventional ABS scenario where the macrocell cannot transmit in any of the RBs (i.e. $\varepsilon_i = N$) of the ABS subframes.

Summarizing the abovementioned considerations, transmissions to the CRE users can be allocated only in the reserved RBs of the ABS subframes with transmit power per RB $P_{TS,k}$, while transmissions to the normal users will be allocated preferably in the ABS subframes (both reserved and non-reserved), however they are allowed to be performed in the Normal subframes if there are not sufficient ABS

subframes. In all the cases the transmit power per RB will be $P_{TS,k}$. Finally, macrocell transmissions are preferably allocated in the Normal subframes, however when the resources are not adequate they are allowed to utilize the (N- ε_i) non-reserved RBs of the ABS subframes. In both cases the transmit power per RB will be $P_{TM,i,high}$. The abovementioned allocation criteria for both macro and small cell users in Case 2 are graphically summarized in Figure 34b.

Algorithm 3: Scheduling Algorithm in the i-th macrocell for a frame

compute $m_{u,RB}(f,t)$ *for each user* $u \in U_{M,i}$ *,for all RBs*
initialize $\Sigma_u=0$ *for each user* $u \in U_{M,i}$
for *each normal subframe t* //Normal subframes
  for $(f=1;f \le N)$
    U_{aux}=*set of users in* $U_{M,i}$ *with* $R_{u,RB(f,t)} \ge R_{b,min}$ *and* $\Sigma_u \le R_{b,max}$
    $u^* = \arg\max_{u \in U_{aux}} m_{u,RB(f,t)}$
    allocate RB(f,t) to user u with* $P_{TM,i,high}$
    $\Sigma_{u^*} = \Sigma_{u^*} + R_{u^*,RB(f,t)}$
  end for
end for
for *each ABS subframe t* //ABS subframes
  if $(ds<Ths)$ // Case 1
    for $(f=1;f \le N)$
      U_{aux}=*set of users in* $U_{I,i}$ *with* $R_{u,RB(f,t)} \ge R_{b,min}$ *and* $\Sigma_u \le R_{b,max}$
      $u^* = \arg\max_{u \in U_{aux}} m_{u,RB(f,t)}$
      allocate RB(f,t) to user u with* $P_{TM,i,low}$
      $\Sigma_{u^*} = \Sigma_{u^*} + R_{u^*,RB(f,t)}$
    end for
  end if
  else if $(ds>Ths)$ // Case 2
    for $(f=\varepsilon+1;f \le N)$ //only non-reserved RBs
      U_{aux}=*set of users in* $U_{M,i}$ *with* $R_{u,RB(f,t)} \ge R_{b,min}$ *and* $\Sigma_u \le R_{b,max}$
      $u^* = \arg\max_{u \in U_{aux}} m_{u,RB(f,t)}$
      allocate RB(f,t) to user u with* $P_{TM,i,high}$
      $\Sigma_{u^*} = \Sigma_{u^*} + R_{u^*,RB(f,t)}$
    end for
  end else if
end for

Algorithm 4: Scheduling Algorithm in the k-th small cell for a frame

compute $m_{u,RB}(f,t)$ *for each user* $u \in U_{S,k}$ *,for all RBs*
initialize $\Sigma_u=0$ *for each user* $u \in U_{S,k}$
for *each ABS subframe t* // ABS subframes
  if $(ds<Ths)$ // Case 1
    for $(f=1;f \le N)$ //all the RBs
      U_{aux}=*set of users in* $U_{CRE,k}$ *with* $R_{u,RB(f,t)} \ge R_{b,min}$ *and* $\Sigma_u \le R_{b,max}$
      if $U_{aux} = \varnothing$
        U_{aux}=*set of users in* $U_{N,k}$ *with* $R_{u,RB(f,t)} \ge R_{b,min}$ *and* $\Sigma_u \le R_{b,max}$
      end if
      $u^* = \arg\max_{u \in U_{aux}} m_{u,RB(f,t)}$
      allocate RB(f,t) to user u with* $P_{TS,k}$
      $\Sigma_{u^*} = \Sigma_{u^*} + R_{u^*,RB(f,t)}$
    end for
  else if $(ds>Ths)$ // Case 2
    for $(f=1;f \le \varepsilon)$ //reserved RBs
      U_{aux}=*set of users in* $U_{CRE,k}$ *with* $R_{u,RB(f,t)} \ge R_{b,min}$ *and* $\Sigma_u \le R_{b,max}$
      if $U_{aux} = \varnothing$
        U_{aux}=*set of users in* $U_{N,k}$ *with* $R_{u,RB(f,t)} > R_{b,min}$ *and* $\Sigma_u < R_{b,max}$
      end if
      $u^* = \arg\max_{u \in U_{aux}} m_{u,RB(f,t)}$
      allocate RB(f,t) to user u with* $P_{TS,k}$
      $\Sigma_{u^*} = \Sigma_{u^*} + R_{u^*,RB(f,t)}$
    end for
    for $(f=\varepsilon+1;f \le N)$ //non-reserved RBs
      U_{aux}=*set of users in* $U_{N,k}$ *with* $R_{u,RB(f,t)} > R_{b,min}$ *and* $\Sigma_u < R_{b,max}$
      $u^* = \arg\max_{u \in U_{aux}} m_{u,RB(f,t)}$
      allocate RB(f,t) to user u with* $P_{TS,k}$
      $\Sigma_{u^*} = \Sigma_{u^*} + R_{u^*,RB(f,t)}$
    end for
  end else if
end for
for *each normal subframe t* //Normal subframes
  for $(f=1;f<=N)$
    U_{aux}=*set of users in* $U_{N,k}$ *with* $R_{u,RB(f,t)} > R_{b,min}$ *and* $\Sigma_u < R_{b,max}$
    $u^* = \arg\max_{u \in U_{aux}} m_{u,RB(f,t)}$
    allocate RB(f,t) to user u with* $P_{TS,k}$
    $\Sigma_{u^*} = \Sigma_{u^*} + R_{u^*,RB(f,t)}$
  end for
end for

The pseudo-code of the scheduling algorithms for allocating the different RBs in each frame according to the abovementioned proposed criteria are presented in *Algorithm 3* and *Algorithm 4* for the macrocells and the small cells, respectively. The user prioritization for the scheduling process is carried out based on the Proportional Fair algorithm [96]. In particular, for each user u (where $u \in U_{M,i}$ when the scheduling is

carried out for the i-th macrocell and $u \in U_{S,k}$ for the scheduling at the k-th small cell) the following priority metric is defined, associated with each $RB(f,t)$:

$$m_{u,RB(f,t)} = \frac{R_{u,RB(f,t)}}{W_u} \tag{45}$$

where $R_{u,RB(f,t)}$ is the achievable bit rate by the user u in $RB(f,t)$ and W_u is the bit rate experienced by the user averaged over a window of the last T_W frames depending on the past allocation of RBs for this user. After each frame, W_u is updated taking into account the actual bit rate achieved by user u in its allocated RBs.

Besides, as noted in *Algorithm 3* and *Algorithm 4* given above, in order to avoid allocating a RB with very low bit rate, a user u is only considered as candidate for the assignment of $RB(f,t)$ if $R_{u,RB(f,t)}$ is above a specific threshold $R_{b,min}$. Moreover, the maximum number of RBs that can be allocated to a single user u in one frame is limited by the fact that the aggregation of the bit rates $R_{u,RB}(f,t)$ in the RBs allocated to this user should be below a maximum value $R_{b,max}$. This aggregated bit rates for a given user u is denoted as Σ_u in the pseudo-code, and is updated each time that an RB is allocated to this user u.

4.2.3 Simulation Results

The performance of the proposed solution has been carried out by means of simulations. In order to study the benefits brought by the presented strategies, comparisons have been carried out against the classical ABS scheme [85]. In this section, the simulation environment, the parameter setting and the numerical results are presented.

4.2.3.1 Simulation Scenario

The simulation scenario is comprised by a macrocell and two small cells in its coverage area. Two different configurations are considered according to the distribution of the small cells, as shown in Figure 35. In the first scenario (Figure 35a) one of the small cells is located close to the macro BS, while in the second scenario (Figure 35b) both small cells are located relatively far away from the macro BS. 90 users are non-homogeneously distributed in the scenario. Moreover, a number of users that is varied throughout the simulations is distributed in form of a Hot Spot (HS), as depicted in Figure 35. Depending on the scenario under study, the position of the HS is changed.

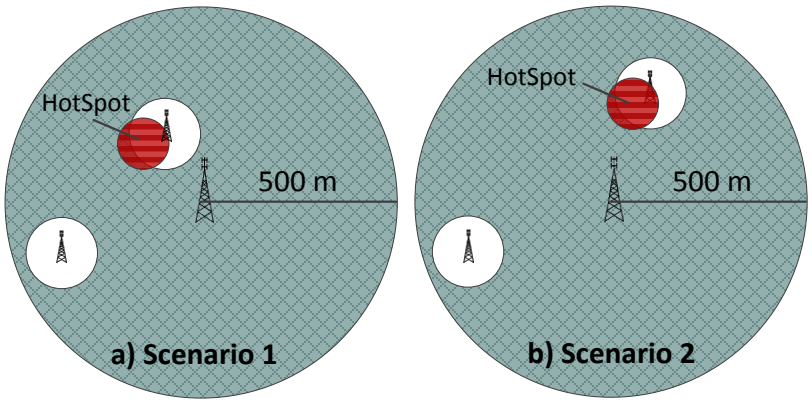

Figure 35: Simulation Scenarios a) Scenario 1 b) Scenario 2

The total propagation losses of a user u with the i-th macrocell and the k-th small cell are denoted as $L_{M,u,i,RB(f,t)}$ and $L_{S,u,k,RB(f,t)}$, respectively and calculated according to the following formula:

$$L(dB) = 128.1 + 37.6 \log d(km) + S - 10 \log F \quad (46)$$

where d corresponds to the user distance from the cell site, S (dB) is the shadowing modelled as a Gaussian random variable with standard deviation σ = 6 dB and F is the fast fading due to multipath, modelled as an exponential random variable with average 1 assumed independent for each RB and frame. The threshold Ths is set to the value of 250m, while the threshold for the user classification into inner and outer in case 1 is set to L_{th}=101.8 dB that corresponds to an inner cell radius of 200m according to the propagation model. Moreover, for the calculation of the reserved RBs in case 2 equation (44) is applied with $\alpha=2/\mu$. This value is obtained assuming that each CRE user will require on average 2 RBs to transmit.

The rest of the simulation parameters are given in Table IX.

TABLE IX: SIMULATION PARAMETERS

N	Number of RBs per subframe	25
μ	Number of ABS subframes	1 to 6
Δ	Cell Bias	3 dB
$P_{TM,i,high}$	Macrocell Transmit Power (high level)	29 dBm
$P_{TM,i,low}$	Macrocell Transmit Power (low level)	11 dBm
$P_{Ts,k,}$	Small cell Transmit Power	6 dBm
T_W	Window size	10 frames
P_N	Noise Power (per RB)	-115.5 dBm
$R_{b,min}$	Minimum bit rate threshold	50 Kbps
$R_{b,max}$	Maximum bit rate threshold	300 Kbps
Ths	Distance threshold	250m
L_{th}	User classification threshold	101.8dB

The achievable bit rate $R_{u,RB(f,t)}$ is modelled through the Shannon bound as:

$$R_{u,RB(f,t)} = B_{RB} \log_2 \left(1+\gamma_{u,RB(f,t)}\right) \quad (47)$$

where $\gamma_{u,RB(f,t)}$ is the signal to noise and interference ratio experienced by user u in the $RB(f,t)$. Finally, it has to be referred that the metric used for the evaluation of the proposed solution is the average capacity per user. This is computed by averaging over all the simulated frames the capacity C_u that a user u gets in each frame. C_u is computed by aggregating the bit rate in all the RBs allocated to the user u in this frame, that is:

$$C_u = \sum_{RB(f,t) \text{ allocated to user u}} B_{RB} \log_2 \left(1+\gamma_{u,RB(f,t)}\right) \quad (48)$$

The presented results are the average of 100 experiments, where each experiment is associated with a different random user distribution. Moreover, the simulation time of each experiment has been set to 1000 frames. For the evaluation of the results, the classical ABS scheme [85] is used as reference where macrocell data transmissions are not allowed to be allocated in any of the ABS subframes. As such, the ABS subframes are used exclusively by the small cells. More particularly, transmissions to the CRE users are restricted to the ABS subframes, while for the normal users there is also the possibility of exploiting the Normal subframes. Furthermore, only one transmit power level per RB is considered for the macrocell (i.e. $P_{TM,high}$). Finally, it has to be noted that CRE is being applied and that the same considerations with respect to the scheduling criteria and restrictions ($R_{b,min}$, $R_{b,max}$) are taken into account, in order to provide a fair comparison.

4.2.3.2 Numerical Results

Scenario 1: In the first scenario the two small cells are positioned at distances 400 and 150 meters (m) from the macro BS, as depicted in Figure 35a. Then, since the threshold *Ths* is equal to 250m the strategy applied by the proposed algorithm is to perform the splitting in the frequency domain (i.e. case 2) and therefore reserve a number ε of RBs in the ABS subframes for macrocell transmissions. It has to be noted that since only one macrocell is considered, for simplicity reasons the index i is omitted from the notation throughout the presentation of the results.

Figure 36 below depicts the gain (in %) achieved by the proposed eICIC solution with respect to the reference scheme in terms of average user capacity. The results are given as a function of the varying HS users and for different values of the number of ABS subframes (μ). As it can be noticed from the figure, a

significant gain is achieved by the proposed solution that increases with the number of the ABS subframes, reaching a value of 45% for μ=6. A key factor for this performance lies in the proper setting of the number of reserved RBs (ε) according to the number of the CRE small cell users. In particular, when the number of the HS users and consequently the number of the total small cell users is small, the number of the reserved RBs is configured by the algorithm to be also small. On the other hand, as the number of the HS users increases, the algorithm tends to reserve a higher amount of RBs in each ABS subframe. In other words, the proposed scheme can reconfigure the corresponding resources depending on the traffic load. Note also that for small number of ABS subframes, for instance 1 or 2, the behavior of the proposed solution resembles that of the reference scheme, since in this case the algorithm leads to ε=N, meaning that, like in the reference scheme, the macrocell is not allowed to transmit in ABS subframes.

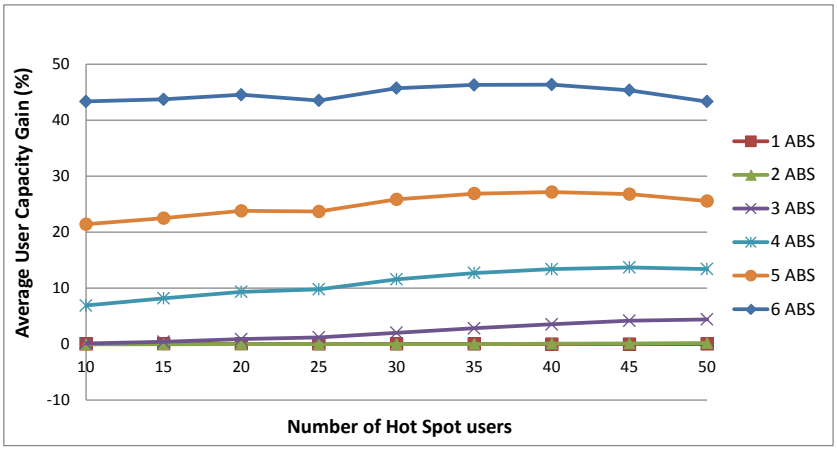

Figure 36: Average User Capacity Gain (%) – Scenario 1

Figure 37 and Figure 38 below, depict the average capacity gain (in %) with respect to the classical ABS approach for the macrocell and the small cell users, respectively. As it can be seen from Figure 37, a very high gain of the order of 70% is achieved in the capacity of the macrocell users, while a small loss that reaches a value of 15% is observed in Figure 38 for the case of the small cell users, especially when the number of the users in the HS is low. This behavior reflects the good performance of the algorithm, because it confirms that when the load of the macrocell is heavy but the load of the small cells is light, the proposed scheme tends to utilize the available resources in such a way that compensates the uneven user distribution. Furthermore, with the increment of the HS users, the algorithm still reserves some RBs in order to serve the traffic of the heavily loaded macrocell, although without generating severe interference to the small cell users. Therefore, it is proved that the proposed solution can adapt to traffic load changes and balance the capacity among the two types of cells, while keeping the introduced interference to the small cell users in low levels.

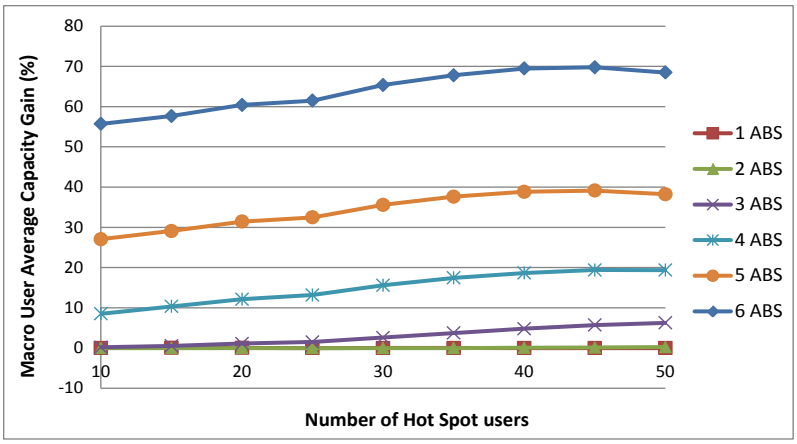

Figure 37: Macrocell User Average Capacity Gain (%) – Scenario 1

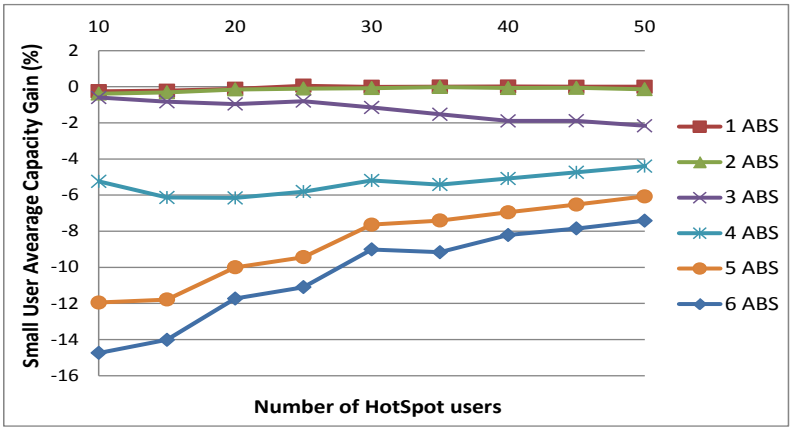

Figure 38: Small Cell User Average Capacity Gain (%) – Scenario 1

Scenario 2: In the second scenario the distance of the two small cells from the macro BS is 400m and 320m, respectively as shown in Figure 35b. Since their distance results to be above the defined threshold (i.e. *Ths*=250m), the algorithm applies case 1 and performs the macrocell splitting into two areas, the inner and the outer, and two transmit power levels are considered, $P_{TM,\,high}$ and $P_{TM,low}$.

In Figure 39 below, it is depicted the average user capacity gain (in %) of the proposed eICIC solution with respect to the classical ABS scheme. Similar observations can be conducted as in scenario 1. In particular, it can be clearly seen that the proposed solution outperforms the reference scheme in terms of average user capacity, while the gain offered by the algorithm increases with the number of the ABS subframes, reaching a value of 17% for the case of μ=6. The benefit results from the fact that the proposed scheme provides additional resources to the macrocell for transmissions to a fraction of its users (i.e. inner users) with the corresponding increase of the capacity.

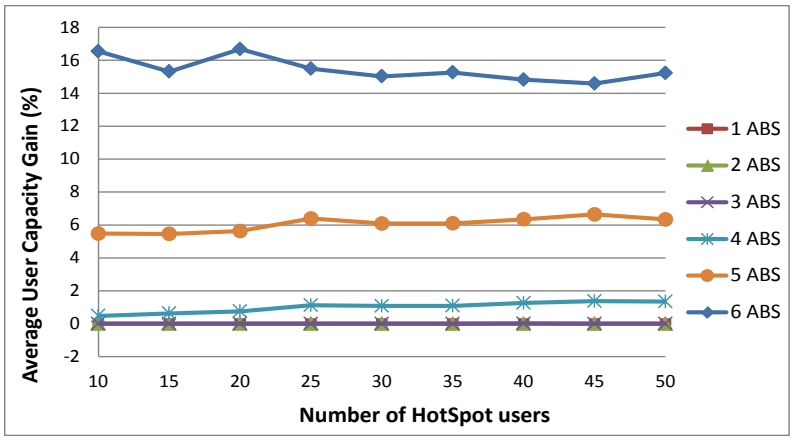

Figure 39: Average User Capacity Gain (%) – Scenario 2

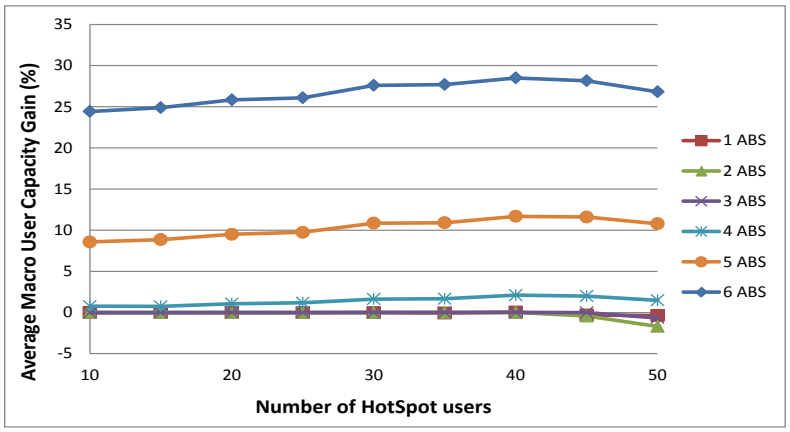

Figure 40: Macrocell User Average Capacity Gain (%) – Scenario 2

Compared to the previous scenario, the gain in this case is not that high. This occurs due to the difference in the macrocell capacity gain. As depicted in Figure 40 presented above, the gain of the macrocell user capacity is quite lower than in Scenario 1 (28% vs 70% for μ=6) because in this case only a fraction of macrocell users (i.e. the inner users) benefits from the additional resources in the ABS subframes. Moreover, transmissions to these users are carried out with lower transmit power, while at the same time a small amount of interference is present due to transmissions to the small cell users. In Scenario 1, all the macrocell users benefit from the reconfigurable amount of additional resources and transmissions were carried out with $P_{TM,i,high}$. As such, the gain of the macrocell users was higher, although there was an impact in the small cell capacity due to the generated interference to the normal users. In this case (Scenario 2), the behavior of the small cell capacity resembles the one presented in Scenario 1 (Figure 38), however the small cell users now experience less interference. This occurs primarily due to the lower transmit power of the macrocell and secondly due to the distance between the inner part of the macrocell and the small cells. It is worth mentioning that the highest loss in the small cells' capacity is of the order of 4% for μ=6. Finally, it has to be referred that despite the fact that the loss

in the small cells capacity is smaller, the major impact in the total user capacity results from the high difference it occurred in the macrocell user capacity gain.

4.3 Time-Frequency-Power eICIC (TFP-eICIC)

Despite the significant benefits brought in the network capacity by the above presented solution ([95]) and the efficiency it provides with respect to the resource utilization, the dependence of the scheme on the position of the small cells in the network topology does not endow the scheme with flexibility. Furthermore, additional signaling is necessary in order to be aware of the small cells position and to select the desired mechanism. Moreover, when the time-power strategy is applied, the most vulnerable CRE users are not completely protected from interference as in the classical ABS scheme, while in the frequency splitting the normal users of the small cells experience a noticeable amount of interference due to the high macrocell transmit power level. On that respect, an extension of [95] has been presented that is based on a combination of the time, frequency and power domains and is known as Time-Frequency-Power eICIC (TFP-eICIC) [97]. More details over the considerations of the proposed scheme are given in this chapter. The system model and the notation used throughout this work are the same as presented in 4.2.1.

4.3.1 Proposed TFP-eICIC Solution

The solution presented in 4.2, has been further modified and enhanced in order to employ only one mechanism that is independent of the position of the small cells and that exploits jointly the time, frequency and power domains with main objective to further improve the efficiency of the resource utilization and to balance in a more effective way the trade-off between the macrocell capacity degradation and the small cell interference reduction. As such, the main idea is to preserve the benefits brought by the ABS and therefore to keep protecting the most vulnerable users of the small cells (i.e. the CRE users), while offering to the macrocells additional resources under special conditions. In particular, the solution preserves the time splitting employed by the ABS scheme, while an additional splitting is introduced with respect to the frequency domain during the ABS subframes and at the same time two transmit power levels are provided for the macrocell transmissions. Therefore, the transmit power per RB for the k-th small cell is fixed and denoted as $P_{TS,k}$, while for the i-th macrocell depending on the subframe that is used to perform its transmissions, two possible transmit power levels per RB are considered. Same as in 4.2 these are denoted as $P_{TM,i,high}$ and $P_{TM,i,low}$.

Considering the *i*-th macrocell and the small cells that fall in its coverage area, the TFP-eICIC scheme is illustrated in Figure 41, which shows in detail the resource management and the allocation principles of the different transmissions depending on the user type.

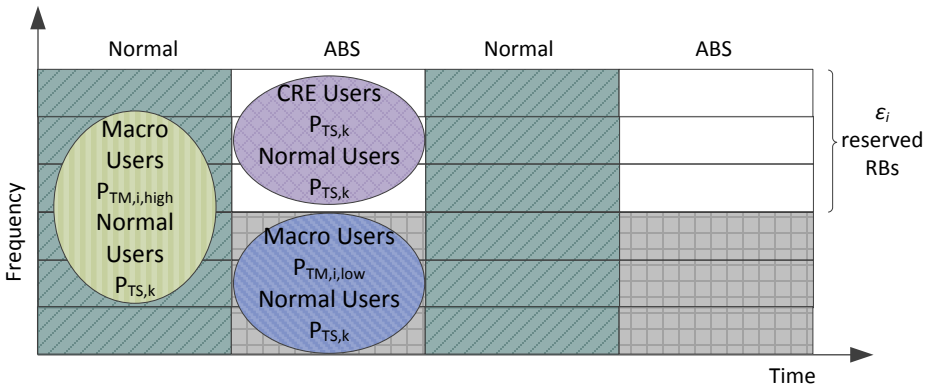

Figure 41: User allocation principles of the TFP-eICIC scheme

As it can be observed, the main aspect of the proposed solution is the additional division of the frequency domain in the ABS subframes. This allows to separate the different cell transmissions during the ABS subframes instead of devoting them exclusively to the small cells, and to exploit different transmit power levels. For this purpose a number of RBs $\varepsilon_i \leq N$ in each ABS subframe is reserved, as depicted in Figure 41. These reserved RBs are primarily devoted for transmissions to the CRE users of the small cells, since they are the most sensitive users to the macrocell interference. This means that no macrocell data transmissions are permitted in these ε_i RBs. Instead, the macrocell transmissions can take place in either the Normal subframes with transmit power $P_{TM,i,high}$ or in the (N-ε_i) non-reserved RBs of the ABS subframes with the restriction of a lower transmit power $P_{TM,i,low}$. In this way, it is possible to keep the generated interference to the small cells at low levels, while we avoid having the macrocell completely silenced during an ABS subframe, resulting in an increase of the macrocell capacity.

Based on these considerations, the allocation criteria of the solution are outlined in the following:

1. Transmissions of the *k*-th small cell to its CRE users can be assigned only in the reserved RBs of the ABS subframes with transmit power $P_{TS,k}$.
2. Transmissions of the *k*-th small cell to its normal users can be allocated in all the RBs of both the ABS and Normal subframes with the following hierarchy: Primarily, the reserved RBs of the ABS subframes are assigned. When these are not adequate, the non-reserved RBs are allocated. Finally, if there are still data to be transmitted but there are not sufficient RBs in the ABS subframes, the RBs of the Normal subframes are used, although at the cost of higher interference. In all the cases the transmit power is $P_{TS,k}$.

3. Transmissions of the macrocell to its users are assigned preferably in the RBs of the Normal subframes. When there is a lack of resources, the macrocells can perform transmissions in the non-reserved RBs of the ABS subframes with $P_{TM,i,low}$.

Same as in 4.2, an important feature of the scheme lies on the reconfiguration of the number of the reserved RBs (ε_i) based on the number of the CRE users using equation (44). As such, ε_i is adjusted in a way that will cover the transmission needs of the CRE users in order to keep them protected from interference, while whenever it is possible, additional resources will be disposed for macrocell transmissions. Finally, the procedure for the allocation of the different RBs in each frame is shown in *Algorithm 5* and *Algorithm 6* given below for the macro and the small cells, respectively. It has to be noted, that the Proportional Fair [96] algorithm is applied as presented in 4.2.2, as well as the $R_{b,min}$ and $R_{b,max}$ restrictions.

Algorithm 5: Scheduling Algorithm in the i-th macrocell

1: *compute* $m_{u,RB(f,t)}$ *for each user* $u \in U_{M,i}$ *,for all RBs*
2: *initialize* $\Sigma_u=0$ *for each user* $u \in U_{M,i}$
3: ***for*** *each normal subframe t* //*Normal subframes*
4: ***for*** *(f=1;f<=N)*
5: U_{aux}=*set of users in* $U_{M,i}$ *with* $R_{u,RB(f,t)} \geq R_{b,min}$ *and* $\Sigma_u \leq R_{b,max}$
6: $u^* = \arg\max_{u \in U_{aux}} m_{u,RB(f,t)}$
7: *allocate RB(f,t) to user u* with* $P_{TM,i,high}$
8: $\Sigma_{u^*} = \Sigma_{u^*} + R_{u^*,RB(f,t)}$
9: ***end for***
10: ***end for***
11: ***for*** *each ABS subframe t* //*ABS subframes*
12 ***for*** *(f= ε +1;f<=N)* //*non-reserved RBs*
13: U_{aux}=*set of users in* $U_{M,i}$ *with* $R_{u,RB(f,t)} \geq R_{b,min}$ *and* $\Sigma_u \leq R_{b,max}$
14: $u^* = \arg\max_{u \in U_{aux}} m_{u,RB(f,t)}$
15: *allocate RB(f,t) to user u* with* $P_{TM,i,low}$
16: $\Sigma_{u^*} = \Sigma_{u^*} + R_{u^*,RB(f,t)}$
17: ***end for***
18: ***end for***

Algorithm 6: Scheduling Algorithm in the k-th small cell

1: *compute* $m_{u,RB(f,t)}$ *for each user* $u \in U_{S,k}$ *,for all RBs*
2: *initialize* $\Sigma_u=0$ *for each user* $u \in U_{S,k}$
3: ***for*** *each ABS subframe t* // *ABS subframes*
4: ***for****(f=1;f<= ε)* //*reserved RBs*
5: U_{aux}=*set of users in* $U_{CRE,k}$ *with* $R_{u,RB(f,t)} \geq R_{b,min}$ *and* $\Sigma_u \leq R_{b,max}$
6: ***if*** $U_{aux} = \varnothing$
7: U_{aux}=*set of users in* $U_{N,k}$ *with* $R_{u,RB(f,t)} \geq R_{b,min}$ *and* $\Sigma_u \leq R_{b,max}$
8: ***end if***
9: $u^* = \arg\max_{u \in U_{aux}} m_{u,RB(f,t)}$
10: *allocate RB(f,t) to user u* with* $P_{TS,k}$
11: $\Sigma_{u^*} = \Sigma_{u^*} + R_{u^*,RB(f,t)}$
12: ***end for***
13: ***for*** *(f= ε+1;f<=N)* //*non-reserved RBs*
14: U_{aux}=*set of users in* $U_{N,k}$ *with* $R_{u,RB(f,t)} \geq R_{b,min}$ *and* $\Sigma_u \leq R_{b,max}$
15: $u^* = \arg\max_{u \in U_{aux}} m_{u,RB(f,t)}$
16: *allocate RB(f,t) to user u* with* $P_{TS,k}$
17: $\Sigma_{u^*} = \Sigma_{u^*} + R_{u^*,RB(f,t)}$
18: ***end for***
19: ***end for***
20: ***for*** *each normal subframe t* //*Normal subframes*
21: ***for*** *(f=1;f<=N)*
22: U_{aux}=*set of users in* $U_{N,k}$ *with* $R_{u,RB(f,t)} \geq R_{b,min}$ *and* $\Sigma_u \leq R_{b,max}$
23: $u^* = \arg\max_{u \in U_{aux}} m_{u,RB(f,t)}$
24: *allocate RB(f,t) to user u* with* $P_{TS,k}$
25: $\Sigma_{u^*} = \Sigma_{u^*} + R_{u^*,RB(f,t)}$
26: ***end for***
27: ***end for***

4.3.2 Simulation Results

The evaluation of the proposed solution has been carried out through simulations and comparisons with existing solutions. In particular, the classical ABS [85], the LP-ABS [91]-[93] and the solution

presented in 4.2 [95], are used as benchmarks schemes. The simulation scenario, the evaluation criteria and the numerical results are presented in detail in this section.

4.3.2.1 Simulation Scenario

The simulation scenario consists of a macrocell and three small cells in its coverage area. Two different deployments of the small cells are studied, as depicted in Figure 42 below. In the first case (scenario 1), all the small cells are deployed in a high distance from the macro BS as shown in Figure 42a, while in scenario 2 (Figure 42b), one of the small cells is located close to the macro BS so the small cell users will experience higher interference. In both scenarios, a total of 110 users are randomly distributed following a uniform distribution. Moreover, two Hot Spots are included as shown in Figure 42. Hot Spot 1 (HS 1) consists of 20 users, while the number of users of Hot Spot 2 (HS 2) is varied throughout the simulations.

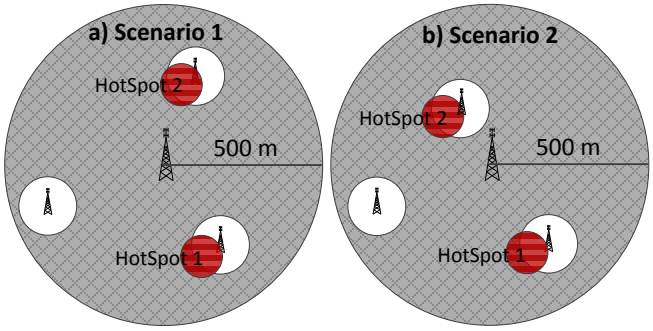

Figure 42: Simulation Scenarios a) Scenario 1 b) Scenario 2

The total propagation loses of user u with the i-th macrocell (i.e. $L_{M,u,i,RB(f,t)}$) and the k-th small cell (i.e. $L_{S,u,k,RB(f,t)}$) are calculated according to equation (46) presented in section 4.2.3.1. The calculation of the reserved RBs is carried out as in 4.2.2 according to equation (44) with the same assumption of $\alpha=2/\mu$..The rest of the simulation parameters are presented in Table X.

TABLE X: SIMULATION PARAMETERS

N	Number of RBs per subframe	25
μ	Number of ABS subframes	1 to 6
Δ	Cell Bias	3 dB
$P_{TM,,high}$	Macrocell Transmit Power (high level)	29 dBm
$P_{TM,,low}$	Macrocell Transmit Power (low level)	23 dBm
$P_{Ts,k,}$	Small cell Transmit Power	6 dBm
T_W	Window size	10 frames
P_N	Noise Power (per RB)	-115.5 dBm
$R_{b,min}$	Minimum bit rate threshold	50 Kbps
$R_{b,max}$	Maximum bit rate threshold	300 Kbps

The performance of the proposed solution is carried out based on the average user capacity (equation (48)) as presented in section 4.2.3.1. Finally, it has to be noted that the results presented in this section are the average of 100 experiments with different random user distributions. The duration of each experiment corresponds to 1000 frames.

4.3.2.2 Reference Schemes

The reference schemes used for the comparisons with the proposed solution are presented in the following:

1. The classical ABS scheme [85] as presented in 4.2.3.1. Briefly, transmissions to the CRE are allocated only in the ABS subframes, while for the normal users the RBs of the Normal subframes can also be used. Macrocell data transmissions are restricted only to the Normal subframes. For the macrocell only one level of transmit power is considered i.e. $P_{TM,i,high}$.
2. The LP-ABS scheme [91]-[93], where macrocell transmissions can be allocated in any RBs of the ABS subframes with the restriction of a lower transmit power (i.e. $P_{TM,i,low}$). Transmissions to the normal users of the small cells can be carried out also in the Normal subframes.
3. The solution of [95] as presented in 4.2.

It has to be noted that the CRE technique is applied in all the solutions. Moreover, all the simulations have been carried out under the same principles, criteria and limitations for the resource allocation as the TFP-eICIC scheme in order to have a fair comparison.

The results are given in terms of gain (in %) that the proposed solution, the LP-ABS and the solution of [95] achieve with respect to the classical ABS scheme. Moreover, in all the figures the solid lines represent the proposed solution, while the LP-ABS and the solution of [95] are given in dashed and dotted lines, respectively.

4.3.2.3 Numerical Results

Scenario 1: In this scenario all the small cells are located at high distance from the macro BS with purpose to examine the case that the small cells are less affected from the macrocell interference. Figure 43 below depicts the average user capacity gain (in %) of the proposed solution, the LP-ABS and the solution of [95] with respect to the classical ABS. It has to be noted that in this case the solution of [95] applies the time-power strategy, where the macrocell is allowed to exploit the ABS subframes to perform transmissions to the users of its inner part with $P_{TM,i,low}$.

As it can be seen in the figure, the proposed solution outperforms the rest of the strategies. The gain achieved with respect to the classical ABS reaches the value of 20%, thanks to the modification in the management of the ABS subframes. In particular, in TFP-eICIC the macrocells benefit from the additional resources, while the small cells users and especially the CRE users are protected from high interferences. In addition, the proposed solution performs better in comparison to the other two schemes due to the fact that interference is seen only by the normal small cell users, while the CRE users are completely protected from macrocell interference. On the contrary, in [95] interference that comes from transmissions to a fraction of the macrocell users (inner users) affects all the small cell users, while in LP-ABS the interference comes from all the macrocell transmissions to its users and affects all the small cell users. It has to be noted that the obtained gain of all the schemes with respect to the classic ABS reduces when decreasing the number of ABS subframes, since in all the cases less resources can be exploited by the macrocells to perform their transmissions.

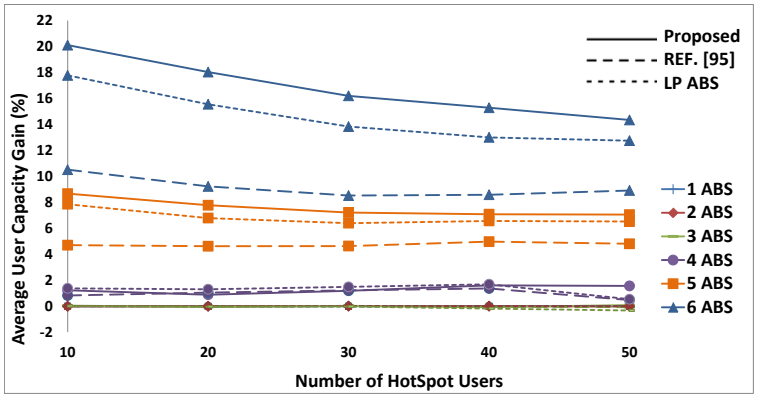

Figure 43: Average User Capacity Gain (%)

The average macrocell and CRE user capacity gains (in %) are presented in Figure 44 and Figure 45, respectively. Starting from Figure 44, it can be observed that the schemes that bring the most significant improvements in the macrocell user capacity are the TFP-eICIC and the LP-ABS. This occurs due to the fact that these two solutions offer more resources for macrocell transmissions to all of its users, while in the solution of [95] only a fraction of the macrocell users benefits from the additional resources (i.e. inner users). However, it can be clearly seen that the proposed solution presents the better performance.

Finally, in Figure 45 it can be clearly noticed that the capacity degradation that the CRE users experience due to the interference introduced in LP-ABS and in [95], is stronger, while for the TFP-eICIC scheme is around zero.

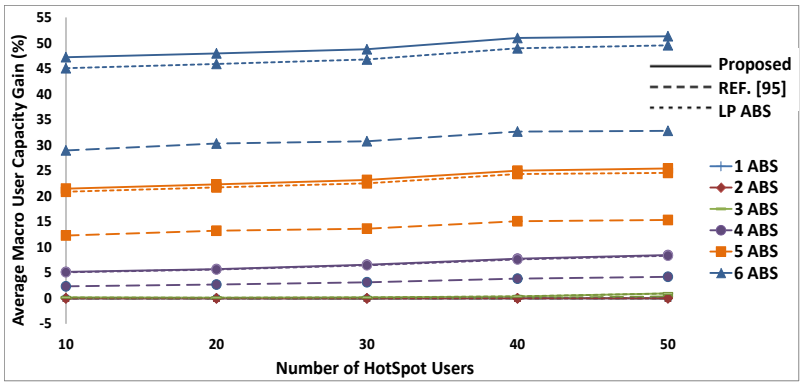

Figure 44: Average Macrocell User Capacity Gain (%)

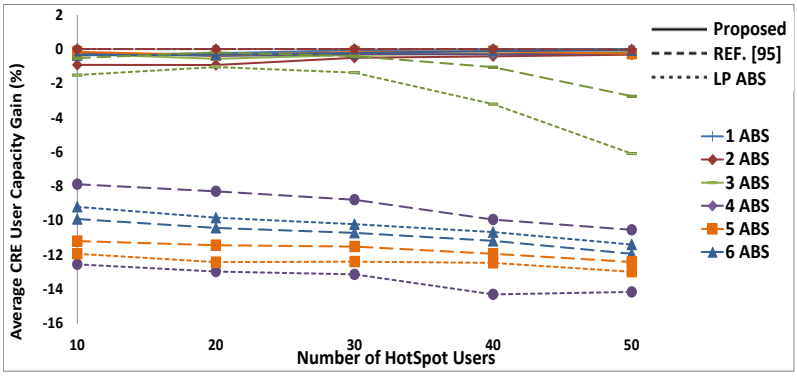

Figure 45: Average CRE User Capacity Gain (%)

Scenario 2: In this scenario one of the small cells is located in a closer distance from the macro BS, therefore its users are more susceptible to interference. It has to be noted that in this case the solution of [95] applies a similar strategy as the proposed TFP-eICIC scheme by reserving a number of RBs in the frequency domain for transmissions to the CRE users, while providing the rest for macrocell transmissions; however by considering only one level of transmit power (i.e. $P_{TM,i,high}$).

Figure 46 below depicts the average user capacity gain (in %) provided by all the considered strategies with respect to the classical ABS.

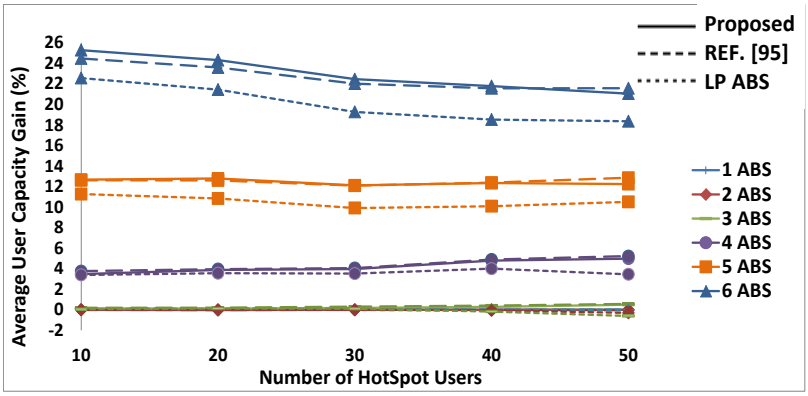

Figure 46: Average User Capacity Gain (%)

Form the figure it can be observed that the TFP-eICIC presents a significant gain with respect to the classical ABS that reaches a value of 26% and therefore it can be clearly stated that it utilizes more efficiently the available resources. Moreover, it can be seen that it outperforms the rest of the strategies, although the difference is not that noticeable, especially when compared to the approach of [95]. This resemblance occurs from the fact that apart from the different transmit power levels a similar approach is followed by the two solutions under this topology. The advantage of the TFP-eICIC with respect to [95] is the lower transmit power that reduces the generated interference levels to the normal small cells users. As far as for the LP-ABS, the difference occurs due to the fact that in TFP-eICIC scheme transmissions to the CRE users can be allocated to reserved RBs that are free of interference, while this is not the case for the LP-ABS, where the macrocell generates a higher level of interference.

Table XI: Macro and CRE Capacity Gain for 6 ABS

Hot Spot Users	Macro user GAIN (%)			CRE Gain (%)		
	Proposed	**LP-ABS**	**[95]**	**Proposed**	**LP-ABS**	**[95]**
10	53.81	51.15	53.94	-0.34	-8.89	-0.53
40	59.79	57.53	61.32	0.44	-11.41	-0.06

Finally, Table XI presents the gain in the macrocell and CRE user capacity for this scenario in the case of μ=6. Similar observations as in Scenario 1 can be conducted. TFP-eICIC, LP-ABS and the solution of [95], achieve a similar gain for the macrocell user case, however in TFP-eICIC the CRE users are more protected from interference as in the classical ABS.

4.4 Optimized TFP-eICIC using Genetic Algorithms (OTFP-eICIC)

By exploiting jointly the time, frequency and power domains, the TFP-eICIC scheme presented in the previous chapter has been proved to improve significantly the resource utilization and the capacity of the macrocells, while keeping the generated interference in the small cells in low levels. However, additional benefits can be achieved by determining properly the partitions in the three domains. As such, the solution has been optimized using genetic algorithms with main target the further improvement of the performance of the scheme. In particular, the parameters that are optimized are the number of ABS Subframes, the number of reserved RBs, the lower transmit power level, and the CRE bias of each small cell, in order to take also under consideration the load balancing. The proposed solution is known as OTFP-eICIC and it has been presented in [98]. In the following chapters the optimization framework is presented in detail, together with the simulation-based performance evaluation.

4.4.1 Capacity Estimation

The target of the optimization is the maximization of the network capacity. As such, in order to apply an optimization framework there is the need to estimate the capacity according to a given configuration of the system parameters. On that respect, the procedure that is followed for the estimation of the aggregated capacity as a function of the system parameters is presented in the following. Before proceeding to the presentation, it has to be referred that the system model and the notation used throughout this work is as presented in section 4.2.1. Moreover the resource management follows the principles presented in section 4.3.1 with only difference that the restriction $R_{b,max}$ in this case is modified so as to define a maximum number of RBs that can be allocated to a single user u, instead of a maximum bit rate. This limitation is denoted as RB_{max} (instead of $R_{b,max}$ in 4.3.1) and is introduced in order to avoid the allocation of a high number of RBs to only one user.

The estimation of the aggregated capacity is carried out based on the fact that the different resources $RB(f,t)$ can be classified in different subsets in one frame depending on the given configuration of the parameters ε and μ of the algorithm, as presented in Figure 47 below. In this way, we define as A_N the subset that includes the RBs that belong to the Normal subframes, as A_{NR} the subset that includes the non-reserved RBs of the ABS subframes and finally as A_R the subset that includes the reserved RBs of the ABS subframes. As such, for any macrocell $m \in M$ the total number of RBs in each subset can be calculated as $N_{N,m} = N \cdot \lambda_m$, $N_{NR,m} = (N - \varepsilon_m) \cdot \mu_m$ and $N_{R,m} = \varepsilon_m \cdot \mu_m$, for the A_N, A_{NR} and A_R subsets, respectively. It has to be noted that this classification is valid for the m-th macrocell and for the small cells that fall inside its coverage area.

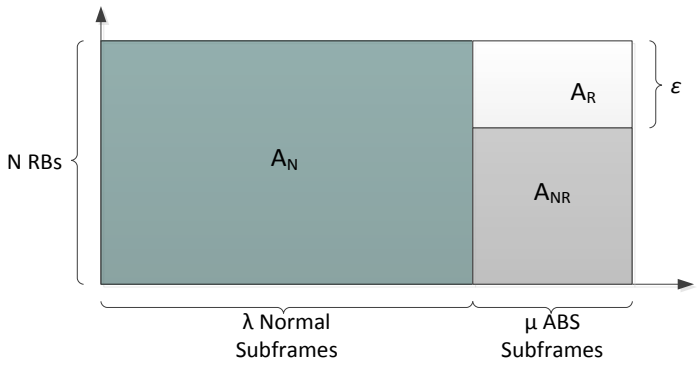

Figure 47: Classification of the resources in subsets. For simplicity, the figure considers that all the ABS subframes are contiguous, though this does not necessarily has to be the case

In this way, the total capacity can be estimated by aggregating the average capacity for each cell $m \in M \cup S$, either macrocell or small cell, and each subset $A_x \in \{A_N, A_R, A_{NR}\}$.

$$C = \sum_{m} \sum_{A_x} RB_{oc,A_x,m} B_{RB} G_{MUD} \log_2 \left(1 + \hat{\gamma}_{A_x,m}\right) \quad (49)$$

where $RB_{oc,Ax,m}$ is the estimation of the RBs that are occupied in the subset A_x of cell m and $\hat{\gamma}_{A_x,m}$ is an estimation of the Signal to Noise and Interference Ratio (SINR) seen by the users of cell m in the RBs of subset A_x. $RB_{oc,Ax,m}$ will be computed in section 4.4.1.1, while the computation of $\hat{\gamma}_{A_x,m}$ will be presented in section 4.4.1.2.

G_{MUD} stands for the multiuser diversity gain, which is a gain factor used to capture the capacity increase achieved due to the diversity of the channel conditions seen by the different users. In particular, in the case that the number of the users is high, there is higher probability that the PF scheduler will select a user with better SINR conditions, resulting in this way in higher capacity [99][100]. As such, G_{MUD} takes different values depending on the estimated $\hat{\gamma}_{A_x,m}$ and the number of the users in cell m.

4.4.1.1 Computation of $RB_{oc,Ax,m}$

The estimation of $RB_{oc,Ax,m}$ is carried out by taking into account the allocation principles and the classification of the resources for each cell, as presented in 4.3.1 and in 4.4.1, respectively. As such, for any macrocell $m \in M$ we have:

$RB_{oc,A_N,m}$: This is the estimation of the occupied resources in the subset A_N. As it is known, all the macrocell transmissions will be allocated preferably in the Normal subframes and therefore in the subset A_N. Moreover, the total number of users in the m macrocell is $|U_{M,m}|$, where $|\cdot|$ denotes cardinality. Assuming that a user can only get up to RB_{max} resources, then the total number of occupied resources in the subset A_N will be the minimum between the resources required by all the users in the macrocell $|U_{M,m}| \cdot RB_{max}$ and the number of total resources $N_{N,m}$:

$$RB_{oc,A_N,m} = \min\left(\left|U_{M,m}\right| \cdot RB_{\max}, N_{N,m}\right) \quad (50)$$

$RB_{oc,A_R,m}$: Represents the estimation of the occupied resources in the A_R subset. Since no macrocell transmissions are permitted in subset A_R, the occupied resources will be zero:

$$RB_{oc,A_R,m} = 0 \quad (51)$$

$RB_{oc,A_{NR},m}$: This is the estimation of the occupied resources in the A_{NR} subset. Since the macrocell transmissions are performed preferably in the A_N subset, then in order to estimate the occupied resources in the A_{NR} subset it should be considered only the required RBs after having allocated first the RBs in the A_N subset ($RB_{oc,A_N,m}$). Thus, the occupied resources in A_{NR} will be the minimum between $|U_{M,m}|\cdot RB_{max}$ minus the occupied resources in the A_N subset ($RB_{oc,A_N,m}$), and the total of $N_{NR,m}$ resources:

$$RB_{oc,A_{NR},m} = \min\left(\left|U_{M,m}\right|\cdot RB_{\max} - \min\left(\left|U_{M,m}\right|\cdot RB_{\max}, N_{N,m}\right), N_{NR,m}\right) \quad (52)$$

The estimation of the occupied resources with respect to the $m \in S$ small cell is carried out using the same rationality, however it has to be noted that the partitions in the time and frequency domain and therefore the number of RBs in each subset are defined by the $m^* \in M$ macrocell that is received with the highest power by the small cell. As such, starting from the A_R subset the estimations are as follows:

$RB_{oc,A_R,m}$: Since the small cell transmissions are assigned preferably in the A_R subset, then the estimation of the resources in the A_R subset will be the minimum between the resources needed for the all the small cell users ($|U_{S,m}|\cdot RB_{max}$) and the total N_{R,m^*} resources available:

$$RB_{oc,A_R,m} = \min\left(\left|U_{S,m}\right|\cdot RB_{\max}, N_{R,m^*}\right) \quad (53)$$

$RB_{oc,A_{NR},m}$: Small cell transmissions to the normal users can be carried out in the A_{NR} subset after having allocated first the resources of the A_R subset. As such, the resources of the A_R subset allocated to normal users should be calculated first. In order to do so, it should be considered that the resources of the A_R subset are allocated preferably to CRE users. Therefore, the resources available for the normal users will be N_{R,m^*} - min($|U_{CRE,m}|\cdot RB_{max}$, N_{R,m^*}), i.e. the resources in A_R after extracting those assigned to CRE users. Then, the number of RBs allocated to normal users in the A_R subset will be given by the minimum between the resources required by the normal users $|U_{N,m}|\cdot RB_{max}$ and the available ones, that is min($|U_{N,m}|\cdot RB_{max}$, N_{R,m^*} - min($|U_{CRE,m}|\cdot RB_{max}$, N_{R,m^*})). Therefore, the estimated number of occupied resources in the A_{NR} area will be given by:

$$RB_{oc,A_{NR},m} = \min\left(\left|U_{N,m}\right|\cdot RB_{\max} - \min\left(\left|U_{N,m}\right|\cdot RB_{\max}, N_{R,m^*} - \min\left(\left|U_{CRE,m}\right|\cdot RB_{\max}, N_{R,m^*}\right)\right), N_{NR,m^*}\right) \quad (54)$$

$RB_{oc,A_{NR},m}$: Small cell transmissions in the A_N subset can be carried out only for the normal users. The allocation is done after having assigned first the resources in the A_R and A_{NR} subsets, respectively. Then, following similar reasoning as in the previous case, we get:

$$RB_{oc,A_N,m} = \min\left(\left|U_{N,m}\right| \cdot RB_{\max} - \min\left(\left|U_{N,m}\right| \cdot RB_{\max}, N_{R,m^*} + N_{NR,m^*} - \min\left(\left|U_{CRE,m}\right| \cdot RB_{\max}, N_{R,m^*} \right) \right), N_{N,m^*} \right) \quad (55)$$

4.4.1.2 *Computation of* $\hat{\gamma}_{A_x,m}$

The estimation of the Signal to Noise and Interference Ratio for a RB belonging to the subset A_x is calculated as:

$$\hat{\gamma}_{A_x,m} = \frac{\overline{\overline{P_{m,A_x}}}}{\overline{L_{m,m,A_x}}} \over P_N + I_{A_x,m} \quad (56)$$

where P_N denotes the noise power per RB, $P_{m,Ax}$ denotes the transmit power of cell m in a RB belonging to the subset A_x and is given by:

$$P_{m,A_x} = \begin{cases} P_{TS,m} & \forall A_x,\ \forall m \in S \\ P_{TM,m,high} & \text{if } A_x = A_N,\ \forall m \in M \\ P_{TM,m,low} & \text{if } A_x = A_{NR},\ \forall m \in M \\ 0 & \text{if } A_x = A_R,\ \forall m \in M \end{cases} \quad (57)$$

$\overline{L_{m,j,Ax}}$ is the average path loss of the users allocated in the subset A_x of cell m with respect to cell j:

$$\overline{L_{m,j,Ax}} = \frac{1}{\left|U_{Ax,m}\right|} \sum_{u \in U_{Ax,m}} \overline{L_{u,j}} \quad (58)$$

In (58) $\overline{L_{u,j}}$ is the average propagation loss of user u with respect to cell j after having averaged the fast fading, and $U_{Ax,m}$ denotes the set of users of cell m that can be allocated in the RBs of subset A_x, given by:

$$U_{A_N,m}=\begin{cases}U_{M,m} & \text{if m}\in M\\ U_{N,m} & \text{if m}\in S\end{cases}\quad U_{A_R,m}=\begin{cases}\varnothing & \text{if m}\in M\\ U_{S,m} & \text{if m}\in S\end{cases}\quad U_{A_{NR},m}=\begin{cases}U_{M,m} & \text{if m}\in M\\ U_{N,m} & \text{if m}\in S\end{cases} \tag{59}$$

Finally, $I_{Ax,m}$ is the interference seen by the users of cell m in a RB of the subset A_x, estimated as:

$$I_{A_x,m}=\sum_{\substack{j\in M\cup S\\ j\neq m}}\left[\frac{P_{j,A_x}}{L_{m,j,A_x}}\cdot\frac{RB_{oc,Ax,j}}{N_x}\right] \tag{60}$$

where N_x is the number of RBs in subset A_x, i.e. $N_x=N_R$ for A_R, $N_x=N_{NR}$ for A_{NR} and $N_x=N_N$ for A_N.

4.4.2 Genetic Algorithm-based Optimization

4.4.2.1 Problem Formulation

Based on the framework presented in section 4.4.1 for the estimation of the capacity, the optimization problem to derive the optimum values of the parameters for the OTFP-eICIC scheme (i.e. the number of ABS subframes μ_i, the number of reserved RBs ε_i and the lower transmit power $P_{TM,i,low}$ for the i-th macrocell, and the CRE bias Δ_k of the k-th small cell) can be formulated as follows:

$$\begin{aligned}&\underset{\mu_i,\varepsilon_i,P_{TM,i,low},\Delta_k}{\arg\max}\quad C\\ &s.t.\\ &\quad 0\le\mu_i\le 10\qquad \mu_i\in\mathbb{Z}\\ &\quad 0\le\varepsilon_i\le N\qquad \varepsilon_i\in\mathbb{Z}\\ &\quad 0\le P_{TM,i,low}\le P_{TM,i,high}\quad P_{TM,i,low}\in\mathbb{R}\\ &\quad 0\le\Delta_k\le\Delta_{\max}\quad \Delta_k\in\mathbb{R}\end{aligned} \tag{61}$$

where Δ_{max} is the maximum value of the CRE bias.

The above presented optimization problem is classified as mixed integer non-linear programming (MINLP) type. Such type of problems is known to be NP-hard and can be solved using heuristic methods. For this reason, genetic algorithms have been selected in this work as optimization tool since they belong to the category of heuristic search algorithms. Genetic algorithms rise from the natural evolution and are considered a useful tool due to their simplicity and their ability to investigate search among several

potential solutions [101][102]. The main idea of genetic algorithms lies on imitating the evolution of the organisms, such as "competition for survival" of the best and usage of operators that recombine the possible solutions.

4.4.2.2 Genetic Algorithm Description

In order to apply genetic algorithms, a vector $\mathbf{s}=[p_1,\ldots, p_R]$ is defined that is known as the *individual* or *chromosome* in the genetic algorithms terminology and that is comprised of the potential configurations of the network. As such, each individual contains the R parameters or *genes* ($p_1,\ldots, p_R$) that are subject of optimization. In this work, the R genes correspond to the number of the ABS Subframes μ_i, the number of the reserved RBs ε_i, the lower transmit power level $P_{TM,i,low,}$ for each macrocell i =1,...,V and the CRE biases Δ_k of each small cell k=1,...,P. Each parameter p_r, r=1,...,R can take a discrete number of possible values ranging from $p_{r,min}$ to $p_{r,max}$ in steps of $step_r$.

The algorithm is executed iteratively, and in each iteration also referred to as *generation* and denoted as z, a number S_{POP} of candidate configurations (individuals) known as *population* is selected. Then, each individual is evaluated using a function known as *fitness* or *cost function*. In this context, the fitness function of individual **s** is the estimated network capacity $C(\mathbf{s})$ that results from equation (49) according to the configuration of the parameters corresponding to the individual **s**.

When the algorithm is triggered, it begins with the selection of the S_{POP} individuals that compose the population of the first generation z=1. Each individual is obtained by assigning to each parameter p_r a random value uniformly selected among the set of possible values from $p_{r,min}$ to $p_{r,max}$ in steps of $step_r$.

In each iteration (or generation) z, the procedure presented below is followed, as illustrated in Figure 48:

1. The capacity $C(\mathbf{s}_x)$ is calculated for each individual s_x of the population, x=1, ..., S_{POP}.
2. The algorithm retains the individual **s*** with the maximum capacity among the individuals of generation z and the individuals of previous generations.
3. The algorithm proceeds with the creation of a new population of individuals for the next generation z+1 by applying the following set of operators to the individuals of generation z:

   Selection: The selection of two individuals of the current generation, known as *parents*, is carried out with this operator. Then, the parents are used to create two new individuals, known as *children* for the next generation. The target is to allow the best individuals to survive with higher

chances in order to pass their "good" genes to the next generations. For this purpose, the individuals in this process are selected according to their cost, so that individuals with higher capacity have higher probability to be selected. In this work, the selection process is carried out with the so called *roulette-wheel selection* [103], where an individual $\mathbf{s}_x$ is selected according to the following probability:

$$P_s(\mathbf{s}_x) = \frac{C(\mathbf{s}_x)}{\sum_{y=1}^{S_{POP}} C(\mathbf{s}_y)} \tag{62}$$

Recombination: The main idea of this operator is to preserve some of the characteristics (genes) of the best individuals of the current generation with purpose to create children for the next generation with chances to be "fitter" than the parents. On that respect, the recombination starts from the two parents obtained in the selection process and the so-called *1-point cross-over* methodology is applied in order to obtain two children. The procedure is depicted in Figure 49 where as it can be seen a *cross-point* is selected randomly that defines the position from which the genes of the two parents will be separated and swapped with each other.

Mutation: The last operator is responsible for introducing some randomness in the genes of the children with target to expand the search space [102]. For each gene, the probability that a mutation is applied is given by 1/R. If the gene is selected for mutation, its value is altered by randomly selecting a value from the range of values this gene can take.

The result of the execution of the above presented processes is to have two new individuals for the next generation. Then, these processes are repeated $S_{POP}/2$ times until obtaining the S_{POP} individuals that will constitute the next generation.

4. Steps 1 to 3 are repeated for each generation until reaching a maximum number of iterations (z_{max}), when the algorithm is terminated.

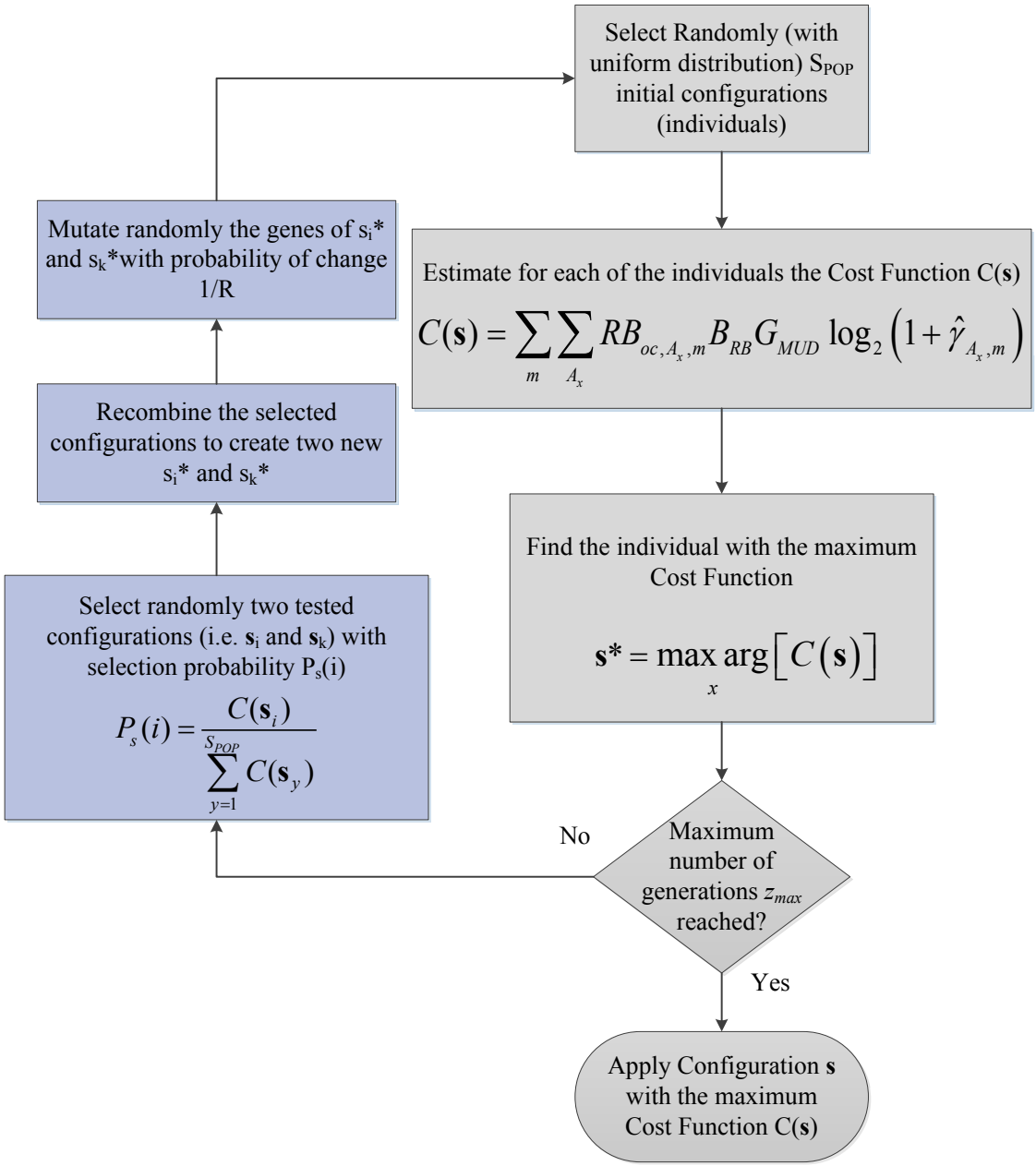

Figure 48: Flow-chart of the Genetic Algorithm-based Optimization

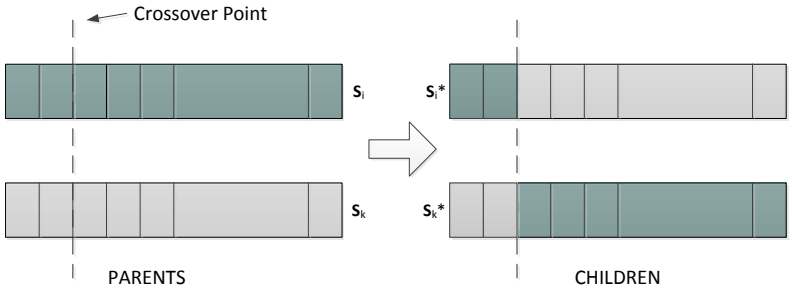

Figure 49: Recombination Process

4.4.2.3 Implementation Considerations

Although the implementation of the proposed solution depends on the capabilities offered by the management systems that are available at the network and that can differ between manufacturers and/or operators, a brief discussion is carried out about some high level considerations on how this implementation could be addressed.

The proposed solution targets the adjustment of the parameters of each macrocell BS and the parameters of the small cells that belong to the coverage area of this macrocell. According to 3GPP specifications ([104] and [105]) there are different options for the selection of the network element where the algorithm will be executed. A first option is to execute it in the management system. In particular, it can run either in the Network Management or in the Element Management levels that configure the parameters of the network and the different network elements, respectively [104]. Another option for the implementation of the proposed solution would be a decentralized approach in which the algorithm is executed at the Network Element level [105], i.e. at the macrocell BS in this case. This solution would require that connectivity exists between the small cells and the macrocell BS, e.g. through the X2 interface, in order to exchange measurements related to the propagation losses between the different users/cells. These measurements are required to estimate the capacity of each potential configuration analyzed by the genetic algorithm using expressions (49) to (60).

Another consideration is the computational complexity and the frequency at which the algorithm should be executed. Since the parameters that are obtained by the optimization process will impact on the scheduling algorithm behavior (i.e. *Algorithm 5* and *Algorithm 6*), then the change of these parameters and consequently the algorithm execution should occur on a relatively long-term basis, involving multiple scheduling cycles in order to assure a proper operation. On that respect, the algorithm is intended to be triggered when significant changes are detected in the environment (e.g. significant variations on the average propagation losses seen by the users, etc). As such, the algorithm does not need to be executed under very stringent real time constraints, reducing in this way the computational complexity. Another factor that is related with the algorithm complexity is the population size S_{POP}. Therefore, a proper setting of this parameter can result in the reduction of the execution time. In any case genetic algorithms offer the possibility of parallel processing implementation due to the independent evaluation of each individual, which contributes also to reducing the execution time of the algorithm. Finally, it has to be noted that simulations performed throughout this work, where parallelism was not exploited, have showed that the required time for the algorithm execution did not exceed 4 minutes per experiment, proving that even in the serial implementation the algorithm complexity is quite low.

4.4.3 Simulation Results

The proposed optimized solution (OTFP-eICIC) has been evaluated by means of simulations. In this section a detailed description of the simulation setting and the numerical results obtained throughout this work are presented. The presentation is mainly divided into two parts. In the first part the proposed solution is compared against existing schemes, such as the classical ABS [85] and the LP-ABS of [91]-[93] in order to study the efficiency of the scheme. The second part focuses on the benefits brought by the genetic optimization; therefore a comparison is carried out between the genetic based optimized approach and the solution of [97], where the configuration of the parameters is fixed. Additionally in the second part, the configurations selected by the genetic optimization strategy depending on the network load are analyzed and discussed.

4.4.3.1 Simulation Scenario

For the evaluation of the proposed solution two different simulation scenarios have been considered in order to study different macrocell interference conditions. On that respect, the analysis is carried out in the first scenario for a macrocell with three cells located in a relatively high distance from the macro BS, while in the second scenario one of the small cells has been located quite close to the BS. In the latter case, the users of the small cell experience higher levels of interference from the macrocell.

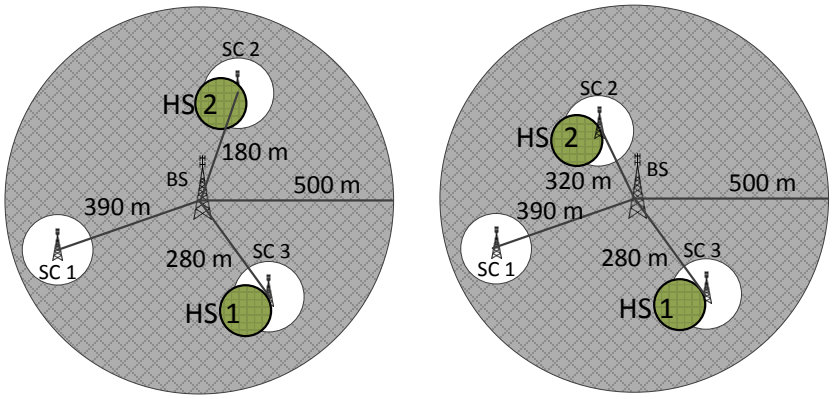

(a) **(b)**

Figure 50: Simulation Scenarios (a): Scenario 1, (b): Scenario 2.

Two Hot Spots are considered in small cells 2 and 3 as shown in Figure 50. Hot Spot 1 (HS 1) consists of 20 users, while the number of users of Hot Spot 2 (HS 2) is varied throughout the simulations. In addition, 120 users, denoted as non-Hot Spot (non-HS) users are distributed uniformly in the scenario. For the calculation of the propagation losses of a user u with the i-th macrocell or the k-th small cell equation (46) is used with the same parameters.

The considered configuration space of the parameters to be optimized is as follows: The number of ABSs μ can vary between 0 and 10 with step 1, the number of the reserved RBs ε can be between 0 and 25 with step 1, the lower transmit power $P_{TM,low}$ can get values between -14 and 28 (dBm) with step 2 dB and finally the CRE biases Δ for the small cells can take values from 0 to 24 dB in step of 1 dB according to the limits specified in [106] and [107]. It has to be noted, that since only one macrocell is studied, the index i from the parameter notation is omitted for simplicity reasons. Table XII presents the rest of the simulation parameters.

TABLE XII: SIMULATION PARAMETERS

N	Number of RBs per subframe	25
$P_{TM,,high}$	Macrocell Transmit Power (high level)	29 dBm
$P_{Ts,k,}$	Small cell Transmit Power	6 dBm
T_W	Window size	10 frames
P_N	Noise Power (per RB)	-115.5 dBm
$R_{b,min}$	Minimum bit rate threshold	50 Kbps
RB_{max}	Maximum Number of allocated RBs	3 RBs
S_{POP}	Population Size	40
z_{max}	Maximum Number of Generations	10000
G_{MUD}	Multiuser Diversity Gain	Obtained from [100]

The simulation results presented in this section are the average of 30 experiments, where each experiment corresponds to a different spatial user distribution and lasts 1000 frames.

Finally, the metrics used for the performance evaluation are the average capacity per user and the aggregated capacity. It is reminded that the average capacity per user is the capacity C_u that a user u experiences in each frame averaged along the whole simulation time, for all the users and for all the experiments. It results from the aggregation of the bit rates in all the RBs that have been allocated for transmissions to this user according to equation (48) as presented in section 4.2.3.1. The aggregated capacity is the total capacity seen by all the users of all the cells, averaged for all the experiments.

4.4.3.2 Comparison with Benchmark Schemes

In order to study the efficiency of the OTFP-eICIC scheme, comparisons have been carried out with existing solutions in terms of average user and aggregated capacity. These solutions are the classical ABS scheme [85] as presented in 4.2.3.1 and the LP-ABS scheme [91]-[93] as presented in 4.3.2.2, which include the CRE technique and follow the same principles, criteria and limitations for the resource allocation as the OTFP-eICIC scheme with the target of a fair comparison.

The comparison of the average user capacity as resulted for the proposed OTFP-eICIC solution and the two benchmark schemes is presented in Figure 51 and Figure 52 for scenario 1 and scenario 2, respectively. The results are given as a function of the HS 2 users variations. Moreover, since the reference schemes follow a static parameter configuration the results are presented for μ equal to 2, 3, 4 and 5, which are the values that provided the highest capacities.

From the figures it can be clearly seen that the proposed optimized solution outperforms both benchmark schemes. As it can be observed for the two reference schemes, the number of ABS subframes that gives the highest system capacity depends on the network load. This suggests that a fixed configuration is not optimal. On the other hand, the genetic algorithm of the OTFP-eICIC approach finds the most appropriate configuration of the involved parameters in each case, which results in the increment of the capacity with gains of up to 24% with respect to the classical ABS and up to 12% with respect to the LP-ABS for both scenarios.

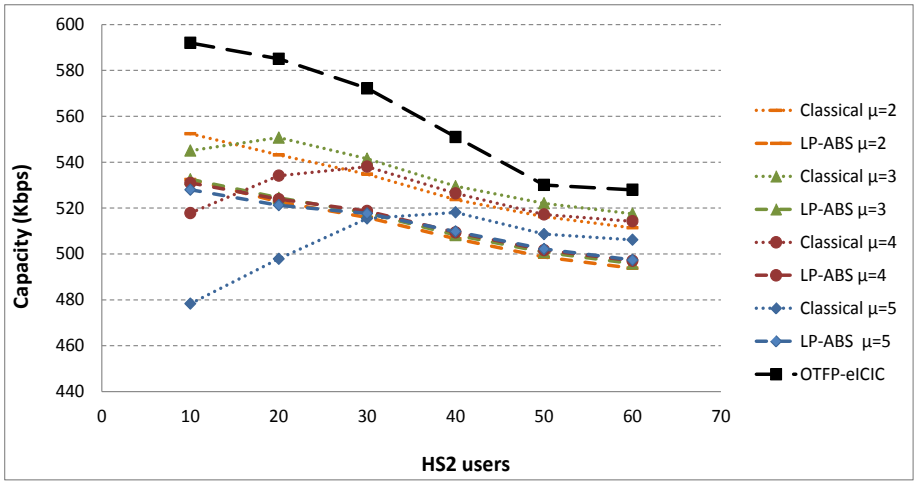

Figure 51: Comparison between different schemes in terms of Average User Capacity in Scenario 1

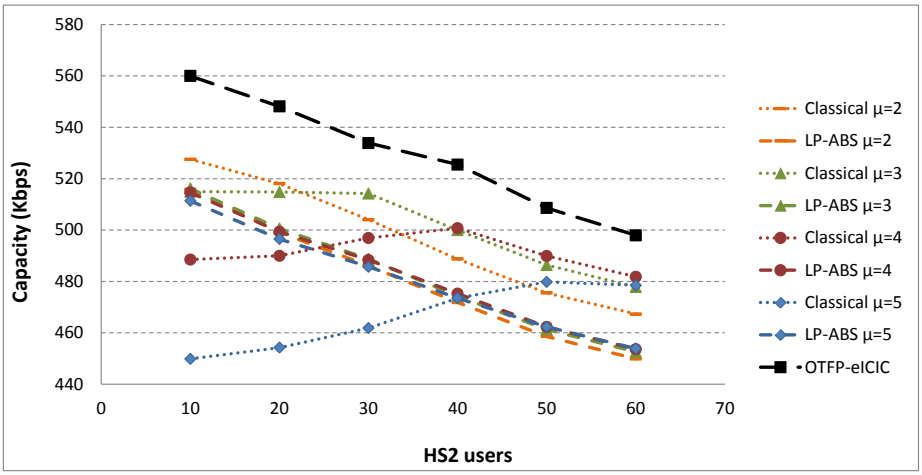

Figure 52: Comparison between different schemes in terms of Average User Capacity in Scenario 2

Furthermore, the comparison of the aggregated capacity with respect to variations of the number of the users in HS2 is presented in Figure 53 and Figure 54 for scenario 1 and scenario 2, respectively. As it can be observed, an important improvement is offered by the proposed solution with respect to the two reference schemes. For the case of the classical ABS the gain reaches a value of 15%, while the gain with respect to LP-ABS reaches a value of 13%. Overall, it can be clearly stated that the OTFP-eICIC successfully configures the network parameters with result the maximization of the network capacity.

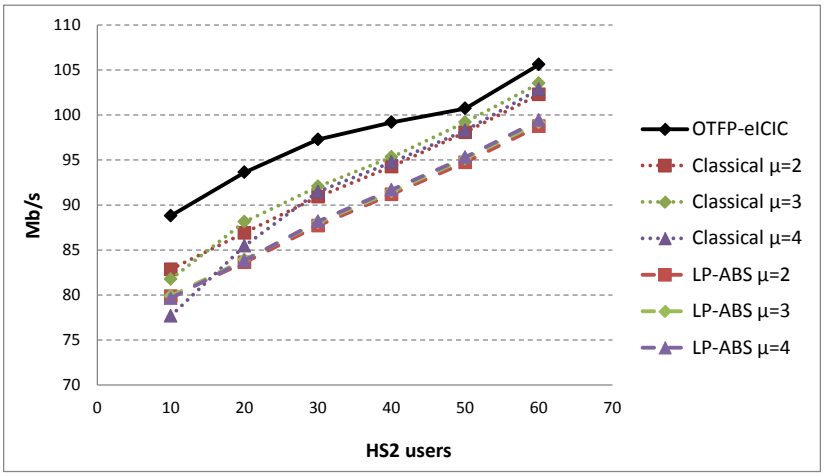

Figure 53: Comparison between different schemes in terms of Aggregated Capacity in Scenario 1

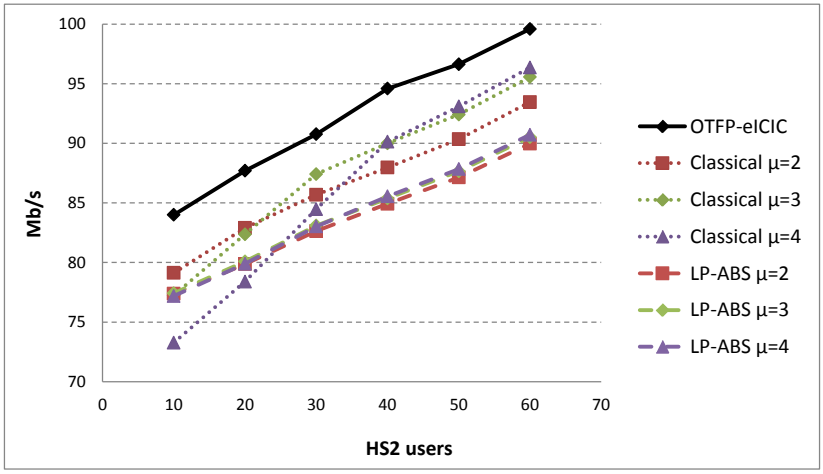

Figure 54: Comparison between different schemes in terms of Aggregated Capacity in Scenario 2

4.4.3.3 Analysis of the Optimization Impact

The second part of the analysis focuses on the benefits brought by the optimization process in terms of capacity improvement. On that respect, this section presents a comparison of the OTFP-eICIC approach with the TFP-eICIC of [97], where the parameter configuration is fixed. It has to be noted that number of

the reserved RBs ε in the reference scheme is adjusted with respect to the number of CRE users according to equation (44) with $\alpha = RB_{max}/\mu$. Moreover in this section, an analysis of the configurations as resulted by the optimization process is carried out.

Let us focus on Scenario 1, where the network deployment consists of the small cells located at high distance from the macrocell BS, and therefore the small cell users are less susceptible to the macrocell interference. Figure 55 presents the gain (in %) in the average user capacity as resulted from the comparison of the optimized proposed solution and the reference scheme. It has to be referred that since the reference scheme follows a static configuration the results are given for different values of the ABS subframes (μ). In particular, the considered values for μ are 2, 3 and 4, which are the ones that provided the highest capacities.

From the figure it can be observed that the optimization process results in a significant improvement of the network capacity with gains reaching the value of 12%. Moreover, it can be noticed that as the number of users in the HS2 decreases, the gain increases. Since both solutions target the increment of the macrocell capacity, this indicates that the optimization process is able to find a configuration that allows the macrocell users to utilize the resources in a more efficient way than in the non-optimized reference scheme and this gain is more noticeable in the case where there are less small cell users. As such, it can be clearly stated that the optimization process improves significantly the network capacity.

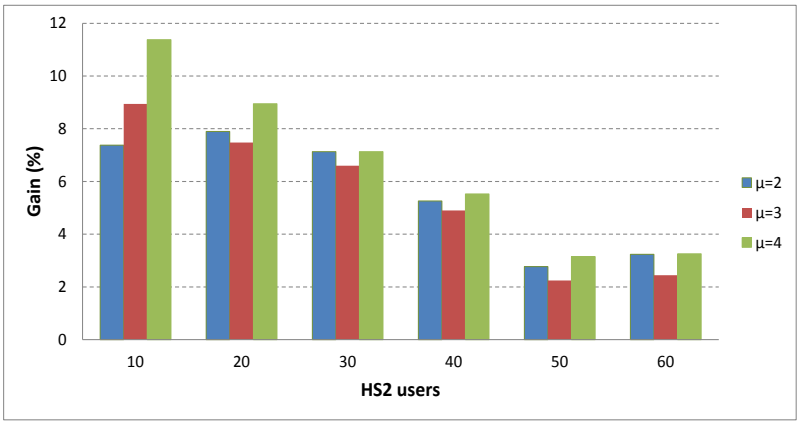

Figure 55: Gain in the average user capacity of the OTFP-eICIC case with respect to the fixed configuration case (TFP-eICIC)

Another comparison has been carried out with respect to variations of the non-HS users, while having a fixed number of users in HS2. As such, Figure 56a depicts the gain (in %) in the average user capacity as resulted for 10 HS2 users, while in Figure 56b the number of HS2 users has been set to 60. As it can be observed from the figures, the OTFP-eICIC scheme improves significantly the capacity. Moreover, it can be noticed that the gain increases with the number of non-HS users, which are mainly macrocell users. Finally, it is worth of mentioning that when the number of the HS2 users is set to 10, the highest gain is

obtained with respect to the TFP-eICIC for μ=4, while when the number of the HS2 users is set to 60, the highest gain is obtained for μ=2. This clearly suggests that a fixed configuration is not always optimal for all load conditions.

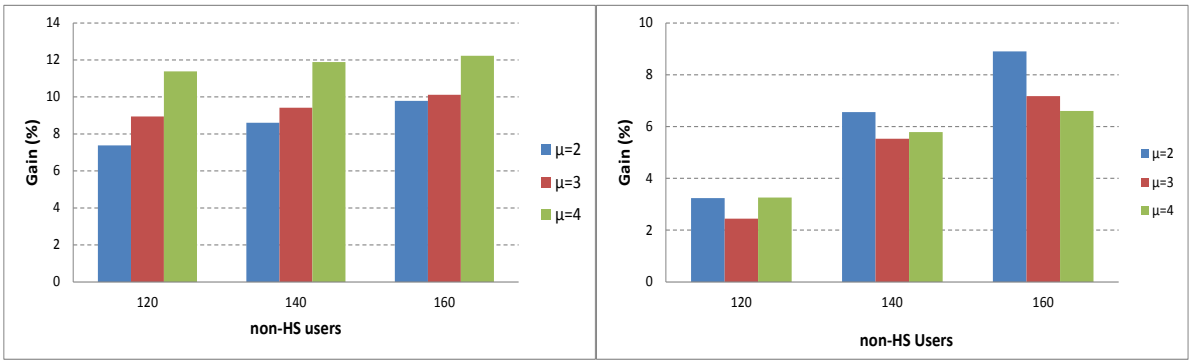

(a) 10 HS2 users **(b) 60 HS users**

Figure 56: Average User Capacity Gain (%) between OTFP-eICIC and TFP-eICIC in scenario 1

As it has already been stated, genetic algorithms are applied in order to find the most appropriate configuration for each experiment according to the network load conditions, with the aim of maximizing the network capacity. On that respect, a discussion is given in the following with respect to the configurations resulted from the optimization process, with the intention to analyze the parameter setting found by genetic algorithms under different situations.

Based on the above, Figure 57 presented below depicts the evolution of the optimized parameters with respect to the variations of the users in the HS2. Figure 57a presents the results of the μ, ε and $P_{TM,low}$ in the same figure for simplicity reasons, while Figure 57b depicts the results for the CRE biases Δ_1, Δ_2, and Δ_3 of small cell 1, 2 and 3, respectively. Moreover, Figure 58a depicts the average number of CRE and normal users in each small cell, while Figure 58b presents the average number of users in the macrocell.

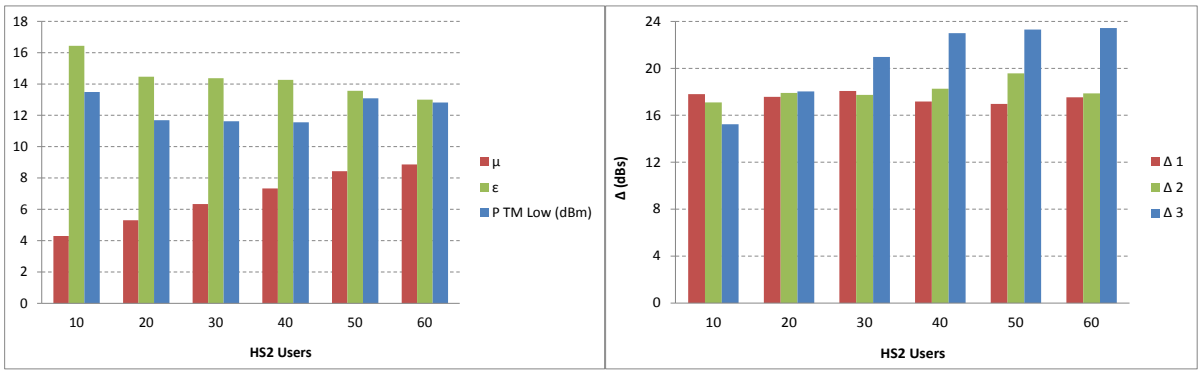

(a) **(b)**

Figure 57: Evolution of the optimized parameters found by the genetic algorithm (a) μ, ε and $P_{TM,low}$, (b) Δ_k

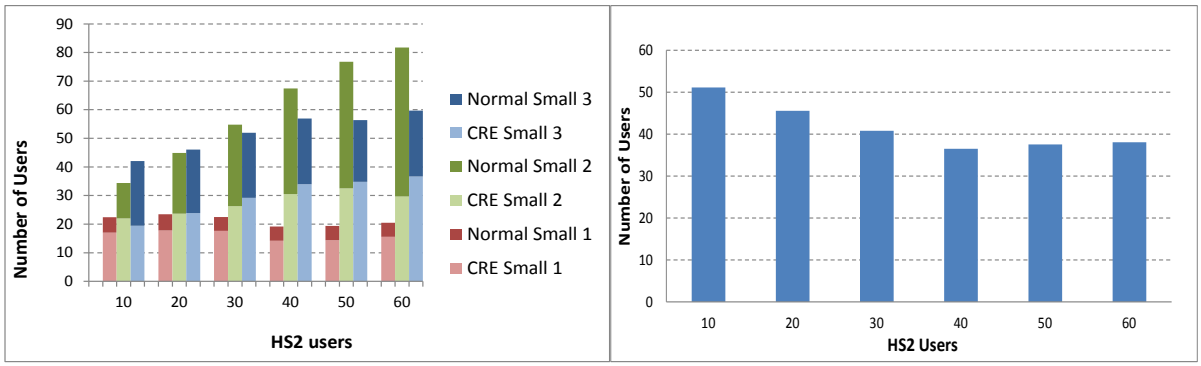

(a) **(b)**

Figure 58: Average number of users in (a) Small cells, (b) Macrocell, as a result of the optimization done by the genetic algorithm

Focusing on the figures given above, it can be observed that as the number of the HS2 users increases, the algorithm tends to increase the total number of reserved RBs (e.g. for the case of 10 HS2 users the number of reserved RBs is $\mu \cdot \varepsilon$=70, while for the case of 60 HS2 users it increases up to $\mu \cdot \varepsilon$=114). This occurs due to the fact that as the users in HS2 increase there will be more CRE users in the small cells 2 and 3 (see Figure 58), meaning that more reserved resources are necessary in order to protect them from the macrocell interference. Furthermore, since the number of normal small cell users is also increased, $P_{TM,low}$ is kept in low levels around 13 dBm, so as to reduce the generated interference from the macrocell.

The configuration of the CRE biases of the small cells (depicted in Figure 57b) is carried out in a way so that the macrocell will be offloaded. More specifically, since the number of reserved RBs increases with the number of the HS2 users, the small cells have in their disposal more resources that are free of interference and therefore they can better absorb more traffic from the macrocell. Thus, as the users in the HS2 are increased, the algorithm tends to increase the values of the CRE biases in order to absorb this traffic. This CRE increase mainly affects small cell 2, where the hotspot HS2 is located, and to a minor extent small cell 3, which also includes a hotspot (HS1) in its proximity.

Similar results are obtained for Scenario 2 when comparing the optimized scheme against the fixed configuration case. Although results are not presented in details for the sake of brevity, the optimized scheme achieves gains up to 11% when the number of HS2 users and non-HS users and the different parameters of the fixed configuration case are varied with the same ranges as in Scenario 1.

5. Conclusions and Future Work

LTE and LTE-A have been a crucial point in the evolution of mobile communication systems. The incorporation of innovating ideas and technologies has opened the way towards possibilities that can surpass the constraints imposed by technology evolution and satisfy the continuously increasing user demands in terms of data rates, coverage and data hungry applications. Resource management and interference mitigation, however, are still great challenges that attract the attention of operators and researches all over the world. In the framework of LTE, ICIC techniques are adopted with target the mitigation of the interference, the capacity increment and the improvement of the overall network performance. On the other hand, the notion of HetNets is introduced in the context of LTE-A, comprised of cells of different sizes and incorporating different technologies. This diversity requires more sophisticated ICIC techniques that take into account the heterogeneity of the network topology. As such, in LTE-A ICIC is enhanced and eICIC techniques take a leading role.

The challenges met by ICIC and eICIC have been addressed in this thesis. Initially ICIC techniques have been studied, the related problems have been identified and new schemes for homogeneous network deployments have been proposed, bringing significant benefits in the network performance. Furthermore, the extension of the concept considering HetNets has also been studied and analyzed. In the second part of the thesis, eICIC methods and the associated challenges have been investigated. In addition, the user association problem in HetNet deployments has also been addressed. Focusing on the network heterogeneity and exploiting the knowledge acquired during the study of the ICIC concept, novel e-ICIC schemes have been proposed resulting in significant improvements. The most important conclusions as resulted throughout this work, as well as a discussion for the future work are given in this chapter.

5.1 Summary of Results

In the first part of the thesis, research has been focused on the ICIC concept. After investigating different existing techniques, work has targeted on the limitations presented when static channel allocations are considered. On that respect, a distributed ICIC scheme known as GS-ICIC that dynamically allocates the available channels has been presented. The algorithm is based on the Gibbs Sampler as optimization tool that targets the minimization of the network interference and consequently the capacity increment. The selection of the Gibbs Sampler is based on the fact that it is a useful tool for

the estimation of parameters or random variables that depend on the state of other variables in their environment (considered as neighbors), which is the case in a cellular network. The estimation is carried out by using the local interactions in order to construct a global model, which is target of minimization. Therefore, the optimization framework was formulated by defining the local and global interferences (energy functions) to be minimized by the algorithm by finding the proper channel allocation. Simulation results have shown the efficiency of the GS-ICIC scheme through comparisons with a classical channel allocation scheme in terms of interference reduction and capacity improvement. The algorithm convergence has been studied showing that most of the experiments converge successfully to an optimal solution. Moreover, the possibility of an online implementation has been discussed through the analysis of the required number of algorithm executions. Results have shown that the algorithm results in the gradual reduction of the interference, therefore having a positive impact in the network performance throughout its execution, making it feasible to be executed online.

Further analysis has been carried out with purpose to study the impact they have on the algorithm performance variations of different algorithm related parameters. As a first step, the possible channel configurations have been varied by applying different restrictions, e.g. assigning only one channel in the inner part of the macrocell. Results have shown that the approach where the inner and the outer parts of the macrocell were restricted form being assigned the same channel, presented the best performance in terms of capacity increment. In addition, different values of the temperature parameter, which is a parameter that impacts on the algorithm convergence, have been tested in order to find the most proper setting. Results have shown that too small values may result in configurations that are not optimal, while values too high require higher simulation time and convergence is not always assured. As such, it has been observed that the temperature parameter must be chosen carefully depending on the network complexity and the requirements of each problem in order to compensate the trade-off between time of convergence and accuracy of the solutions given by the algorithm. Finally, the impact of the number of users on the algorithm performance has been studied. Simulation results have shown that the algorithm achieves quite similar performances independently from the number of the users, although it has to be referred that when this number is small it performs slightly better.

The performance of GS-ICIC has been additionally analyzed through different formulations of the local and global energy functions in order to study the impact in the interference mitigation and the capacity improvement. The first approach, known as UIGS-ICIC, was based on the fact that apart from the experienced interference, the user capacity depends also on the number of the users that share the same bandwidth, i.e. the number of users that are served by the same cell. As such, both the interference and the number of the users have been considered in the energy function. The second approach (USGS-ICIC) targeted the joint minimization of the interference and the maximization of the capacity. For this reason, the SINR has been included in the formulation. Finally, the third approach, known as NUSGS-

ICIC was based on empirical observations and consists on the inclusion of the SINR and a constant parameter. Simulation results have shown that all the approaches outperform a reference scheme in terms of average user and average edge user capacity. Compared to the GS-ICIC scheme however, the UIGS-ICIC and the USGS-ICIC did not present better performances. On the other hand, the NUSGS-ICIC present similar results with respect to the average user capacity, while for the average edge user capacity results have shown that for large inner cell ranges it performs better, but worse when small inner cell ranges are considered. As such, depending on the operators' requirements, either the GS-ICIC or the NUSGS-ICIC can be selected.

The next part of the ICIC investigation has been focused on the consideration of heterogeneous deployments. On that respect, the GS-ICIC scheme has been extended to the HGS-ICIC in order to include small cells in the macrocell deployment. The energy function has been formulated accordingly so as to include the interference of both macrocells and small cells. Moreover, the performance of the algorithm has been analyzed with respect to different scenarios, starting from simpler and moving towards more complicated topologies. Through simulations and comparisons with reference schemes it has been proved that the algorithm successfully configures the available channels and results in the interference mitigation and the capacity improvement.

Finally, in the last part of the study of the ICIC a possible implementation of the HGS-ICIC scheme has been presented, under the name REM-based frequency optimization (RFO). The implementation is based on the utilization of a database known as REM that holds information about the radio environment, such as active users' locations and propagation characteristics, in a dynamic manner. The information can be classified into two types, local and global depending on whether they are related to the local environment or they can impact on a higher number of nodes. RFO exploits local information, such as transmit power levels and propagation losses between the users and the cells of the network in order to estimate the received and generated interference and perform the channel allocation accordingly. Performance evaluation has focused on the impact the REM information error has on the algorithm performance in terms of interference reduction and capacity improvement with respect to a traditional channel allocation scheme. Results have shown that the gain is decreased as the error in the information increases, although the overall performance of the algorithm presents significant improvements with respect to the reference scheme.

The second part of the thesis has been devoted on the study of eICIC related challenges for HetNets. These challenges include the user-to-cell association and the interference management in networks comprised of macrocells and small cells. The work has been initially focused on the interference management. One of the most prominent solutions used in LTE-A is the ABS scheme that is based on the partition of the available subframes into Normal and ABS and that devotes the ABS subframes

exclusively for small cell transmissions with result however the resource underutilization for the macrocells and consequently the capacity degradation. On that respect, a novel solution, known as Time-Frequency/Time-Power eICIC, for the management of the ABS subframes has been presented that is based on two mechanisms that exploit the time-frequency or the time-power domains depending on the deployment of the small cells in the network. The key concept of these mechanisms is based on the fact that the macrocells can perform simultaneous transmissions with the small cells in the ABS subframes under special constraints. In particular, these conditions include the allowed RBs in the frequency domain that can be reconfigured and the maximum allowed transmit power. The efficiency of the solution has been studied through simulations and comparisons with the classical ABS scheme in terms of average user capacity. It has been shown that both mechanisms increase significantly the user capacity, with the Time-Frequency mechanism however presenting higher gains.

The Time-Frequency/Time-Power eICIC scheme has been further improved in order to overcome the constraints presented in the flexibility of the scheme due to the dependence on the small cells position in the network topology and the presence of interference when the time-power mechanism is applied. As such, the Time-Frequency-Power eICIC (TFP-eICIC) has been proposed, employing a smart mechanism that exploits jointly the time, frequency and power domains with purpose to further improve the resource utilization and to balance in a more effective way the trade-off between the macrocell capacity degradation and the small cell interference reduction. The proposed scheme preserves the time splitting employed by the ABS scheme, while an additional splitting is introduced with respect to the frequency domain during the ABS subframes and at the same time two transmit power levels are provided for the macrocell transmissions. In this way, the most vulnerable users of the small cells (i.e. users located in the cell edges) are protected, while additional resources are disposed for macrocell transmissions. The efficiency of the scheme has been evaluated through simulations and comparisons with different benchmark schemes. These include the classical ABS, the LP-ABS that exploits the power domain and the Time-Frequency/Time-Power eICIC. It has been shown that the proposed scheme outperforms all the benchmark schemes in terms of average user capacity, proving that a better resource utilization is achieved.

Finally, the last part of the eICIC investigation has been focused on the optimization of the TFP-eICIC with purpose to include the user-to-cell association, to enhance the performance of the scheme and achieve additional benefits in the network performance. On that respect, the OTFP-eICIC scheme has been presented that involves the proper setting of the partitions in the three domains, including the user-to-cell association parameters, based on genetic algorithms. In particular, the parameters optimized by the algorithm are the number of ABS Subframes, the number of reserved RBs, the lower transmit power level and the CRE bias of each small cell. The optimization process makes use of a cost function that is based on the capacity estimation depending on the configuration under test. As such, genetic algorithms are able

to search among several solutions and converge to an optimal configuration. The evaluation of the scheme has been carried out through simulations and comparisons with several reference schemes. In particular, the classical ABS and the LP-ABS have been used as benchmarks for the comparisons in terms of average and aggregated user capacity, while a further comparison has been carried out with the TFP-eICIC in order to study the benefits brought by the optimization process. In addition, an analysis of the resulted configurations has been performed and the implementation considerations have been discussed. Results have shown that the OTFP-eICIC scheme outperforms all the reference schemes, improving significantly the user capacity. As such, it can be stated clearly that the proposed solution utilizes the available resources in a more efficient way. Moreover, it has been demonstrated that the proper setting of the related parameters carrier out by the OTFP-eICIC can adapt to traffic load changes, while this is not always the case when a static configuration is considered.

5.2 Future Work

This section includes suggestions for future research directions based on the work presented in this PhD thesis. The possible directions can be divided into three groups related to further evaluations that can be carried out, different implementations of the proposed solutions and additional technologies that can be employed. A brief guideline is given in the following.

- Additional Evaluation in other scenarios

  The ICIC and eICIC solutions presented in this work are based on simulations where user mobility and handover are not included. As such, future work can include evaluations of the proposed schemes through simulations of real life scenarios where the environment will be changed in certain instances. Moreover, the OTFP-eICIC scenario can be additionally compared against further solutions that have been presented in the literature and that have been optimized to reconfigure the network parameters.

  Since mobile communications evolution is moving towards 5G, the networks tend to become denser. On that respect, further evaluations of the proposed solutions can be carried out under scenarios that include a high number of small cells in a specific location (e.g. concerts, stadiums etc.), known as ultra-dense networks. In such cases new challenges arise especially related to the interference management. As such, it would be very interesting to study the performance of the proposed solutions in such type of networks.

- Implementation Considerations

In this work it has been given in detail a possible implementation of the GS-ICIC scheme based on the concept of REMs. In the same way, the TFP-eICIC and OTFP-eICIC solutions can be benefit from the information hold in the REMs with respect to radio environment parameters and the conditions that experience the users and the cells of the network. For instance, the algorithm can obtain information about the users that are more susceptible to interference, i.e. the CRE users and perform the calculations based on this information. Nevertheless, specific issues should be devised carefully, such as the rate with which information will be obtained, the element that will execute the algorithms and the reliability of the information hold by the REM databases.

Moreover, the implementation of the OTFP-eICIC solution presented in this work has been carried out based on a serial execution. As it has been discussed in 4.4.2.3, a parallel implementation could reduce significantly the algorithm complexity and the execution time. As such, additional benefits could be achieved if the algorithm would be implemented for example in an FPGA evaluating in parallel each candidate configuration.

- Other Technologies

Another option for extending the work of this thesis would be to consider other features included in the context of LTE and LTE-A. A good example would be the incorporation of Carrier Aggregation (CA) in the implementation of the proposed solutions in order to increase the spectral efficiency and the user data rates, with special focus on the throughputs of the users located in the cell edges. On that respect, the proposed strategies can be modified accordingly so as to assign the proper component carriers to the network users.

Finally, one of the most important aspects would be the extension of this work in order to be compliant with the 5G requirements. As such, additionally study could be carried out with respect to the supported bandwidths and the related challenges resulting from the increment of the users and the technologies that are involved, in order to modify accordingly the proposed schemes. For example, it is envisaged that 5G networks will employ Cloud-Radio Access Networks (C-RAN), Network Function Virtualization (NFV) and Software Defined Networking (SDN). C-RAN refers to cloud-based architectures where certain functions can be executed in the cloud. NFV is related to the software implementation of network functions, such as traffic load management, in general purpose computing and storage resources. SDN separates the control plane and the data plane and therefore the control functions can be implemented on a software controller, known as the SDN controller that serves as the

programmatic interface to the network. It has to be noted that both NFV and SDN can exploit C-RAN for an efficient implementation. C-RAN, NFV and SDN endow the network with scalability and flexibility since the functions can be reconfigured according the current requirements. As such, the implementation of the proposed solutions can be carried out based on these architectures with target an easier and more efficient management of interference and load balance.

6. References

[1] Lopez-Perez, D.; Guvenc, I.; de la Roche, G.; Kountouris, M.; Quek, T.Q.S.; Jie Zhang, "Enhanced intercell interference coordination challenges in heterogeneous networks," *Wireless Communications, IEEE* , vol.18, no.3, pp.22-30, June 2011

[2] 4G Americas – White Paper, "Developing & Integrating *a* High Performance HET-NET", October 2012

[3] R. Qingyang Hu, Yi Qian, "Heterogeneous Cellular Networks", *John Wiley & Sons*, Ltd., 2013

[4] I. Guvenc, T.Q.S Quek, M. Kountouris, D. López-Pérez, "Heterogeneous and Small Cell Networks: Part 1", *IEEE Communications Magazine*, May, 2013,pp.34-35

[5] Ying Loong Lee; Teong Chee Chuah; Loo, J.; Vinel, A., "Recent Advances in Radio Resource Management for Heterogeneous LTE/LTE-A Networks," *Communications Surveys & Tutorials, IEEE* , vol.16, no.4, pp.2142,2180, Fourthquarter 2014

[6] J. G. Andrews, "Seven ways that HetNets are a cellular paradigm shift", *Communications Magazine*, *IEEE*, vol. 51, no.3, pp. 136-144, March 2013

[7] G. Boudreau, J. Panicker, N. Guo, R Chang, N. Wang, and S. Vrzic, "Interference coordination and Cancellation in 4G Networks", *IEEE Communications Magazine*, vol. 47, no. 4, April 2009, pp. 74-81

[8] http://www.3gpp.org/LTE

[9] 3GPP TR-23.401, v 8.4.1, "GPRS enhancements for Evolved Universal Terrestrial Radio Access network (E-UTRAN) Access (Release 8)"

[10] S. Sesia, I. Toufik, M.Baker, "LTE: The UMTS Long Term Evolution", *John Wiley & Sons*, Ltd., 2009

[11] 3GPP, "Overview of 3GPP Release 10 v. 0.1.8", March 2013

[12] http://www.3gpp.org/ftp/Information/WORK_PLAN/Description_Releases/

[13] NEC, "3GPP LTE Evolved Packet System (and what it has to do with Femtocells)", available at: http://sites.cttc.es/femtoschool/andreas-maeder-nec-germany.html

[14] http://www.3gpp.org/The-Evolved-Packet-Core

[15] K. Bogineni, R, Ludwig, P. Mogensen, V. Nandlall, V. Vucetic, B.K. Yi, Z. Zvonar, "LTE Part I: Core network," *Communications Magazine, IEEE*, vol.47, no.2, pp.40-43, February 2009

[16] I. F. Akyildiz, D. M. Gutierrez-Estevez, E. Chavarria Reyes, "The evolution to 4G cellular systems: LTE-Advanced", *Phys. Commun.* 3, 4 (December 2010), 217-244

[17] 3GPP, TR-36.300 v.8.12.0 "Evolved Universal Terrestrial Radio Access (E-UTRA) and Evolved Universal Terrestrial Radio Access network (E-UTRAN); Overall Description; Stage 2", 36.300, March 2010

[18] A. L. Intini, "Orthogonal Frequency Division Multiplexing for Wireless Networks", Report, *University of California, Santa Barbara*, December 2000

[19] V. Tarokh, N. Marchetti, M. I. Rahman, S. Kumar, R. Prasad, "OFDM: Principles and Challenges" in "New Directions in Wireless Communication Research", *Springer US*, pp. 29-62 2009

[20] 3GPP, TR-25.892, v 2.0.0, "Feasibility Study for OFDM for UTRAN enhancement; (Release 6)", June 2006

[21] J. Jayakumari, "MIMO-OFDM for 4G Wireless Systems", I*nternational Journal of Engineering Science and Technology*, vol. 2(7), pp. 2886-2889, 2010

[22] E. Dahlman, S. Parkvall, J. Sköld, P. Beming, "3G Evolution: HSPA and LTE for Mobile Broadband", *Elsevier Ltd*, 2007

[23] L. Hanzo, J. Akhtman, M. Jiang, L. Wang, "MIMO-OFDM for LTE, WiFi and WiMax: Coherent versus Non-Coherent and Cooperative Turbo-Transceivers", *John Wiley & Sons*, Hoboken, 2011.

[24] M. Morelli, C. C-J Kuo, M. O. Pun, "Synchronization Techniques for Orthogonal Frequency Division Multiple Access (OFDMA): A Tutorial Review", *Proceedings of the IEEE*, vol.95, no.7, pp.1394-1427, July 2007

[25] R. Prasad and F.J. Velez, "WiMax Networks: Techno-Economic Vision and Challenges", *Springer*, 2010

[26] R. Agustí, F. Bernardo, F. Casadevall, R. Ferrús, J. Pérez-Romero, O. Sallent, "LTE: Nueva Tendencias en Communicaciones Móviles", *Fundacion Vodafone España*, 2010

[27] C. Ciochina, D. Mottier, H. Sari, "An Analysis of OFDMA, Precoded OFDMA and SC-FDMA for the Uplink in Cellular Systems", *Proceedings from the 6th International Workshop on Multi-Carrier Spread Spectrum*, Herrsching, Germany, vol. 1, pp. 25-36, 2007

[28] L. Zhang, "A survey on Long Term Evolution", available online: http://www.cse.wustl.edu/~jain/cse574-10/ftp/lte.pdf

[29] H. Bolcskei, "MIMO-OFDM Wireless Systems: Basics, Perspectives and Challenges", *Wireless Communications, IEEE*, vol. 13, no. 4, pp. 31-37, Aug. 2006.

[30] H. Holma, A. Toscala, “LTE for UMTS – OFDMA and SC-FDMA Based Radio Access”, *John Wiley & Sons*, 2009

[31] H. G. Myung, D. J. Goodman, “Single Carrier FDMA, a new air interface for Long Term Eolution”, *Wiley & Sons*, 2008

[32] J. Pérez-Romero, O. Sallent, R. Agustí, M. A. Diaz-Guerra, “Radio Resource Management Strategies in UMTS”, *John Wiley & Sons*, 2005

[33] 3GPP TS 36.300 v.8.11.0 “Evolved Universal Terrestrial Radio Access (E-UTRA) and Evolved Universal Terrestrial Radio Access Network (E-UTRAN); Overall Description; Stage 2”, Jan. 2010

[34] O. Iosif, I. Banica, “On the Analysis of Packet Scheduling in Downlink 3GPP System”, *4th International Conference on Communication Theory, Reliability, and Quality of Service*, 2011

[35] 3GPP. TR 36.913 v.9.0.0, “Requirements for further advancements for E-UTRA (LTE-Advanced)”, 2009

[36] 3GPP, http://www.3gpp.org/lte-advanced

[37] Report ITU-R M.2134, “Requirements Related to Technical Performance for IMT-Advanced Radio Interface(s)”, Nov. 2008

[38] 4G Americas, “LTE Carrier Aggregation Technology Development and Deployment Worldwide”, October 2014

[39] G.D. Ntouni, A. Boulogeorgos, D.S. Karas, T.A. Tsiftsis, F. Foukalas, V.M. Kapinas, G.K. Karagiannidis, "Inter-band carrier aggregation in heterogeneous networks: Design and assessment," in *Wireless Communications Systems (ISWCS), 2014 11th International Symposium on* , vol., no., pp.842-847, 26-29 Aug. 2014

[40] Agilent, “Introducing LTE Advanced”, Application Note, available online at: http://cp.literature.agilent.com/litweb/pdf/5990-6706EN.pdf

[41] T. Tran, Y. Shin, O.-S. Shin, “Overview of enabling technologies for 3GPP LTE-advanced”, *EURASIP Journal on Wireless Communications and Networking,* 2012

[42] http://www.radio-electronics.com/info/cellulartelecomms/lte-long-term-evolution/4g-lte-advanced-relaying.php

[43] A. Khandekar, N. Bhushan, V. Ji Tingfang, “LTE-Advanced: Heterogeneous networks”, *Wireless Conference (EW)*, 2010 European, pp. 978-982, April 2010.

[44] 3GPP, TR 36.814 v. 9.0.0, “Evolved Universal Terrestrial Radio Access (E-UTRA); Further advancements for E-UTRA physical layer aspects ”, March 2010

[45] A. Damnjanovic, J. Montojo, W. Yongbin, L. Tao, M. Vajapeyam, Y. Taesang, S. Osok, D. Malladi, “A survey on 3GPP heterogeneous networks”, *Wireless Communications, IEEE*, vol.18, no.3, pp.10,21, June 2011

[46] V. Chandrasekhar, J. G. Andrews, A. Gatherer, “Femtocell networks: a survey”, *Communications Magazine, IEEE*, vol.46, no.9, pp.59-67, September 2008

[47] 3GPP, TR 36.921 v.9.0.0, “Home eNode B radio frequency requirements analysis”, March 2010

[48] M. Rahman, H. Yanikomeroglu, W. Wong, “Interference Avoidance with Dynamic Inter-Cell Coordination for Downlink LTE System”, *Wireless Communications and Networking Conference, WCNC 2009 IEEE*, pp.1,6, 5-8, April 2009

[49] K. Begain, G.I. Rozsa, A. Pfening, and M. Telek, “Performance analysis of GSM networks with intelligent underlay-overlay”, in *Proc. Seventh International Symposium on Computers and Communications* (ISCC 2002), July 2002, pp. 135-141

[50] 3GPP R1-050507 Huawei, “Soft Frequency Reuse Scheme for UTRAN LTE”, 3GPP TSG RAN WG1 Meeting #41, May 2005

[51] 3GPP, TSG-RAN R1-50738, “Interference mitigation considerations and results on frequency reuse”, Siemens, Sept. 2005

[52] M. Sternad, T. Ottosson, A. Ahlen, and A. Svensson, “Attaining both coverage and high spectral efficiency with adaptive OFDM downlinks”, in *Proc. IEEE VTC* 2003 Fall, Oct. 2003, pp. 2486-2490

[53] K. Elsayed et. al., “4G++: Advanced Performance Boosting Techniques in 4th Generation Wireless Systems”, Authority Funded Project, Deliverable D4.1

[54] R. Chang, Z. Tao, J. Zhang, C.-C. Jay Kuo, “Dynamic Fractional Frequency Reuse (D-FFR) for multicell OFDMA Networks using a graph framework” *Wireless Communications and Mobile Computing*, 2011

[55] X. Shui, M. Zhao, P. Dong, and J. Kong, “A novel dynamic soft frequency reuse combined with power re-allocation in LTE uplinks”, WCSP, Oct. 2012, pp.1-6

[56] G. Koudouridis, C. Qvarfordt, Tao Cai, J. Johansson, "Partial Frequency Allocation in Downlink OFDMA Based on Evolutionary Algorithms," *Vehicular Technology Conference Fall (VTC 2010-Fall)*, 2010 IEEE 72nd , pp.1,5, 6-9 Sept. 2010

[57] K. Koutlia, M. Žiak, J. Pérez-Romero, R. Agustí, “On the Use of Gibbs Sampling for Inter-Cell Interference Mitigation under Partial Frequency Reuse Schemes”, *Proc. The Third International Conference on Mobile Services, Resources, and Users* (MOBILITY), Lisbon, Portugal, Nov. 2013

[58] P. Bremaud, “Markov Chains: Gibbs Field, Monte Carlo Simulation, and Queues”, Springer Verlag, 1999

[59] G. Winkler, “Image Analysis, Random Fields and Markov Chain Monte Carlo Methods: A Mathematical Introduction (Stochastic Modelling and Applied Probability)”, Springer-Verlag, New York, Inc., Secaucus, NJ, USA, 1995

[60] P. Pérez, “Markov random fields and images,” *CWI Quarterly*, vol. 11, no. 4, pp. 412–437, 1998

[61] Y. Gong, W. Xu, “Machine Learning for Multimedia Content Analysis”, Springer, 2007

[62] B. Kauffmann, F. Baccelli, A. Chaintreau, V. Mhatre, K. Papagiannaki, C. Diot, “Measurement-based Self Organization of Interfering 802.11 Wireless Access Networks”, in *INFOCOM 2007, 26th IEEE International Conference on Computer Communications. IEEE* , pp.1451-1459, 6-12 May 2007

[63] C. Shue Chen, F. Baccelli, "Self-Optimization in Mobile Cellular Networks: Power Control and User Association," in *Communications (ICC), 2010 IEEE International Conference on* , pp.1-6, 23-27 May 2010

[64] C. Chen, F. Baccelli, L. Roullet, "Joint Optimization of Radio Resources in Small and Macro Cell Networks," in *Vehicular Technology Conference (VTC Spring), 2011 IEEE 73rd*, pp.1-5, 15-18 May 2011

[65] I. Viering M. Dottling, A. Lobinger, “A mathematical perspective of self – optimizing wireless networks”, in *Communications, 2009, ICC '09, IEEE International Conference on* , pp.1-6, 14-18 June 2009, 2009, pp. 1-6

[66] Shin-Ming Cheng, Shou-Yu Lien, Feng-Seng Chu, Kwang-Cheng Chen, "On exploiting cognitive radio to mitigate interference in macro/femto heterogeneous networks," in *Wireless Communications, IEEE* , vol.18, no.3, pp.40-47, June 2011

[67] Y. Zhao, L. Morales, J. Gaeddert,.K.K Bae, Um Jung-Sun, J.H. Reed, "Applying Radio Environment Maps to Cognitive Wireless Regional Area Networks," in *New Frontiers in Dynamic Spectrum Access Networks, 2007. DySPAN 2007. 2nd IEEE International Symposium on* , pp.115-118, 17-20 April 2007

[68] J. Pérez-Romero, A. Zalonis, L. Boukhatem, A. Kliks, K. Koutlia, N. Dimitriou, R. Kurda, "On the use of radio environment maps for interference management in heterogeneous networks," in *Communications Magazine, IEEE* , vol.53, no.8, pp.184-191, August, 2015

[69] B. Sayrac (editor), “D2.4: Final System Architecture”, Deliverable of FARAMIR project, December 2011, available at http://www.ict-faramir.eu/index.php?id=deliverables, accessed 7th Jan. 2016

[70] A. Zalonis et al., “Femtocell Downlink Power Control Based on Radio Environment Maps”, *IEEE Wireless Commun. Netw. Conf. (WCNC)*, Paris, France, April 2012

[71] J. Andrews, S. Singh, Ye Qiaoyang, Lin Xingqin, H. Dhillon, "An overview of load balancing in hetnets: old myths and open problems," *Wireless Communications, IEEE* , vol.21, no.2, pp.18,25, April 2014

[72] A. Weber, O. Stanze, "Scheduling strategies for HetNets using eICIC," in *Communications (ICC), 2012 IEEE International Conference on*, pp.6787-6791, 10-15 June 2012

[73] 3GPP R1-101203, Samsung, “System Performance of Heterogeneous Networks with Range Expansion”, Feb. 2010

[74] Peng Tian, Hui Tian, Jianchi Zhu, Lan Chen, Xiaoming She, "An adaptive bias configuration strategy for Range Extension in LTE-Advanced Heterogeneous Networks," *Communication Technology and Application (ICCTA 2011), IET International Conference on*, pp.336,340, 14-16 Oct. 2011

[75] Ning Zhaolong, Song Qingyang, Guo Lei, Dai Mengfan, Yue Minghong, "Dynamic Cell Range Expansion-based interference coordination scheme in next generation wireless networks," *Communications, China* , vol.11, no.5, pp.98,104, May 2014

[76] Final Report of 3GPP TSG RAN WG1 #66 bis v1.1.0. 3GPP R1-114352, 2011

[77] Xinyu Gu, Wenyu Li, Lin Zhang, "Adaptive cell range control in heterogeneous network," *Wireless Communications & Signal Processing (WCSP), 2013 International Conference on* , vol., no., pp.1,5, 24-26 Oct. 2013

[78] Xinyu Gu, Xin Deng, Qi Li, Lin Zhang, and Wenyu Li, “Capacity Analysis and Optimization in Heterogeneous Network with Adaptive Cell Range Control,” *International Journal of Antennas and Propagation*, vol. 2014, Article ID 215803, 10 pages, 2014

[79] Lopez-Perez, D.; Xiaoli Chu; Guvenc, I., "On the Expanded Region of Picocells in Heterogeneous Networks," *Selected Topics in Signal Processing, IEEE Journal of* , vol.6, no.3, pp.281,294, June 2012

[80] Madan, R.; Borran, J.; Sampath, Ashwin; Bhushan, N.; Khandekar, A.; Tingfang Ji, "Cell Association and Interference Coordination in Heterogeneous LTE-A Cellular Networks," *Selected Areas in Communications, IEEE Journal on* , vol.28, no.9, pp.1479,1489, Dec. 2010

[81] L. Lindbom R. Love, S. Krishnamurthy, C. Yao, N. Miki, and V. Chandrasekhar, “Enhanced inter-cell interference coordination for heterogeneous networks in LTE-advanced: A survey”, 2011. Available: http://arxiv.org/abs/1112.1344, CoRR, abs/1112.1344, 2011

[82] 3GPP, R1-104968, “Summary of the Description of Candidate eICIC Solutions”, Madrid, Spain, Aug. 2010

[83] T. Tran, Y. Shin, O.-S. Shin, “Overview of enabling technologies for 3GPP LTE-advanced”, *EURASIP Journal on Wireless Communications and Networking*, 2012

[84] 3GPP, R1-105081, “Summary of the Description of Candidate eICIC Solutions”, Madrid, Spain, Aug. 2010

[85] 3GPP, R1-104661, “Comparison of Time-Domain eICIC Solutions”, Madrid, Spain, Aug. 2010

[86] Cierny, M.; Haining Wang; Wichman, R.; Zhi Ding; Wijting, C., "On Number of Almost Blank Subframes in Heterogeneous Cellular Networks," *Wireless Communications, IEEE Transactions on* , vol.12, no.10, pp.5061,5073, August 2013

[87] Vasudevan, S.; Pupala, R.N.; Sivanesan, K., "Dynamic eICIC — A Proactive Strategy for Improving Spectral Efficiencies of Heterogeneous LTE Cellular Networks by Leveraging User Mobility and Traffic Dynamics," *Wireless Communications, IEEE Transactions on* , vol.12, no.10, pp.4956,4969, October 2013

[88] S. Singh, J.G. Andrews, "Joint Resource Partitioning and Offloading in Heterogeneous Cellular Networks," *Wireless Communications, IEEE Transactions*, vol.13, no.2, pp.888-901, Feb. 2014

[89] Deb, S.; Monogioudis, P.; Miernik, J.; Seymour, J.P., "Algorithms for Enhanced Inter-Cell Interference Coordination (eICIC) in LTE HetNets," *Networking, IEEE/ACM Transactions on* , vol.22, no.1, pp.137-150, Feb. 2014

[90] Trabelsi, N.; Roullet, L.; Feki, A., "A Generic Framework for Dynamic eICIC Optimization in LTE Heterogeneous Networks," *Vehicular Technology Conference (VTC Fall), 2014 IEEE 80th* , vol., no., pp.1,6, 14-17 Sept. 2014

[91] 3GPP, R1-113635, “Performance Evaluation of FeICIC with zero and reduced power ABS”, Huawei, HiSilicon, San Francisco, USA, Nov. 2011

[92] 3GPP, R1-120223, “Potential Issues regarding Low power ABS”, Panasonic, Dresden, Germany, Feb. 2012

[93] B. Soret, K. I. Pedersen, “Macro Transmission Power Reduction for HetNet Co-channel Deployments”, *IEEE, Global Telecommunications Conference (GLOBECOM)*, pp. 4342-4346, Dec. 2012

[94] Hao Zhou; Hailun Xia; Caili Guo; Rui Han; Yaguang Wu, "Adaptive ABS Configuration Scheme with Joint Power Control for Macro-Pico Heterogeneous Networks," *Vehicular Technology Conference (VTC Fall), 2014 IEEE 80th* , vol., no., pp.1,5, 14-17 Sept. 2014

[95] K. Koutlia, J. Pérez-Romero, R. Agustí, "Novel eICIC scheme for HetNets exploiting jointly the frequency, power and time dimensions", in *Personal, Indoor, and Mobile Radio Communication (PIMRC), 2014 IEEE 25th Annual International Symposium on*, pp.1078-1082, 2-5 Sept. 2014

[96] C. Wengerter, J. Ohlhorst, A.G.E. von Elbwart, "Fairness and throughput analysis for generalized proportional fair frequency scheduling in OFDMA*", IEEE 61st VTC 2005-Spring*, Jun. 2005

[97] K. Koutlia, J. Pérez-Romero, R. Agustí, "On enhancing Almost Blank Subframe Management for efficient eICIC in HetNets", *2014 IEEE 81st Vehicular Technology Conference (VTC Spring)*, May 2015

[98] K. Koutlia J. Pérez-Romero, R. Agustí, "On jointly exploiting the frequency, time and power dimensions for optimizing eICIC in Heterogeneous Networks", *Journal on Wireless Communications and Networking*, *EURASIP*, (submitted for publication)

[99] J.-G. Choi, S. Bahk, "Cell-Throughput Analysis of the Proportional Fair Scheduler in the Single-Cell Environment," *Vehicular Technology, IEEE Transactions on* , vol.56, no.2, pp.766-778, March 2007

[100] F. B. Alvarez, Contribution to Dynamic Spectrum Assignment in Multicell OFDMA Networks, PhD Thesis, UPC, April 2010

[101] M. Mitchell, "An introduction to Genetic Algorithms", *MIT Press* 1999

[102] J. W. Chinneck, "Practical Optimization: A Gentle Introduction" [Online]. Available: http://www.sce.carleton.ca/faculty/chinneck/po.html, ch. 14

[103] D.E. Goldberg, "Genetic Algorithms in search, Optimization and Machine Learning," *Addison-Wesley Reading*, Massachusetts, 1989

[104] 3GPP, TS 32.101 v12.0.0, "Telecommunication management; Principles and high level requirements (Release 12)", September 2014

[105] 3GPP TS 32.500 v12.1.0, "Self-Organizing Networks (SON); Concepts and requirements (Release 12)", December 2014

[106] 3GPP, TS 36.331 v12.5.0, "E-UTRA; Radio Resource Control", March 2015

[107] 3GPP, TS 36.304 v12.4.0, "E-UTRA; User Equipment procedures in idle mode", March 2015